

Weather and Forecasting

Investigating synoptic, mesoscale features SNOW six events

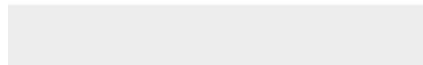
--Manuscript Draft--

Manuscript Number:	
Full Title:	Investigating synoptic, mesoscale features SNOW six events
Article Type:	Article
Corresponding Author:	Ralph Wade Johnson, Ph.D. program University Of Missouri Columbia, Missouri UNITED STATES
Corresponding Author's Institution:	University Of Missouri
First Author:	Ralph Wade Johnson, Ph.D. program
Order of Authors:	Ralph Wade Johnson, Ph.D. program
Abstract:	<p>This investigative study evaluates phenomena that that contributed to the heavy snowfall during six selected events - four mainly central United States and two Southeast, Middle Atlantic, Northeastern/New England. The physical and dynamical processes emphasized for their respective roles include 700hPa vertical motions or omega $\omega \geq -0.60$ pa/s, cyclogenesis and cyclone tracks, jet streak induced ageostrophic circulations, 850hPa temperature gradients, 850hPa warm and cold advection, latent heat release, 850hPa frontogenesis, 850hPa low level jet, 700hPa relative humidity (RH), 850hPa meridional and zonal wind, 700hPa v-component of storm motion, 700hPa heights and zonal winds, 300hPa heights and zonal winds.</p> <p>This research compares and analyzes 700hPa omega, pressure at mean sea level, 850hPa temperature along with other variables mentioned above that made contributions to the event physical and dynamical processes. This focus is on the physical and dynamical processes individually or collectively contributed to produce the heavy snowfall that occurred that occurred during these events. This study compares the role pf latent and sensible heat fluxes over ocean and land in cyclone development. In addition, while development of the heavy snow event represents complex interaction among many physical processes that occur on the synoptic and mesoscales, ENSO and teleconnections provide an important framework within which the winter storm evolves.</p>
Suggested Reviewers:	<p>Paul Markowski, PhD Chief Editor, American Meteorological Society markowski.waf@ametsoc.org DR Paul Markowski, along with DR Anthony Lupo are aware submit a manuscript that meets the AMS standards for publishable work!!!!</p> <p>Lynn McMurdie, PhD Editor McMurdie.WAF@ametsoc.org DR Lynn McMurdie, along with DR Paul Markowski and DR Anthony Lupo - University of Missouri are well aware of my efforts to submit a manuscript that meets the AMS standards for publishable work.</p>



[Click here to access/download](#)

Cost Estimation and Agreement Worksheet
Cost Estimation and Agreement Worksheet (7c).pdf



Response to Reviewers – 2/03/2017 Update

“Investigating the synoptic and mesoscale features in six selected heavy snow events” has been revised to “Investigating the synoptic and mesoscale features in six selected heavy snow events – Jet Streak Circulations and Latent, Sensible Heat Fluxes” Ralph Wade Johnson - Author

Manuscript does not identify a “gap” in scientific knowledge to and add new knowledge to the body of scientific work.

RE: Discussion of analyses that compares or contrast the contribution of latent, sensible heat fluxes during mainly continental heavy snow events with mainly ocean heavy snow events is presented for each of the six events studied. Since most of the emphasis has been on the contribution of oceanic latent, sensible heat fluxes to heavy snow events, this bridges the “gap” by recognizing that although the roles are different they are equally important whether the event is mainly over land or ocean (coastal).

Also, this study identifies a possible “gap” in scientific knowledge between scientific knowledge between heavy rain and heavy snow events. The use of SPC Hourly Mesoscale Analysis Archive parameters to diagnose the 25-26 December 2010 and 1-2 February 2011 events partially fills this “gap”, in particular 850hPa convergence, 250-850hPa differential divergence and 250hPa divergence.

The arguments presented in the manuscript should be free of errors in logic and the conclusions should follow from the original evidence presented.

RE: Since there is no relationship between the ENSO phase and the occurrence of snowstorms, it has been shown for all six events that heavy snow is a “manifestation of complex interactions or contributions of many physical processes that occur on the synoptic and mesoscales.

For all events, 850hPa temperature, meridional wind, zonal and the 700hPa v-component of storm variables have been changed to only as variables that interacted or contributed to heavy snow during each of the six events.

Zonal winds crossing geopotential height contours, as an indication jet streak ageostrophic circulations has been REMOVED from the manuscript. Jet streak ageostrophic circulations are represented by SPC Hourly Mesoscale Analysis Archive images of 300hPa isotachs, height and ageostrophic wind.

The transition from a closed circulation at 900hPa to a trough at 600hPa and subsequent latent heat release are primary synoptic and mesoscale processes statement(s) have been removed from the manuscript.

Latent Heat Release for the 25-26 December 2010 and 1-2 February 2011 events has been explored by SPC Hourly Mesoscale Analysis Archive images of 700-500hPa mean RH and 700-500hPa layer – average omega.

Previous work and current understanding must to cited and represent correctly.

RE: Quote marks, as proper acknowledgement of literature references, have placed around Martin 1998 source used in 19 January 1995 event discussion and Kocin and Uccellini 2004 source used in manuscript Summary.

RE: Editing this manuscript, according Lynn McMurdie, Ph.D. Editor – AMS Weather and Forecasting has indeed been a learning experience!! If further editing is needed prior to recommendation for publication, PLEASE inform me!! There may be other standards that need to be met?! I am ready to be “refreshed” and learn more!!

I plan to use the standards that you have taught while editing my final AMS 28th Conference on Weather Analysis and Forecasting manuscript.

THANKS again, Ralph Wade Johnson – Author

1

1 **Investigating synoptic, mesoscale features six events**

2

3 Ralph Wade Johnson*

4

5 Department of Soil, Environmental and Atmospheric Sciences

6 302 Anheuser Busch Natural Resources Building

7 University of Missouri

8 Columbia MO 65211 USA

9

10 Submitted to:

11 Weather and Forecasting

12 December 2016

13

14 *Corresponding Author: Ralph Wade Johnson

15 Department of Soil, Environmental and Atmospheric Sciences, 302 Anheuser Busch

16 Natural Resources Building, Columbia MO 65211 rwjb75@mail.missouri.edu

17

18 ABSTRACT

19 This investigative study evaluates meteorological phenomena that played roles in

20 the heavy snowfall during six selected events – four mainly central United States and

21 two Southeast, Middle Atlantic, Northeast/New England. The physical and dynamical
22 processes emphasized for their respective roles include 700hPa vertical motions or
23 omega (ω) $\geq -0.60 \text{ pa s}^{-1}$, Cyclogenesis and cyclone tracks, Jet streak-induced
24 ageostrophic circulation, 850hPa temperature gradients, 850hPa warm air advection
25 (WAA), latent heat release (LHR), 850hPa cold air advection, 850hPa frontogenesis,
26 850hPa low level jet (LLJ), 700hPa relative humidity (RH) $\geq 80\%$, 850hPa meridional
27 wind, 850hPa zonal wind, 700hPa v-component of storm motion, 700hPa heights and
28 zonal winds, 300hPa heights and zonal winds.

29 This research compares and analyzes 700hPa omega, pressure at mean sea level,
30 850hPa temperature along with other variables mentioned above that made
31 contributions to the event physical and dynamical processes. The focus is on how the
32 physical and dynamical processes individually or collectively contributed to produce the
33 heavy snowfall that occurred during these events. This study compares the role of latent
34 and sensible heat fluxes over ocean and land in cyclone development. In addition, while
35 development of the heavy snow event represents complex interaction among many
36 physical processes that occur on the synoptic and mesoscales, ENSO and
37 teleconnections provide an important framework within which the winter storm evolves.

38

39 1. Introduction

40 The six events included in this investigative study are 30-31 January 1982, 14-
41 15 December 1987, 19 January 1995, 1-2 February 2011, 13-14 March 1993 and
42 25-26 December 2010. The events were compared according to the region(s) that

43 they impacted and the physical and/or dynamical processes that were analyzed
44 and/or documented during periods of heaviest snowfall. The 30-31 January 1982
45 event was compared with 14-15 December 1987, since they both produced heavy
46 snowfall over the central United States, in particular from southwest Missouri to
47 northeast Illinois/southeast Wisconsin/northern Indiana. The 19 January 1995 event
48 was compared with 1-2 February 2011, since they both produced a similar pattern
49 of heavy snowfall from southwest Missouri to northeast Missouri/southeast Iowa,
50 central/northeast Illinois to southeast Wisconsin. The 13-14 March 1993 event was
51 compared with 25-26 December 2010, since they both produced heavy snowfall
52 over parts of the southeast United States, the Middle Atlantic States, northeast and
53 New England.

54 The main focus of this research is to show that heavy snow events, regardless of
55 development region, are result of a "manifestation of a complex interaction" (Kocin
56 and Uccellini 2004 Volume I) or contribution(s) of among many synoptic and
57 mesoscale phenomena. The variables and physical/dynamical processes include
58 700hPa maximum negative omega, 700hPa RH \geq 80%, pressure at mean sea level,
59 850hPa temperature (gradients), 850hPa meridional wind, 850hPa zonal wind,
60 700hPa v-component of storm motion. Emphasis is on how they contributed to
61 produce latent heat release (LHR), 850hPa frontogenesis, 850hPa warm and cold
62 advection, cyclogenesis and the event regional distribution of snowfall. Also,
63 700hPa heights and zonal winds, 300hPa heights and zonal winds are included to
64 diagnose the contribution of this vertical plane to the snowfall during the selected six
65 events.

66 A goal of this research is to show that latent and sensible heat fluxes at surface
67 “complex interact” or contribute with the variables, synoptic and mesoscale
68 processes mentioned above during cyclone development associated with heavy
69 snow during each of the six events. However, the role of latent and sensible heat
70 fluxes in cyclone development associated with heavy continental snows is less
71 notable than one associated with Middle Atlantic and Northeast events. Another
72 goal is to provide an indication of latent heat release by showing 700hPa relative
73 humidity and 700hPa omega images during periods of maximum snow
74 accumulation for each of the six events.

75 (Kocin and Uccellini 2004 Volume I) discuss the large-scale circulation patterns,
76 (variables, synoptic and mesoscale processes) that contribute to episodes of Middle
77 Atlantic and Northeast heavy snow events. However, the central purpose or focus of
78 this research analyzes ENSO, teleconnections, variables, synoptic and mesoscale
79 processes that contribute to episodes of central United States heavy snow events.
80 This objective is accomplished in the figure presentation section.

81

82 2. Data sources and analysis methods

83 a. Data

84 **NCEP North American Regional Reanalysis (NARR) 3-Hourly Composite**
85 **Mean Archives**¹ were used to download pressure at mean sea level, 700hPa
86 omega and categorical snow at surface panels representative of dates and hours
87 when most intense snowfall occurred during selected cases, in particular those 1

88 January 1979 through 31 July 2015. **NCEP NARR 3-Hourly Composite Mean**
89 **Archives** were also used to download 700hPa omega (maximum), pressure at
90 mean sea level, 850hPa temperature, categorical snow at surface, 850hPa
91 meridional wind, 850hPa zonal wind, 700hPa v-component of storm motion for
92 selected events listed above. Since it was unavailable from NCEP NARR 3-Hourly,
93 700hPa RH \geq 80% data was downloaded from **NCEP NCAR 6-Hourly composite**
94 **mean archives**³

95 Additional NCEP 3-Hourly Composite Mean Archive synoptic and mesoscale
96 phenomena variables are downloaded for events that impacted more than one
97 region during their development and maturity. These include the 700hPa heights
98 and zonal winds and 300hPa heights and zonal winds. For 13-14 March 1993,
99 event latent, sensible heat fluxes at surface and event pressure at mean sea level
100 at six hour intervals during most intense cyclogenesis are included.

101

102 b. Analysis

103 Analysis are done for NCEP NARR 3-Hourly Composite Mean 700hPa
104 maximum negative omega, pressure at mean sea level, 850hPa temperatures,
105 850hPa meridional and zonal wind, 700hPa v-component of storm motion,
106 sensible and latent heat fluxes at surface, 700hPa and 300hPa heights, 700hPa
107 and 300hPa zonal winds to determine how they contributed to cyclogenesis, jet
108 streak-induced ageostrophic circulation, latent heat release (LHR), 850hPa warm
109 air and cold air advection, 850hPa temperature gradients, 850hPa frontogenesis,

110 850hPa low level jet (LLJ) in the selected events. NCEP NARR 3-Hourly
111 Composite Mean 900hPa analyses (lower troposphere closed circulation) and
112 600hPa analyses (middle troposphere trough) have been used to diagnose LHR
113 during each of the six events. **The Storm Prediction Center² (SPC)** uses
114 850hPa frontogenesis, 850hPa temperature advection and differential vorticity
115 advection in their analyses. As mentioned above, comparison of the above
116 parameters as indicators of the physical and dynamical processes has been
117 done by regions impacted by the heavy snowfall during the winter storms. The
118 selection of dynamical and physical processes has been in accord with Kocin
119 and Uccellini Volume II (2004) analyses of thirty-two selected major snowstorms.

120 Relevant higher resolution image patterns from the SPC Hourly Mesoscale
121 Analysis Archive are included to provide emphasis of the contribution of these
122 parameters to snowfall during the selected events. These are: Group (1) is
123 700hPa height, wind, temperature, 700-500hPa mean RH (fill). Group (2) is
124 300hPa isotachs (fill), height and ageostrophic wind and 700-500hPa layer-
125 average omega (magenta – up). Group (3) is 850hPa Pettersen frontogenesis
126 (fill), 850hPa height, temperature and wind. Group (4) is 850hPa temperature
127 advection (fill), 850hPa height, temperature and wind. Group (5) is 850hPa
128 convergence (red), 250-850hPa differential divergence (fill), 250hPa divergence
129 (purple). Group (6) is Surface temperature, dewpoint and pressure mean sea
130 level. Group (7) Near freezing surface wet bulb temperature, sea level pressure
131 and wind. The SPC Hourly Mesoscale Analysis Archive for these parameters is
132 available 1800 UTC 1 February 2011, 2100 UTC 1 February 2011, 0000 UTC 2

133 February 2011. (According to surface observations, this is the 6-hour increment
134 period of maximum 1-2 February 2011 event snow accumulation.) Also, the SPC
135 Hourly Mesoscale Analysis Archive for these parameters is available 0600 UTC
136 26 December 2010, 0900 UTC 26 December 2010, 1200 UTC 26 December
137 2010. (According to surface observations, this is the 6-hour increment period of
138 maximum 25-26 December 2010 event snow accumulation.)

Commented [JRW(1)]: um

139 Other parameter images from the SPC Hourly Mesoscale Analysis Winter
140 Weather Archive that are relevant to the 1-2 February 2011 and 25-26 December
141 2010 maximum events snow accumulation are 800-750hPa EPVg (shaded) and
142 Conditional Instability which includes 850hPa frontogenesis (red), 650-500hPa
143 EPVg (shaded) and Conditional Instability which includes 700hPa frontogenesis
144 (red) and Critical Thickness – 1000-500hPa (red), 1000-700hPa (green), 1000-
145 850hPa (blue), 850-700hPa (yellow) and surface temperature 0°C (magenta).
146 According to surface observations, the 6-hour increment period of maximum 1-2
147 February 2011 event snow accumulation for 800-750hPa EPVg, 650-500hPa
148 EPVg and Critical Thickness includes 2100 UTC 1 February 2011. According to
149 surface observations, the 6-hour increment period of maximum 25-26 December
150 2010 event snow accumulation 800-750hPa EPVg, 650-500hPa EPVg and
151 Critical Thickness includes 0800 – 0900 UTC 26 December 2010.

152 Comparison of parameters, physical and dynamical processes are done by
153 region(s) in which the selected events occurred. This is shown in Tables 1, 2 and
154 3 that also include surface, 850hPa and 700-500hPa frontogenesis, [EPVg and
155 CI (850-750hPa) (650-500hPa)] used in SPC analyses. Also, NCEP NARR 3-

156 Hourly and NCEP NCAR 6-Hourly variables are included in the tables. The tables
157 depict which variables, physical and dynamical processes that are common, as
158 well as unique to the events compared and hence unite understanding of the
159 case studies. Also, this research, including tables, has been done to show
160 specific contributions for jet streak circulations, including ageostrophic, latent,
161 sensible heat fluxes (ocean, gulf and continent) and latent heat release that
162 produced heavy snowfall during each of the selected events. However, a main
163 goal of this research is not to analyze the variables, physical, dynamical
164 processes and SPC Hourly Mesoscale Analysis Archive parameters but
165 emphasize their contributions to the regional distribution of snowfall and areas of
166 heavy snow in each of the six events. Unfortunately, SPC Hourly Mesoscale
167 Analysis Archive parameters-24 hour are available 18 October 2005 to present
168 which only includes the 25-26 December 2010 and 1-2 February 2011 events.

169 ¹www.esrl.noaa.gov/psd/cgi-bin/narr/plothour.pl

170 ²www.spc.noaa.gov

171 ³www.esrl.noaa.gov/psd/data/composites/hour

172

173 **3. Synoptic and Mesoscale Analyses – Central United States**

174 **a. 30-31 January 1982 Event**

175 **i. Overview**

176 This event was chosen since it was associated with cyclogenesis that
177 produced notable rains prior to heavy snows over the middle Mississippi valley.
178 Also, extensive elevated convection was recorded during moderate/heavy
179 snowfall. The storm regional distribution of snowfall was primarily central United
180 States, including Great Lakes.

181 Moore and Blakley (1988) documented that moderate/heavy snowfall
182 accompanied by lightning and thunder occurred between 0100UTC 31 January
183 1982 and 1400UTC 31 January 1982 at Lambert Saint Louis International
184 Airport. According to Moore and Blakley (1988), surface observations for Saint
185 Louis Lambert Airport 2200-1400UTC 30-31 January 1982 indicated large
186 pressure fluctuations throughout the period with a periodicity of several hours,
187 most likely related to thunderstorm activity. Such pressure fluctuations may also
188 indicate mesoscale gravity waves during this event (Schneider 1990a). The
189 banded structure of moderate-to-heavy snowfall from east-central Missouri
190 through northeast-to-east Illinois into north-central Indiana were accompanied by
191 $700\text{hPa } \omega \leq -1.2 \text{ pa s}^{-1}$ over east-central Missouri and west central Illinois
192 (indicated Figure 1C) and possible mesoscale gravity wave activity during this
193 event. The presence of these vertical motions, heavy snow along relatively
194 narrow band north-northwest of inverted trough, and a marked warm front
195 extending across south-central Missouri-central and southern Illinois-central and
196 southern Indiana 0000-1200UTC 31 January 1982 indicate that thunder-snow
197 was elevated. Thunder-snow ~400 km north of surface cyclone over east-central

198 Arkansas at 0600UTC 31 January 1982 (Moore and Blakely 1988) is indication
199 of the presence of elevated convection during this event (Market et al. 2002).

200 **II. Analyses of variables and synoptic, mesoscale processes**

201 Figure 2 Images [A], [B], [D] show how 850hPa temperature, 850hPa
202 meridional wind and 850hPa zonal wind interacted during this event. Figure 2
203 Image [C] indicates how the 700hPa v-component of storm motion contributed
204 along with [A], [B] and [D] to produce the regional distribution of snowfall shown
205 in Figure 1 Image D.

206 Figure 2 Images [B], [C] indicate an advection role of the 850hPa low level
207 jet (LLJ) during this event. Figure 2 [A], [B], [C] indicate how the 850hPa LLJ
208 contributed along with 850hPa temperature (gradients) – [A] and v-component of
209 storm motion – [C] to produce heavy snowfall during this event. Figure 1 Images
210 B and C provide an indication of latent heat release during this event.

211 The complex interactions or contributions include 700hPa trough–ridge
212 systems [Figure 18 Image A] provide divergence and ascent (700hPa maximum
213 negative omega) [Figure 1 Image C] for cyclogenesis [shown Figure 1 Image A].
214 Jet streak circulations embedded within this trough-ridge system [indicated
215 Figure 18 Images A, B, C, D] help focus ascent patterns [Figure 1 Image C],
216 transport potential vorticity (Kocin and Uccellini 2004 Volume I – their Figure
217 7.1c) toward the developing cyclonic circulation (Figure 1 Image A), enhance
218 low-level temperature gradients, for example 850hPa [shown Figure 2 Images A
219 and B] and middle level moisture transports [shown Figure 1 Image B and Figure

220 2 Image C] that are required heavy snowfall (Kocin and Uccellini 2004 Volume
221 l).

222 Since 700hPa and 300hPa zonal winds (Figure 18 Images B and D) are
223 available, convergence and divergence, vorticity advection and the presence of
224 jet streak circulation can be diagnosed from 700hPa–300hPa vertical plane
225 geopotential height fields during this event (Figure 18 Images A and C).

226 Figure 23 [Images A, B] show the role of sensible and latent heat fluxes in
227 development of cyclones associated with heavy continental snow events is
228 somewhat less defined than those associated with middle Atlantic and northeast
229 events. However, notable contributions of latent and sensible fluxes can be seen
230 in vicinity of the cyclone [Image C] associated with this event. Also, Image [C]
231 indicates role of the “cold” anticyclone over western Minnesota during this event.

232

233 **b. 14-15 December 1987 Event**

234 **I. Overview**

235 This event was chosen because of the observed and documented presence
236 of mesoscale gravity wave interaction during the event. Again, elevated
237 convection was recorded during moderate/heavy snowfall. The storm regional
238 distribution of snowfall was primarily central United States, including Great
239 Lakes.

240 There is considerable interest for including this previously studied event
241 here. First, Moore and Lambert (1993) found EPV, CSI, convective instability
242 and elevated convection were important processes during 14-15 December
243 1987 winter storm. Second, Pokerandt et al. (1996) document that within this
244 event, a series of mesoscale gravity waves that formed and lasted for over 10
245 hours within a rapidly developing mid-latitude cyclone. According to Schneider
246 1990a, the large-amplitude mesoscale wave disturbances had a maximum
247 surface pressure perturbation of $\sim 10\text{hPa}$ and produced severe winter weather
248 including wind gusts to 30 m s^{-1} , cloud to ground lightning and much localized
249 periods of heavy snow.

250 Near the time when observed mesoscale waves had large amplitude, many
251 mesoscale surface pressure perturbations were evident in the Pokerandt et al.
252 (1996) model. When observed waves had just entered west-central Illinois
253 (0600-0800UTC 15 December 1987), their model had a wave from southwest
254 WI into northeast IL, another with amplitude $\sim 4\text{hPa}$ from east-central IA into
255 west-central IL, several others from southern MI southwest to southern MO. So,
256 0300 – 0900UTC 15 December 1987 NCEP/NARR $\omega \leq -0.90\text{ pa s}^{-1}$ (shown Figure
257 3C) fields have observational relationship to mesoscale gravity waves at mature
258 stage of this event.

259 **II. Analyses of variables and synoptic, mesoscale processes**

260 Figure 4 Images [A], [B], [D] show how 850hPa temperature, 850hPa
261 meridional wind and 850hPa zonal interacted during this event. Image [C]

262 shows how the 700hPa v-component of storm motion contributed along with [A],
263 [B] and [D] to produce the regional distribution of snowfall shown in Figure 3
264 Image D. Figure 3 Images B and C provide an indication of latent heat release
265 during this event.

266 Figure 4 Images [B], [C] an advection role of the 850hPa low level jet (LLJ)
267 during this event. Images [A], [B], [C] show how the 850hPa LLJ “complexly
268 interacted” or contributed along with 850hPa temperature (gradients) – [A] and
269 v-component of storm motion – [C] to produce heavy snowfall during this event.

270 The complex interactions or contributions include 700hPa trough-ridge
271 systems [Figure 19 Image A] that provide divergence ascent (700hPa maximum
272 negative omega) [Figure 3 Image C] for cyclogenesis [indicated Figure 3 Image
273 A]. Jet streak circulations embedded within this trough-ridge system [indicated
274 Figure 19 Images A, B, C, D] help focus ascent patterns [Figure 3 Image C],
275 transport potential vorticity (Kocin and Uccellini 2004 Volume I – their figure
276 7.1c) toward the developing cyclonic circulation [Figure 3 Image A], enhance
277 low-level temperature gradient, for example 850hPa [indicated Figure 4 Images
278 A and B] and middle level moisture transports [indicated Figure 3 Image B and
279 Figure 4 Image C] that are required for heavy snowfall (Kocin and Uccellini 2004
280 Volume I).

281 Since 700hPa and 300hPa zonal winds (Figure 19 Images B and D) are
282 available, convergence and divergence, vorticity advection and the presence of

283 jet streak circulations can be diagnosed from 700hPa – 300hPa vertical plane
284 geopotential height fields during this event (Figure 19 Images A and C).

285 Figure 24 [Images A, B] show the contributions of sensible and latent heat
286 fluxes in development of cyclones associated with heavy continental snow
287 events is somewhat less defined than those associated with middle Atlantic and
288 northeast events. However, notable contributions of latent and sensible heat
289 fluxes can be seen in vicinity of the cyclone [Image C] associated with this event.
290 Similar to middle Atlantic and northeast events, notable latent and sensible heat
291 fluxes are associated with the succeeding anticyclone over the Gulf of Mexico
292 [Images A, B].

293 Table 1 has been done to show common or unique variable,
294 physical/dynamical processes that produced the regional distribution snowfall
295 and areas of heavy snowfall during the 30-31 January 1982 and 14-15
296 December 1987 events. Since both of these events were central United States,
297 Table 1 compares variables, physical/dynamical processes documented or
298 observed/analyzed that contributed during 30-31 January 1982 that were also
299 documented or observed/analyzed during 14-15 December 1987. The
300 exceptions were 850hPa **Q** vector/isotherm fields (30-31 January 1982) and
301 mesoscale gravity wave interaction (14-15 December 1987).

302

303 **c. 19 January 1995 Event**

304 **I. Overview**

305 This event was chosen due to the “sharp” gradient of regional snowfall
306 intensity, for example, heavy southwest – central Missouri and light/very light
307 east central Missouri/west central Illinois. Again, elevated convection was
308 observed and recorded, in particular central – southwest Missouri, although
309 lesser extent than 30-31 January 1982 and 14-15 December 1987 events. The
310 storm regional distribution of snowfall is over central United States, in particular
311 middle Mississippi valley.

312 “Martin 1998 model analyses of the 19 January 1995 event found that
313 saturated regions of CSI did not appear in the simulated frontal environment,
314 suggesting it may not have been an important factor. Instead frontogenesis in the
315 presence of “across-front” differences in the effective static stability [as measured
316 in terms of equivalent potential vorticity (EPV) was found to be the circumstance
317 responsible for the intensity and dimensions of the snow band. Martin 1988
318 determined that release of convective instability in the ascending branch of the
319 thermally direct frontal circulation provided the convective component to the
320 band, manifested in cloud-to-ground lightning and occasional bursts of 5 cm h^{-1}
321 snowfall rates.” Figure 5C shows 700hPa omega did indeed interact or contribute
322 with the thermally direct frontal circulation to provide the convective components
323 that produced categorical snow at the surface.

324 The results of Martin 1998 further revealed: Ascent of warm, moist air in the
325 trowel portion of the warm-occluded structure that developed in this case was
326 shown to contribute to the heavy snowfall. Frontogenesis along the warm-frontal
327 portion of the warm-occluded structure forced the lifting of air into and through

328 the trowel. Also, it is suggested that the trowel, which was a focus of
329 frontogenesis to the northwest of the cyclone center in this case, is easily
330 identifiable given emerging visualization technologies, that is, 1998 and current
331 advances in radiosonde observations.

332 **II. Analyses of variables and synoptic, mesoscale processes**

333 Figure 6 Images [A], [B], [D] indicate how 850hPa temperature, 850hPa
334 meridional wind and 850hPa zonal wind interacted during this event. Image [C]
335 indicates how the 700hPa v-component of storm motion contributed along with
336 [A], [B] and [D] to produce the regional distribution of snowfall shown in Figure 5
337 Image D.

338 Figure 6 Images [B], [C] show the advection role of the low level jet (LLJ)
339 during this event. Images [A], [B], [C] show how the 850hPa LLJ “complexly
340 interacted” or contributed along with 850hPa temperature (gradients) – [A] and v-
341 component of storm motion – [C] to produce heavy snowfall during this event.
342 Figure 5 Images B and C provide an indication of latent heat release during this
343 event.

344 The complex interactions or contributions include 700hPa trough-ridge
345 systems [Figure 20 Image A] that provide divergence and ascent (700hPa
346 maximum negative omega) [Figure 5 Image A]. Jet streak circulations embedded
347 within this trough-ridge system [shown Figure 20 Images A, B, C, D] help focus
348 ascent patterns [Figure 5 Image C], transport potential vorticity (Kocin and
349 Uccellini 2004 Volume I – their Figure 7.1c) toward the developing cyclonic

350 circulation [Figure 5 Image A], enhance low-level temperature gradients, for
351 example 850hPa [shown Figure 6 Images A and B] and middle level moisture
352 transports [shown Figure 5 Image B and Figure 6 Image C] that are required for
353 heavy snowfall (Kocin and Uccellini 2004 Volume I).

354 Since 700hPa and 300hPa zonal winds (Figure 20 Images B and D) are
355 available, convergence and divergence, vorticity advection and the presence of
356 jet streak circulations can be diagnosed from 700hPa – 300hPa vertical plane
357 geopotential height fields during this event (Figure 20 Images A and C).

358 Figure 25 [Images A, B] show the contribution of sensible and latent heat
359 fluxes in development of cyclones associated with heavy continental snow events
360 is somewhat less defined than those associated with middle Atlantic and
361 northeast events. However, notable contributions of latent and sensible heat
362 fluxes can be seen in vicinity of the cyclone [Image C] associated with this event.

363

364 **d. 1-2 February 2011 Event**

365 **I. Overview**

366 This event was chosen for its cyclone intensity that brought a variety of
367 precipitation to the central United States; types included heavy snow – west,
368 southwest/central Missouri/east Iowa/central-northeast Illinois, southeast
369 Wisconsin, snow/ice pellets (sleet), freezing rain – east central Missouri/west
370 central Illinois, freezing rain/extensive “glazing” – central/southern Indiana. There
371 was observed and documented elevated convection, in particular

372 southwest/central Missouri (compare to 14-15 December 1987 and 19 January
373 1995), central Illinois. The regional distribution of storm snowfall was not only
374 central United States, including lakes Michigan, Superior, Huron, but lakes Erie
375 and Ontario and Northeast United States.

376 HPC surface analysis – 0000 UTC 2 February 2011, along with upper air
377 analysis indicated “comma head” region associated with a 996hPa cyclone.
378 Referring to Rauber et al. 2014 and Rosenow et al. 2014, an upper-tropospheric dry
379 air stream associated with a cyclone’s dry slot frequently intrudes over lower-level
380 Gulf of Mexico air in the comma head of strong cyclones. This creates two zones of
381 precipitation within the comma head: a northern zone characterized by deep
382 stratiform clouds and topped by “cloud-top generating” cells, and a southern zone
383 marked by elevated convection. The Rauber et al. 2014 research found that 1049
384 total lightning flashes occurred within the comma head region of the 1-2 February
385 2011 cyclone from 1850 UTC 1 February to 1104 UTC 2 February 2011, providing
386 evidence that elevated convection (see Table 2 – 1-2 February 2011 event column)
387 was dominant in the region of moderate to heavy snowfall associated with this
388 winter storm.

389 Figures 35 through 42 show relevant SPC Hourly Mesoscale Analysis Archive
390 parameters that contributed to regional maximum observed snowfall accumulation
391 during the selected time increment 1800 UTC 1 February – 0000 UTC 2 February
392 2011. These include [700-500hPa mean RH], [300hPa isotachs, ageostrophic wind,
393 700-500hPa layer-average omega], [850hPa Pettersen frontogenesis], [850hPa
394 temperature advection], [850hPa convergence, 250-850hPa differential divergence,

395 250hPa divergence], [surface temperature, dewpoint], [near freezing surface wet
396 bulb temperature], [800-750hPa EPVg-conditional instability], [650-500hPa EPVg-
397 conditional instability] and [critical thickness].

398 **II. Analyses of variables and synoptic, mesoscale processes**

399 Figure 8 Images [A], [B], [D] indicate how 850hPa temperature, 850hPa
400 meridional wind and 850hPa zonal interacted during this event. Image [C] shows
401 how 700hPa v-component of storm motion contributed along with [A], [B] and [D] to
402 produce the regional distribution of snowfall shown Figure 7 Image [D].

403 Figure 8 Images [B], [C] indicate an advection role of the 850hPa low level jet
404 (LLJ) during this event. Images [A], [B], [C] show how the 850hPa LLJ contributed
405 along with 850hPa temperature (gradients) – [A] and v-component of storm motion
406 – [C] to produce heavy snowfall during this event. Figures 35 and 36 provide an
407 indication of latent heat release during this event.

408 The complex interactions or contributions include 700hPa trough-ridge systems
409 [Figure 9 Image A] that provide divergence and ascent (700hPa maximum negative
410 omega) [Figure 7 Image C] required for cyclogenesis [shown Figure 7 Image A]. Jet
411 streak circulations embedded within this trough-ridge system [shown Figure 9
412 Images A, B, C, D] help focus ascent patterns [Figure 7 Image C], transport
413 potential vorticity (Kocin and Uccellini 2004 Volume I-their Figure 7.1 c) toward the
414 developing cyclonic circulation [Figure 7 Image A], enhance low-level temperature
415 gradients, for example 850hPa [shown Figure 8 Images A and B] and middle level
416 moisture transports [shown Figure 7 Image B and Figure 8 Image C] that are

417 required for heavy snowfall (Kocin and Uccellini 2004 Volume I). Since 700hPa and
418 300hPa zonal winds (Figure 9 Images B and D) are available, convergence and
419 divergence, vorticity advection and the presence of jet streak circulations can be
420 diagnosed from the 700hPa – 300hPa vertical plane geopotential height fields
421 during this event (Figure 9 Images A and C).

422 Also, mesoscale processes such as 850hPa frontogenesis and LLJ [shown
423 Figure 8 Images A, D and B] contribute to enhancing the baroclinic environment for
424 cyclogenesis and focus moisture transports and ascent that enhance the snowfall
425 rate(s). Cold anticyclones (synoptic scale) generally have to be positioned to the
426 north of the developing cyclone to sustain the source of level cold air required for
427 snow (Kocin and Uccellini 2004 Volume I). For the 1-2 February 2011 event, this is
428 shown in Figure 7 Image A, as a (105000 Pa High) over west North Dakota,
429 northwest South Dakota, northeast Wyoming and east Montana.

430 Figure 26 [Images A, B] show the contribution of sensible and latent heat fluxes
431 in development of cyclones associated with heavy continental snow events is
432 somewhat less defined than those associated with middle Atlantic and northeast
433 events. However, notable contributions of latent and sensible heat fluxes can be
434 seen in vicinity of the cyclone [Image C] associated with this event, in particular
435 Lakes Superior, Michigan and Huron.

436 Table 2 was done to show variables, physical/dynamical processes common
437 and unique to 19 January 1995 and 1-2 February 2011 events. Since mesoscale
438 gravity wave interaction was only indicated from surface analysis during 1-2

439 February 2011, the only unique documented physical/dynamical process was
440 cyclonic advection of θ_e (19 January 1995).

441

442 **4. Synoptic and Mesoscale Analyses – middle Atlantic and northeast**
443 **US events**

444 **a. 13-14 March 1993**

445 **I. Overview**

446 This event was chosen for the contribution that latent, sensible heat fluxes
447 and latent heat release played in cyclone development during various stages of
448 the storm. Again, the extent and intensity of elevated convection, respect to
449 snowfall, was of considerable interest (compare to other selected events). The
450 storm regional snowfall distribution (contrast to other selected events) included
451 not only lakes Superior, Michigan and Huron, but Erie and Ontario, sections of
452 the southeast United States, east Tennessee – central Alabama, the
453 Appalachians, Middle Atlantic and Northeast United States, plus sections of New
454 England.

455 Reference Kocin and Uccellini 2004 Volume II, the 850hPa isotherm pattern
456 had taken on the classic “S” on 13 March, as warm-air advection (WAA) was
457 concentrated north and east of the surface low and cold-air advection (CAA)
458 occurred to the south and west. These areas of WAA and CAA occur over a
459 region of “strong” upward vertical motion ($\omega \leq -1.3$) from southeast Virginia to
460 southern New England [indicated Figure 10C] and correspond to heavy snow
461 and ice pellets over this same region during the same time period [indicated

462 Figure 10D]. As indicated Figure 10A, intense cyclogenesis played an important
463 role in the 700hPa $\omega \leq -1.3$ region depicted by Figure 10C.

464 Kocin et al. 1995 provide additional information that indicates the interaction
465 of parameters listed in Table 3 and their role during the 13-14 March 1993 event:
466 The 850hPa analysis at 1200UTC 13 March shows that a “massive circulation”
467 developed in the lower troposphere over the southern United States,
468 accompanied by an increase in temperature gradients along the baroclinic zone
469 in northern Florida, eastern Georgia and the Carolinas, plus an increase of
470 observed wind speeds (for those stations still reporting winds) surrounding the
471 cyclone. In addition, the 850hPa low center became collocated with the 0°C
472 isotherm with strong WAA located northeast of the center and strong CAA to the
473 south. The 0°C to -2°C isotherm corresponds closely to the rain/snow line, with
474 the greatest manually digitized radar video integrator and processor (VIP) echo
475 levels found in the southeasterly 850hPa flow from the Atlantic Ocean to North
476 Carolina and into the Middle Atlantic States as moisture-laden air in the warm
477 sector of the cyclone ascends over the colder air west of the coast-line.

478 . **Analyses of variables and synoptic, mesoscale processes**

479 Figure 11 Images [A], [B], [D] indicate how 850hPa temperature, 850hPa
480 meridional wind and 850hPa zonal wind interacted during this event. Image [C]
481 shows how the 700hPa v-component of storm motion contributed along with [A],
482 [B] and [D] to produce the regional distribution of snowfall shown in Figure 10
483 Image D.

484 Figure 11 Images [B], [C] an advection role of the low level jet (LLJ) during
485 this event. Images [A], [B], [C] show how the 850hPa low level jet (LLJ)
486 “complexly interacted” or contributed with 850hPa temperature (gradients) – [A]
487 and v-component of storm motion – [C] to produce heavy snowfall during this
488 event. Figure 10 Images B and C provide an indication of latent heat release
489 during this event.

490 Sensible and latent heat fluxes over the Gulf of Mexico and Atlantic Ocean
491 vicinity of the developing cyclone act to contribute to the cyclone’s rapid
492 intensification (Kocin and Uccellini 2004 Volume I). Figures 12, 13, 14, 15
493 [Images A, B and C 1200 – 1800 UTC 13 March 1993, 1800 UTC 13 March -
494 0000 UTC 14 March 1993, 0000 – 0600 UTC 14 March 1993, 0600 - 1200 UTC
495 14 March 1993] clearly show how these \leq meso- α scale phenomena contributed
496 to the cyclone’s rapid intensification. This intensification was associated with the
497 heavy snowfall over the Appalachians and western New York during this event.

498 The complex interactions or contributions include 700hPa trough-ridge
499 systems [Figure 21 Image A] that provide divergence and ascent (700hPa
500 maximum negative omega) [Figure 10 Image C] for cyclogenesis [shown Figure
501 10 Image A]. Jet streak circulations embedded within this trough-ridge system
502 [shown Figure 21 Images A, B, C, D] help focus ascent patterns [Figure 10
503 Image C], transport potential vorticity (Kocin and Uccellini 2004 Volume I – their
504 Figure 7.1c) toward the developing cyclonic circulation [Figure 10 Image A],
505 enhance low-level temperature gradients, for example 850hPa [shown Figure 11
506 Images A and B] and middle level moisture transports [indicated Figure 10 Image

507 B and Figure 11 Image C] that are required for heavy snowfall (Kocin and
508 Uccellini 2004 Volume I).

509 Since 700hPa and 300hPa zonal winds (Figure 21 Images B and D) are
510 available, convergence and divergence, vorticity advection and the presence of
511 jet streak circulations can be diagnosed from 700hPa-300hPa vertical plane
512 geopotential height fields during this event (Figure 21 Images A and C).

513 II. Latent Heat Release – real time

514 The transition from a closed circulation (1200 – 1800 UTC 13 March 1993) at
515 900hPa (Figure 28 Image A) to a trough (1200 – 1800 UTC 13 March 1993) at
516 600hPa (Figure 28 Image B) is a synoptic-scale process that can possibly result
517 in latent heat release and development of (1200 – 1800 UTC 13 March 1993)
518 cyclone (Figure 28 Image C). It is the intent of Figure 28 Images A, B, C and
519 reference Kocin and Uccellini (2004) Volume I to provide an indication of latent
520 heat release during cyclone development (1200 – 1800 UTC 13 March 1993).

521 The transition from a closed circulation (1800 UTC 13 March – 0000 UTC 14
522 March 1993) at 900hPa (Figure 29 Image A) to trough (1800 UTC 13 March –
523 0000 UTC 14 March 1993) at 600hPa (Figure 29 Image B) is a synoptic-scale
524 process that can possibly result in latent heat release and development of (1800
525 UTC 13 March – 0000 UTC 14 March 1993) cyclone (Figure 29 Image C). It is
526 the intent of Figure 29 Images A, B, C and reference Kocin and Uccellini (2004)
527 Volume I to provide an indication of latent heat release during cyclone
528 development (1800 UTC 13 March – 0000 UTC 14 March 1993).

529 The transition from a closed circulation (0000 – 0600 UTC 14 March 1993) at
530 900hPa (Figure 30 Image A) to trough (0000 – 0600 UTC 14 March 1993) at
531 600hPa (Figure 30 Image B) is a synoptic-scale process that can possibly result
532 in latent heat release and subsequent development of (0000 – 0600 UTC 14
533 March 1993) cyclone (Figure 30 Image C). It is the intent of Figure 30 Images A,
534 B, C and reference Kocin and Uccellini (2004) Volume I to provide an indication
535 of latent release during cyclone development (0000 – 0600 UTC 14 March 1993).

536 The transition from a closed circulation (0600 – 1200 UTC 14 March 1993)
537 at 900hPa (Figure 31 Image A) to trough (0600 – 1200 UTC 14 March 1993) at
538 600hPa (Figure 31 Image B) is a synoptic-scale process that can possibly result
539 in latent heat release and subsequent development of (0600 – 1200 UTC 14
540 March 1993) cyclone (Figure 31 Image C). It is the intent of Figure 31 Images A,
541 B, C and reference Kocin and Uccellini (2004) Volume I to provide an indication
542 latent heat release during cyclone development (0600 – 1200 UTC 14 March
543 1993). Although not high resolution patterns, Figure 10 Image B (700hPa RH
544 $\geq 80\%$) and Image C (700hPa $\Omega \leq -1.3 \text{ pa s}^{-1}$) are can be considered as
545 indicators of latent heat release during this event.

546

547 **b. 25 – 26 December 2010**

548 **I. Overview**

549 Also, this event was chosen for the role that latent, sensible heat fluxes and
550 latent heat release played in storm cyclone development off the middle Atlantic

551 and Northeast United States coasts. However, contrast to 13-14 March 1993
552 event, the minimum pressure at mean sea level is about 13hPa higher and the
553 latent, sensible heat fluxes were about half the magnitude. Again, elevated
554 convection was of interest during this event, although to a lesser extent than 13-
555 14 March 1993. The storm regional distribution of snowfall is of interest, as east
556 central Missouri, northeast/east Illinois, north Alabama, middle/east Tennessee,
557 west North Carolina, Virginia, Middle Atlantic/Northeast states and New England
558 received notable accumulations.

559 Figures 43 through 50 show relevant SPC Hourly Mesoscale Analysis
560 Archive parameters that contributed to the regional maximum snowfall observed
561 during the selected time increment 0600 – 1200 UTC 26 December 2010. These
562 include [700-500hPa mean RH], [300hPa isotachs, ageostrophic wind, 700-
563 500hPa layer- average omega], [850hPa Pettersen frontogenesis], [850hPa
564 temperature advection], [850hPa convergence, 250-850hPa differential
565 divergence, 250hPa divergence], [surface temperature, dewpoint], [near freezing
566 surface wet bulb temperature], [800-750hPa EPVg-conditional instability], [650-
567 500hPa EPVg-conditional instability] and [critical thickness].

568 **II. Analyses of variables and synoptic, mesoscale** 569 **processes**

570 Figure 17 Images [A], [B], [D] indicate how 850hPa temperature, 850hpa
571 meridional wind and 850hPa zonal wind interacted during this event. Image [C]
572 shows how the 700hPa v-component of storm motion contributed along with [A],

573 [B] and [D] to produce the regional distribution of snowfall shown in Figure 16
574 Image D.

575 Figure 17 Images [B], [C] indicates an advection role of the 850hPa low level
576 jet (LLJ) during this event. Images [A], [B], [C] show how the 850hPa LLJ
577 contributed with 850hPa temperature (gradients) – [A] and v-component of storm
578 motion – [C] to produce heavy snowfall during this event. Figures 43 and 44 are
579 synoptic, mesoscale indicators of latent heat release.

580 The complex interactions or contributions include 700hPa trough-ridge
581 systems [Figure 22 Image A] that provide divergence and ascent (700hPa
582 maximum negative omega) [Figure 16 Image C] for cyclogenesis [shown Figure
583 16 Image A]. Jet streak circulations embedded within this trough-ridge system
584 [shown Figure 22 Images A, B, C, D] help focus ascent patterns [Figure 16
585 Image C], transport potential vorticity (Kocin and Uccellini 2004 Volume I – their
586 Figure 7.1c) toward the developing cyclonic circulation [Figure 16 Image A],
587 enhance low-level temperature gradients, for example 850hPa [indicated Figure
588 17 Images A and B] and middle level moisture transports [shown Figure 16
589 Image B and Figure 17 Image C] that are required for heavy snowfall (Kocin and
590 Uccellini 2004 Volume I).

591 Since 700hPa and 300hPa zonal winds (Figure 22 Images B and D) are
592 available, convergence and divergence, vorticity advection and the presence of
593 jet streak circulations can be diagnosed from 700hPa-300hPa vertical plane
594 geopotential height fields during this event (Figure 22 Images A and C).

595 Figure 27 indicates the role of sensible and latent heat fluxes similar to 13-14
596 March 1993 where such meso α scale phenomena contributed to the cyclone's
597 intensification during this event. Although only about half the intensity, the 25-26
598 December 2010 sensible and latent heat fluxes [Images A, B] are located vicinity
599 and southwest of the event cyclone over the Atlantic Ocean and Gulf of Mexico
600 [Image C].

601 Table 3 was done to show variables, physical/dynamical processes common
602 and unique to 13-14 March 1993 and 25-26 December 2010 events. Although
603 both these storms were primarily Middle Atlantic and Northeast United States
604 coasts, there were variables, physical/dynamical processes unique to each.
605 These are differential positive vorticity advection (700-450hPa), EPVg and CI
606 (850hPa-750hPa) (650-500hPa) (25-26 December 2010) and Isentropic Potential
607 Vorticity, Potential Vorticity Advection into cyclone center (13-14 March 1993).

608 5. Summary

609 This research has analyzed and compared six major heavy snow events. The
610 four from the central United States are 30-31 January 1982, 14-15 December
611 1987, 19 January 1995 and 1-2 February 2011. The other two are 13-14 March
612 1993 and 25-26 December 2010 which impacted parts of the Southeast, Middle
613 Atlantic and Northeast United States regions. Although the events were analyzed
614 individually, they were compared 30-31 January 1982 – 14-15 December 1987, 19
615 January 1995 – 1-2 February 2011 and 13-14 March 1993 and 25-26 December
616 2010 (Tables 1, 2, 3), according to the regions impacted by heavy snowfall.



617 Analysis of maximum negative 700hPa omega areas, 700hPa RH \geq 80% areas,
618 minimum pressure at mean sea level areas, regional categorical snow at surface,
619 850hPa temperature (gradient) areas, 850hPa meridional and zonal wind areas,
620 700hPa v-component of storm motion areas for all six events. Reference Kocin
621 and Uccellini (2004) Volume 1, this research has shown that a major winter storm,
622 regardless of region, is “manifestation” of a complex interaction or contributions
623 among variables that indicate several physical and/or dynamical processes, which
624 occur on the synoptic to mesoscales. These meteorological phenomena are: 1)
625 Upper-level trough-ridge systems provide divergence and ascent required for
626 cyclogenesis. 2) Jet streaks embedded within this trough-ridge system help focus
627 the ascent patterns, and enhance low-level temperature gradients and moisture
628 transports that are required for heavy snowfall (1-2 February 2011). 3) “Cold”
629 anticyclones generally have to be positioned to the north or northwest of the
630 developing cyclone to sustain the source of low-level arctic or polar continental air
631 required for heavy snow (1-2 February 2011).

632 4) Referring to Kocin and Uccellini (2004) Volume I, surface cyclogenesis
633 associated with Northeast snowstorms, for example 13-14 March 1993, involves
634 either a primary low pressure center that develops near the Gulf of Mexico or a
635 secondary low pressure that develops along the Southeast or middle Atlantic coast
636 and tracks north/northeast along to approximately 200 kilometers offshore (Figure
637 12, 13, 14, 15 - Image C). These cyclone systems encompass a wide range of
638 processes throughout the depth of the troposphere that promote interactions of
639 relatively warm and cold air, in particular 850hPa (Figure 11 Images A, B, D),

640 entrain large amounts of water vapor into regions of precipitation, in particular
641 700hPa (Figure 10 Image B), organize, focus and enhance ascent, in particular
642 700hPa (Figure 10 Image C). All of which are necessary for the production of
643 heavy snow during this event.

644 5) "The evolution of the cyclones that produce these snowstorms is linked to
645 upper level trough-ridge and embedded jet streak patterns that evolve in a manner
646 consistent with baroclinic instabilities and self-development concept(s) (Kocin and
647 Uccellini 2004 Volume I). Self-development depends on the following conditions
648 that have been analyzed for the selected events of this study: a) the existence of
649 an upper level trough-ridge system and jet streaks focus on the divergence aloft, a
650 necessary condition for maximizing mass divergence and ascent immediately
651 downstream of the developing surface low; b) an asymmetrical distribution of
652 clouds and precipitation to focus latent heat release and associated dynamic
653 feedbacks on the downstream ridge and polar jet streak, both factors that can
654 enhance the middle troposphere divergence north and east of the storm center; c)
655 warming is due to an enhanced low level jet and warm air advection pattern
656 immediately north and east of the developing coastal or continental cyclone." The
657 concept accounts for the adiabatic, quasi-geostrophic framework that has been
658 applied to cyclogenesis (Holton and Hakim 2013, chapter 6) and also for the
659 various interactions among dynamical and diabatic processes indicated for each of
660 the selected events analyzed.

661 6) The influence of curvature effects in minimizing the contribution of jet
662 streaks to upper-level ageostrophic winds and divergence, and their associated

663 vertical motion fields, is discussed in studies by Kocin et al. (1986), Uccellini and
664 Kocin (1987), Moore and Vanknowe (1992) and Loughe et al. (1995). These
665 studies indicate that curvature complicates the simple two-dimensional
666 relationship(s) (as shown by Kocin and Uccellini 2004 Volume I – their Figure 7.1b)
667 between the ageostrophic wind field associated with jet streaks and divergence.
668 Diabatic processes especially those related to latent heat release, can also
669 enhance the vertical motions associated with jet streak circulations (Uccellini et al.
670 1987). Despite the complications introduced by curvature and diabatic processes,
671 Loughe et al. (1995) demonstrates that these transverse circulations make a
672 significant contribution to the divergence aloft and resultant vertical motion patterns
673 in the entrance and exit region of the jet streak.

674 Mesoscale ($\leq \alpha$) processes such as 850hPa frontogenesis, low level jet (LLJ)
675 contribute to enhancing the baroclinic environment for cyclogenesis and focus the
676 middle troposphere moisture transports and ascent (maximum negative omega)
677 that enhance snowfall rates (30-31 January 1982, 14-15 December 1987, 19
678 January 1995, 1-2 February 2011, 13-14 March 1993 and 25-26 December 2010
679 events). Sensible and latent heat fluxes over the Gulf of Mexico and Atlantic
680 Ocean (13-14 March 1993 event) and latent heat release (LHR) within the
681 developing cyclone (30-31 January 1982, 14-15 December 1987, 19 January
682 1995, 1-2 February 2011, 13-14 March 1993 and 25-26 December 2010 events) all
683 act to contribute to the cyclone's "rapid" intensification. When all these physical
684 and/or dynamical processes are combined during cyclogenesis in such a manner
685 to maximize the low/middle troposphere thermal advections and moisture

686 transports, enhance ascents (maximum negative omega), yet still maintain a deep
687 enough layer of (surface to 850hPa) $\leq 0^{\circ}\text{C}$, heavy snow will, likely, be the outcome,
688 regardless of event region. However, these processes do not indicate a specific
689 contribution for LHR in the selected event cyclogenesis.

690 **6. Conclusions**

691 The selected case results further indicate the deepening rates of extratropical
692 cyclones are related to “complex interactions” (Kocin and Uccellini 2004 Volume I)
693 or contributions between thermodynamic and dynamic processes which are
694 dependent on the horizontal and vertical distributions of the pressure gradient
695 force especially as it relates to the transition from a closed circulation to a trough
696 between 900 and 600hPa and subsequent latent heat release. Again, referring to
697 Kocin and Uccellini (2004) Volume I, within the transition layer between a closed
698 circulation in the lower troposphere and trough aloft, the release of latent heat
699 poleward and east the developing cyclone would be especially important for
700 enhancing the parcel accelerations, divergent airflow (shown in Figures 28 – 36
701 Image B), surface pressure tendency and associated “rapid” development of the
702 cyclone (shown in Figures 28 – 36, in particular 28 – 31, Image C).

703 This study provides evidence of how latent heat release is involved in storm
704 cyclogenesis during each of the 25-26 December 2010 and 1-2 February 2011
705 events. For the other events, although not high resolution, NCEP/NARR images of
706 700hPa RH and 700hPa omega provide an indication latent release. For the 13-14
707 March 1993 event, air parcels ascending from the lower troposphere to the middle

708 troposphere, for example 900hPa to 600hPa, can possibly provide an indication of
709 latent heat release.

710 This study identifies a possible “gap” in scientific knowledge between heavy
711 rain and heavy snow events. The use of SPC Hourly Mesoscale Analysis Archive
712 parameters to diagnose the 25-26 December 2010 and 1-2 February 2011 events
713 partially fills this “gap”, in particular 850hPa convergence, 250-850hPa divergence
714 and 250hPa divergence.

715 A novel result of this study is that it shows large-scale circulation pattern(s)
716 which includes ENSO and teleconnections, (variables, synoptic and mesoscale
717 processes) contribute to episodes of regional snowfall distribution and areas of
718 heavy snow during six selected events. Although Kocin and Uccellini (2004)
719 Volume I schematically show how synoptic and mesoscale processes, including
720 LHR (their Figure 8.1 Images A and B) contribute to heavy snowfall along the
721 Northeast urban corridor, this research has shown that such processes, including
722 LHR, can contribute to heavy snowfall over the central United States. It is through
723 understanding the large-scale circulation pattern(s), (variables, synoptic and
724 mesoscale processes) contributing to episodes of central United States winter
725 storms that further advances in the prediction of these events can be made.

726 Danard (1964) recognized that the inability of the first numerical models to
727 accurately predict cyclogenesis was partially due to the neglect of latent heat
728 release. He found that it was necessary to include latent heat release in model
729 simulations to account for the distribution and magnitude of the vertical motion or

730 omega patterns during cyclogenesis and its observed deepening rates.
731 Krishnamurti's (1968) application of the quasi-geostrophic omega equation to the
732 life cycle of a rapidly developing cyclone demonstrates that latent heat release is a
733 major contributor to vertical motions or omega. Throughout this research study,
734 focus has been on maximum negative 700hPa omega patterns, their contribution
735 to intense cyclogenesis due to latent heat release (lower level closed circulation to
736 middle level trough) and other physical/dynamical processes, using NARR variable
737 archives. Although Kocin and Uccellini (2004) Volume I acknowledges that
738 assessing the relative importance of sensible and latent heat processes is difficult,
739 if not counterproductive, an objective of this research is to encourage NOAA/NWS
740 forecasters that being more aware of the contributions of latent heat release and
741 the other synoptic to mesoscale physical processes could definitely improve heavy
742 snowfall forecasts which are dependent on the large-scale circulation pattern(s).

743 Another important goal of this research is to focus as much on the synoptic
744 and mesoscale physical processes, including LHR, as on the forecast parameter
745 or variable. This emphasis is likely to increase the confidence of snowfall amount
746 forecast(s) associated with a major winter storm. Study has reached this goal
747 through presentation analyses, including tables, for each of the six events.

748 Uccellini et al. 1987 use the phrase "full physics" to refer to model simulation
749 that includes planetary boundary layer or sensible, latent heat fluxes and latent
750 heat release. This research has shown that both latent, sensible heat fluxes at
751 surface and latent heat release (lower to middle levels of troposphere) "complex
752 interact" (Kocin and Uccellini 2004 Volume I), "synergistic interact" (Uccellini et al

753 1987) or contributed along with other variables synoptic and mesoscale processes
754 to provide a more “realistic” rate of cyclone development that is prerequisite for
755 accurate model prediction of the storm regional snowfall distribution and heavy
756 snow areas.

757 While the large-scale circulation (ENSO and teleconnections) which provides
758 an important framework on which each of the six events evolve is unique for each
759 event, there are some common patterns. The ENSO patterns are moderate La
760 Nina for 25-26 December 2010 and 1-2 February 2011 events, neutral conditions
761 for 13-14 March 1993 and 30-31 January 1982, weak to moderate El Nino for 19
762 January 1995 and 14-15 December 1987 events. The teleconnection patterns are
763 weak negative AO for 19 January 1995, 30-31 January 1982 and 14-15 December
764 1987 events. However, 13-14 March 1993, both AO and NAO were weak positive.
765 For 1-2 February 2011, January 2011 moderate negative AO became moderate
766 positive February 2011 AO. Reflecting 25-26 December 2010, AO was strong
767 negative and NAO was moderate negative. So, central purpose or theme that
768 unites each of the six cases is the heavy snow that developed during these events
769 was a “manifestation of a complex interaction” or contribution among the many or
770 several physical processes that occur on the synoptic and mesoscales. This has
771 been shown by presentation analyses throughout this study.

772

773

REFERENCES

- 774 Danard, M.B., 1964: On the influence of released latent heat on cyclone development.
775 *J. Appl. Meteor.* **3**, 27-37.
- 776 Holton, J.R. and G.J Hakim, 2013: *An Introduction to Dynamic Meteorology*. 5th ed.
777 Academic Press, 532 pp.
- 778 Kocin, P.J., L.W. Uccellini and R.A. Petersen, 1986: Rapid evolution of a jet stream
779 circulation in a pre-convective environment. *Meteor. Atmos. Phys.*, **35**, 103-138.
- 780 _____, P.N. Schumacher, R.F. Morales Jr. and L.W. Uccellini, 1995: Overview of
781 the 12-14 March 1993 Superstorm. *Bull. Amer. Meteor. Soc.*, **76**, 165-182.
- 782 Kocin, P.J and L.W. Uccellini, 2004: Northeast Snowstorms: Volume I: Overview: *Amer.*
783 *Meteor. Soc.*, 296 pages.
- 784 _____ and _____, 2004: Northeast Snowstorms: Volume II: The Cases.
785 *Amer. Meteor. Soc.*, 821 pages.
- 786 Krishnamurti, T.N., 1968: A study of a developing wave cyclone. *Mon. Wea. Rev.*, **96**,
787 208-217.
- 788 Lough, A., C.-C. Lai and D. Keyser, 1995: A technique for diagnosing three-
789 dimensional circulations in baroclinic disturbances on limited area domains. *Mon.*
790 *Wea. Rev.*, **123**, 1476-1504.
- 791 Market, P.S., C.E. Halcomb and R.L. Ebert, 2002: A climatology of thunder-snow events
792 over the contiguous United States. *Wea. Forecasting*, **17**, 1290-1295.

- 793 Martin, J.E., 1998: The structure and evolution of a continental winter cyclone. Part II:
794 Frontal forcing of an extreme snow event. *Mon. Wea. Rev.*, **126**, 329-348.
- 795 Moore, J. T. and P. D. Blakely, 1988: The Role of Frontogenesis Forcing and
796 Conditional Symmetric instability in the Midwest Snowstorm of 30-31 January 1982.
797 *Mon. Wea. Rev.*, **116**, 2155-2171.
- 798 _____ and G.E. Vanknowe, 1992: The effect of jet-streak curvature on kinematic
799 fields. *Mon. Wea. Rev.*, **120**, 2429, 2432.
- 800 _____ and T. E. Lambert, 1993: The use of equivalent potential vorticity to
801 diagnose regions of conditional symmetric instability. *Wea. Forecasting*, **8**, 301-308.
- 802 Pokrandt, P.J., G.J. Tripoli and D.D. Houghton, 1996: Processes leading to the
803 formation of mesoscale waves in the Midwest cyclone of 15 December 1987. *Mon.*
804 *Wea. Rev.*, **124**, 2726-2752.
- 805 Rauber et al. 2014: Stability and charging characteristics of the comma head Region of
806 continental winter cyclones. *J. Atmos. Sci.*, **71**, 1559-1582.
- 807 Rosenow et al 2014: Vertical motions within generating cells and elevated convection in
808 the comma head of winter cyclones. *J. Atmos. Sci.* **71**, 1538-1558.
- 809 Schneider, R.S., 1990a: Large-amplitude mesoscale wave disturbances within the
810 intense Midwest extratropical cyclone of 15 December 1987. *Wea. Forecasting*, **5**,
811 533-558.
- 812 _____, and G. Vaughan, 2011: Occluded fronts and the occlusion process: A
813 fresh look at conventional wisdom. *Bull. Amer. Meteor. Soc.*, **92**, 443-466.

- 814 Uccellini, L.W. and P.J. Kocin, 1987: An examination of vertical circulations associated
 815 with heavy snow events along the East Coast of the United States. *Wea.*
 816 *Forecasting*, **2**, 289-308.
- 817 _____, L.W., R.A. Petersen, K.F. Brill, P.J. Kocin and J.J. Tuccillo, 1987:
 818 Synergistic interactions between an upper-level jet streak and diabatic processes
 819 that influence the development of a low-level jet and secondary coastal cyclone.
 820 *Mon. Wea. Rev.*, **115**, 2227-2261.
- 821 Weather Prediction Center (WPC) Event Review: 25-27 December 2010 Winter Storm,
 822 Eastern United States.

30–31 January 1982 Event	14–15 December 1987 Event
Variable or Parameter (documented or observation/analysis)	Variable or Parameter (documented or observation/analysis)
850hPa Low Level Jet (LLJ)	850hPa LLJ
850hPa Warm Air Advection (WAA)	850hPa WAA
850hPa Cold Air Advection (CAA)	850hPa CAA
Latent Heat Release (LHR)	Latent Heat Release (LHR)
$\omega \leq -1.2 \text{ pa s}^{-1}$ 700hPa	$\omega \leq -0.90 \text{ pa s}^{-1}$ 700hPa
Frontogenesis (Surface, 850hPa, 700- 500hPa)	Frontogenesis (Surface, 850hPa, 700- 500hPa)
CSI/MSI and EPV	CSI/MSI and EPV
Cyclone tracks and Cyclogenesis	Cyclone tracks and Cyclogenesis
Elevated Convection	Elevated Convection
700hPa RH \geq 80%	Mesoscale Gravity Wave Interaction
Jet streak-induced Ageostrophic circulation	EPVg and CI (800-750hPa) (650- 500hPa)
850hpa Temperature Gradients	Jet streak-induced Ageostrophic circulation

Enhanced IR Satellite Imagery	700hPa RH \geq 80%
850hPa Q vector/isotherm fields	Enhanced Satellite Imagery

823 Table 1. Comparison of variables most relevant to the 30-31 January 1982
824 event with variables most relevant to the 14-15 December 1987 event

19 January 1995 Event	1 - 2 February 2011 Event
Variable or Parameter (documented and/or indicated from surface/upper air analyses)	Variable or Parameter (documented and/or indicated from surface/upper air analyses)
$\omega \leq -0.90 \text{ pa s}^{-1}$ 700hPa	$\omega \leq -1.2 \text{ pa s}^{-1}$ 700hPa
TROWAL	850hPa Temperature ($^{\circ}\text{K}$)
Frontogenesis (850hPa, 700-500hPa)	850hPa Temperature Gradients ($^{\circ}\text{K}$)
Elevated Convection	TROWAL and CSI (Cross-sectional analyses), EPV
EPVg and CI (800-750hPa) (650-500hPa)	Frontogenesis (850hPa, 700-500hPa)
Latent Heat Release (LHR)	Latent Heat Release (LHR)
700hPa RH \geq 80%	700hPa RH \geq 80%
Cyclonic Advection of θ_e	Elevated Convection
Cyclone tracks and cyclogenesis (indicated from surface analyses)	Cyclone tracks and cyclogenesis (indicated from surface analyses)
Jet streak-induced Ageostrophic circulation (indicated from literature)	Jet streak-induced Ageostrophic circulation (indicated from literature)
Low Level Jet (LLJ) (indicated from literature)	Low Level Jet (LLJ) (indicated from literature)
Warm Air Advection (WAA) (indicated from literature)	Warm Air Advection (WAA) indicated from literature)
Cold Air Advection (CAA) (indicated from literature)	Cold Air Advection (CAA) (indicated from literature)
	Mesoscale Gravity Wave Interaction (indicated from surface analyses)

825 **Table 2.** Parameters relevant to 19 January 1995 event comparison to parameters
826 relevant to 1-2 February 2011 event

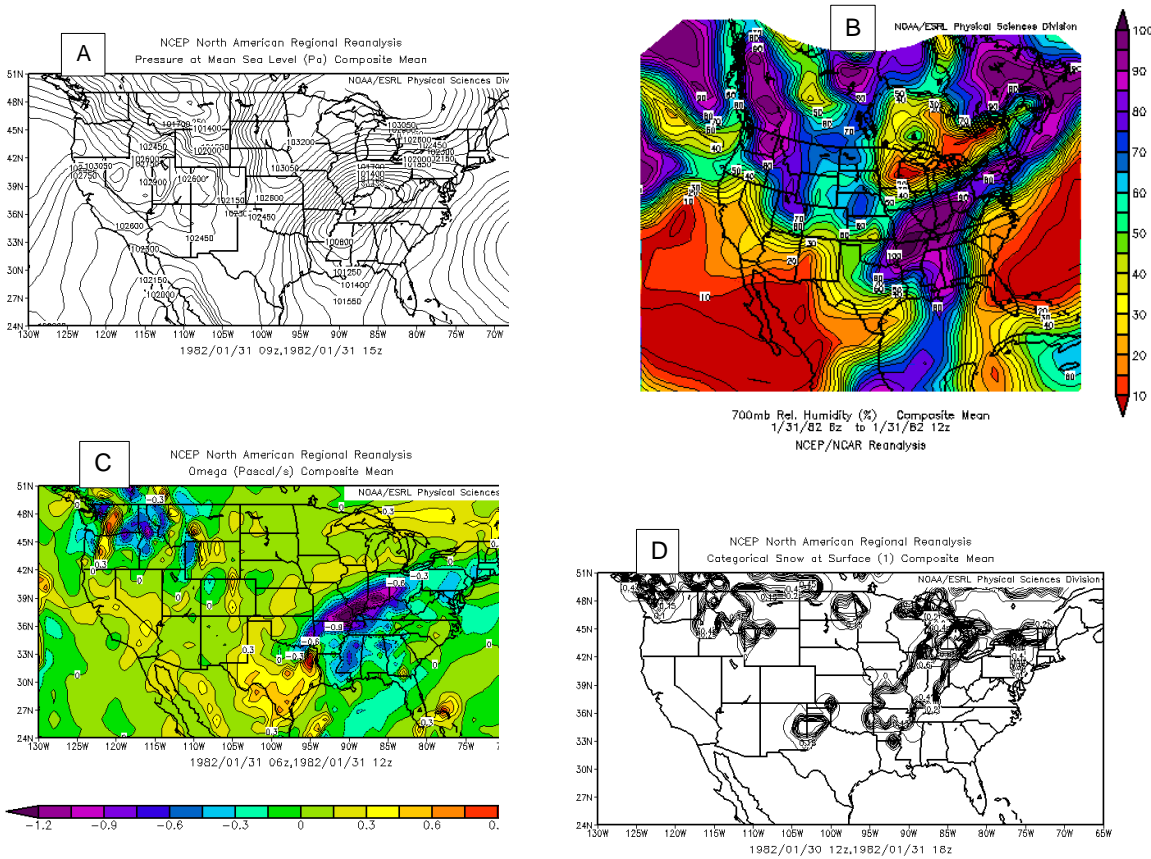
13 - 14 March 1993 Event	25 - 26 December 2010 Event
Variable or Parameter	Variable or Parameter
$\omega \leq -1.3 \text{ pa s}^{-1}$ 700hPa	$\omega \leq -0.90 \text{ pa s}^{-1}$ 700hPa

Enhanced IR Satellite Imagery	Frontogenesis (Surface, 850hPa, 700-500hPa)
850hPa Low Level Jet (LLJ)	Cyclone tracks and Cyclogenesis
CSI/MSI and EPV	Elevated Convection
Frontogenesis (Surface, 850hPa, 700-500hPa)	EPVg and CI (850hPa-750hPa) (650-500hPa)
Cyclone tracks and Cyclogenesis	Differential Positive Vorticity Advection (700-450hPa)
LHR	TROWAL
Elevated Convection	700hPa RH \geq 80%
TROWAL	LHR
700hPa RH \geq 80%	850hPa WAA
850hPa convergence and 250hPa divergence	850hPa CAA
850hPa Warm Air Advection (WAA)	Jet streak-induced Ageostrophic circulation
850hPa Cold Air Advection (CAA)	850hPa LLJ
Isentropic Potential Vorticity	850hPa Temperature Gradients
Latent and Sensible Heat Fluxes at Surface (Gulf of Mexico and Atlantic Ocean)	Latent and Sensible Heat Fluxes at Surface (off middle Atlantic and northeast coasts)
Jet streak-induced Ageostrophic circulation	
Potential Vorticity Advection into cyclone center	
850hPa Temperature Gradients	

827 **Table 3.** Parameters relevant to 13-14 March 1993 event comparison to parameters

828 relevant to 25-26 December 2010 event

829



830

831

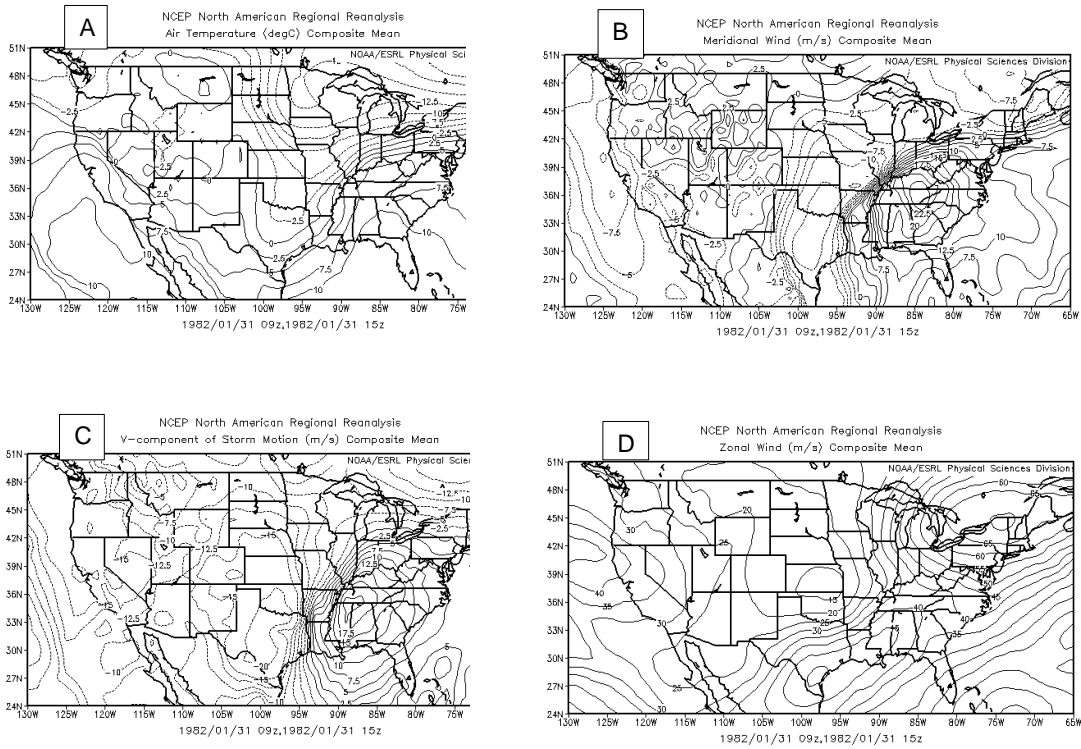
832

833

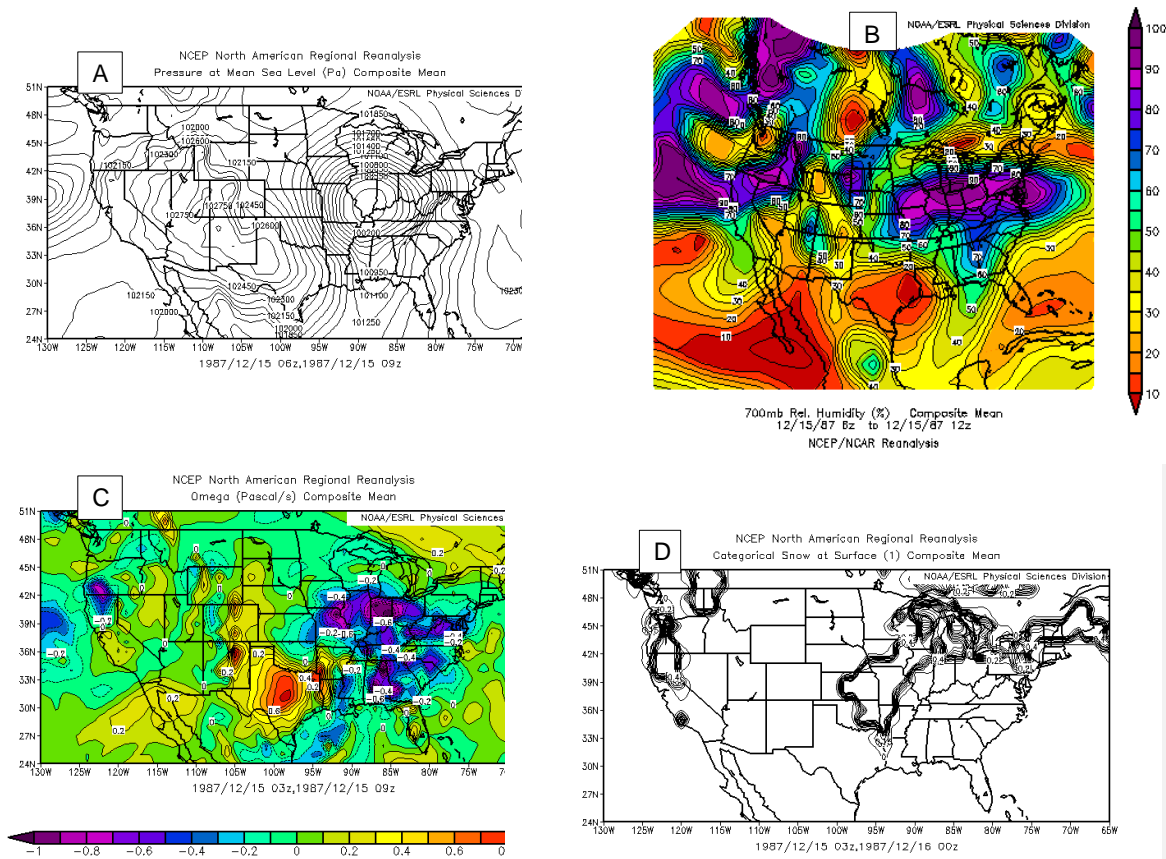
834

835

Figure 1. 30-31 January 1982 - Image [A] is event Pressure at Mean Sea Level ≤ 100400 . Image [B] is event 700hPa RH $\geq 80\%$. Image [C] is event 700hPa Omega ≤ -1.2 . Image [D] is event Categorical Snow at Surface < 1 . Images [A], [B], [C] indicate complex interaction of these variables to produce the regional distribution of snowfall shown in Image [D] and focus on the patterns of middle level moisture and ascent north-northeast of the cyclone center that enhance snowfall rates, subsequently increase accumulations.



836 **Figure 2.** 30-31 January 1982 – Image [A] is event 850hPa Temperature.
 837 Image [B] is event 850hPa Meridional Wind. Image [C] is event 700hPa
 838 V-Component of Storm Motion. Image [D] is event 850hpa Zonal Wind.
 839 Images [A], [B], [C], [D] indicate a complex interaction of these variables
 840 to produce the regional distribution of snowfall shown in Figure 1 Image
 841 [D].



842
843
844
845
846
847

Figure 3. 14-15 December 1987 – Image [A] is event Pressure at Mean Sea Level ≤ 100000 . Image [B] is event 700hPa RH $\geq 80\%$. Image [C] is event 700hPa Omega ≤ -0.9 . Image [D] is event Categorical Snow at Surface < 1 . Images [A], [B], [C] indicate a complex interaction of these variables to produce the regional distribution of snowfall shown in Image [D] and focus on the patterns of middle level moisture and ascent north-northeast of the cyclone center that enhance snowfall rates, subsequently increase accumulations.

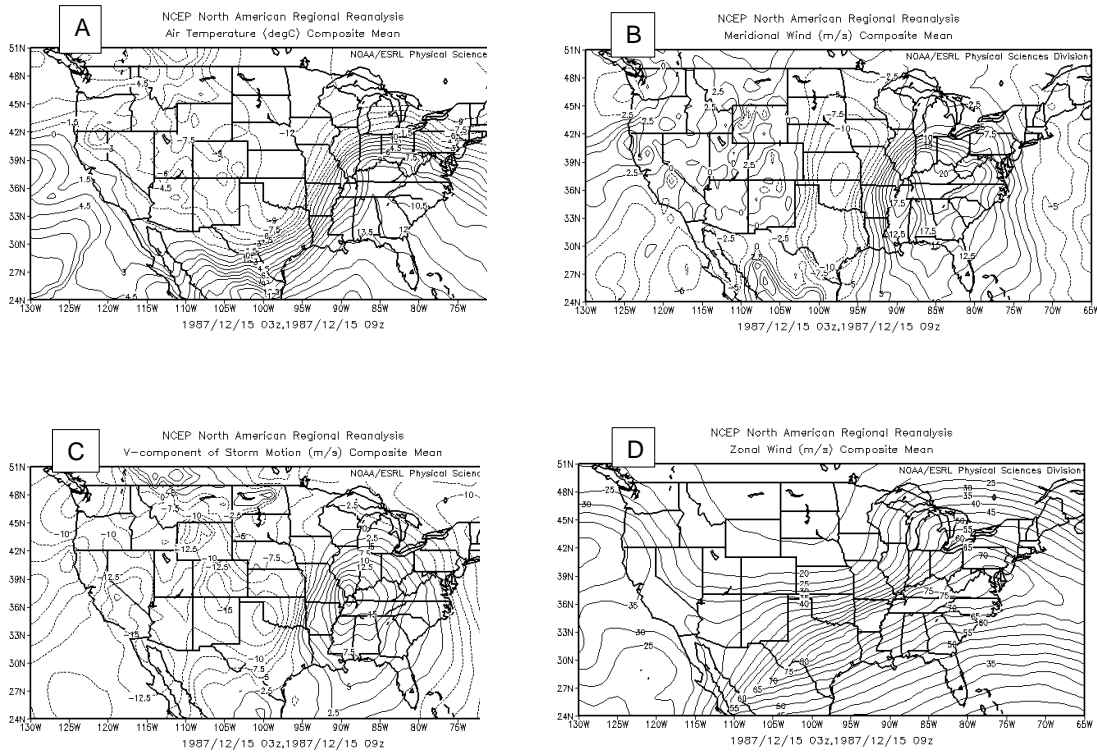


Figure 4. 14-15 December 1987 – Image [A] is event 850hPa Temperature. Image [B] is event 850hPa Meridional Wind. Image [C] is event 700hPa V-Component of Storm Motion. Image [D] is event 850hPa Zonal Wind. Images [A], [B], [C], [D] indicate a complex interaction of these variables to produce the regional distribution of snowfall shown in Figure 3 Image [D].

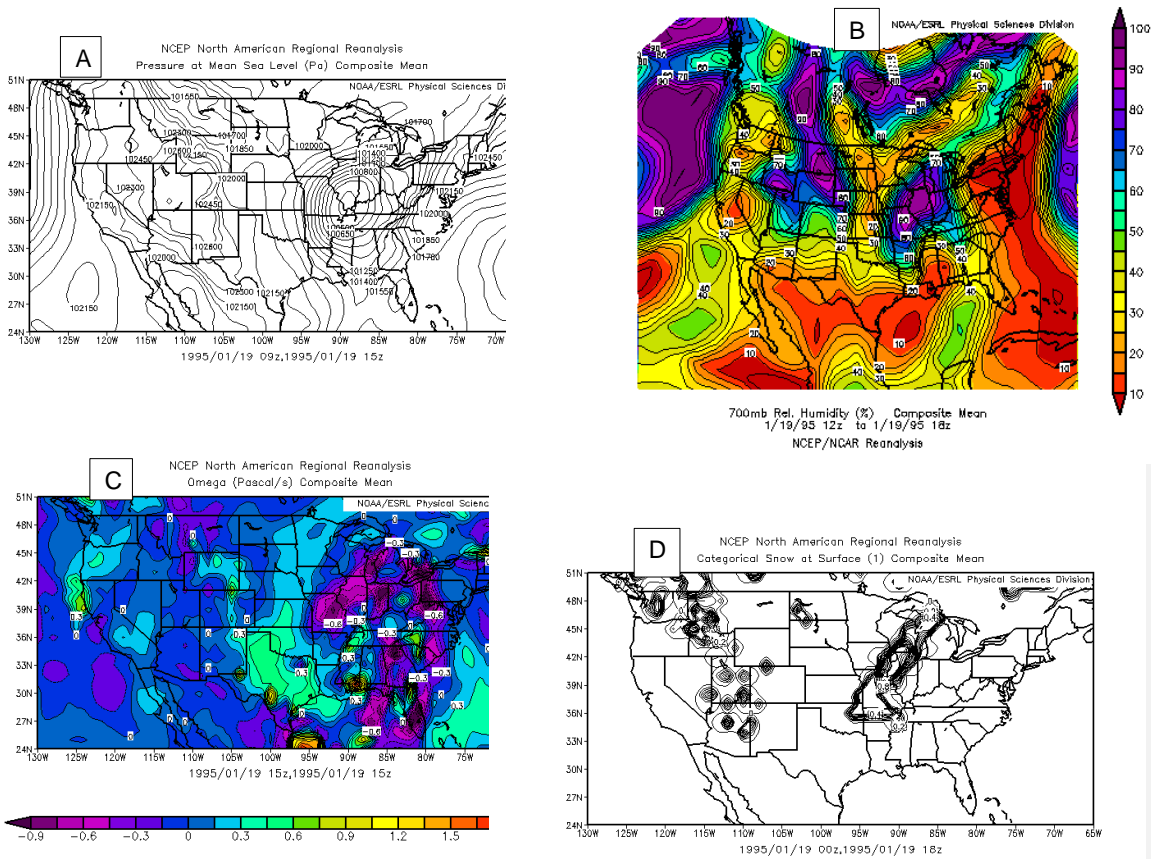
849

850

851

852

853



854

855

856

857

858

859

Figure 5. 19 January 1995 – Image [A] is event Pressure at Mean Sea Level ≤ 100350 . Image [B] is event 700hPa RH $\geq 80\%$. Image [C] is event 700hPa Omega ≤ -0.9 . Image [D] is event Categorical Snow at Surface < 1 . Images [A], [B], [C] indicate a complex interaction of these variables to produce the regional distribution of snowfall shown in Image [D] and focus on the patterns of middle level moisture and ascent north-northeast of the cyclone center that enhance snowfall rates, subsequently increase accumulations.

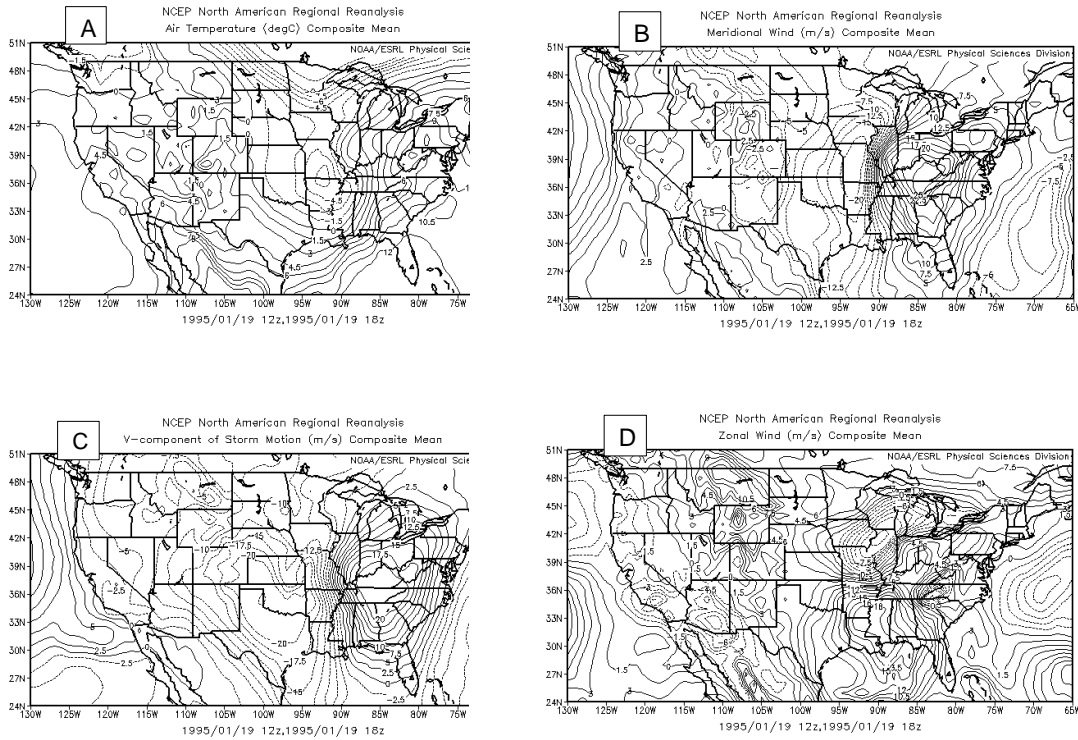


Figure 6. 19 January 1995 – Image [A] is event 850hPa Temperature. Image [B] is event 850hPa Meridional Wind. Image [C] is event 700hPa V-Component of Storm Motion. Image [D] is event 850hPa Zonal Wind. Images [A], [B], [C], [D] indicate a complex interaction of these variables to produce the regional distribution of snowfall shown in Figure 5 Image [D].

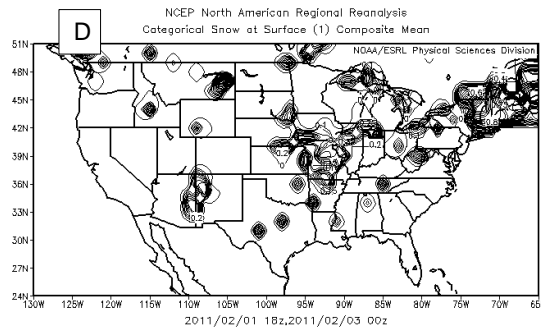
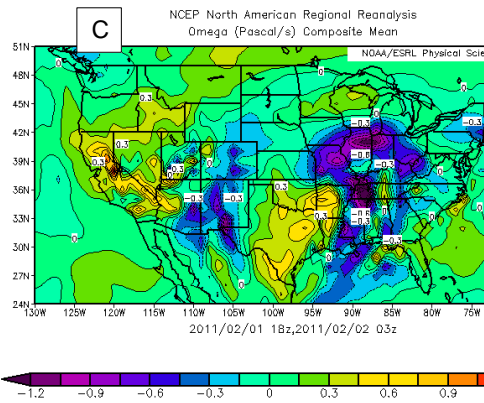
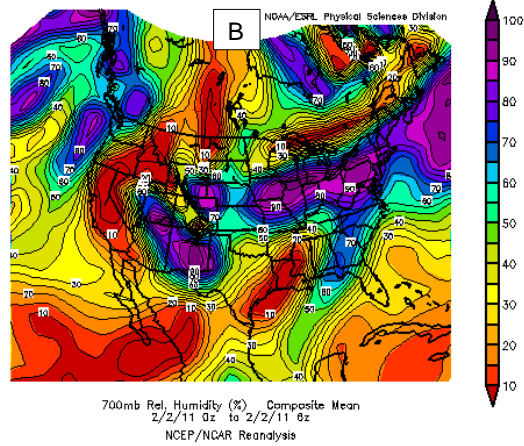
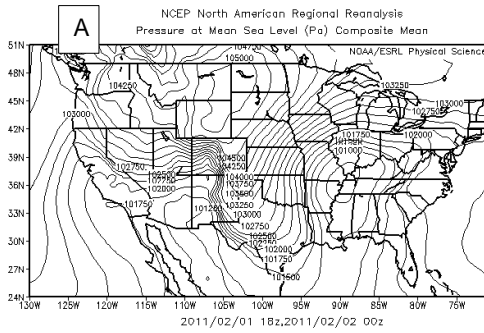
861

862

863

864

865



866

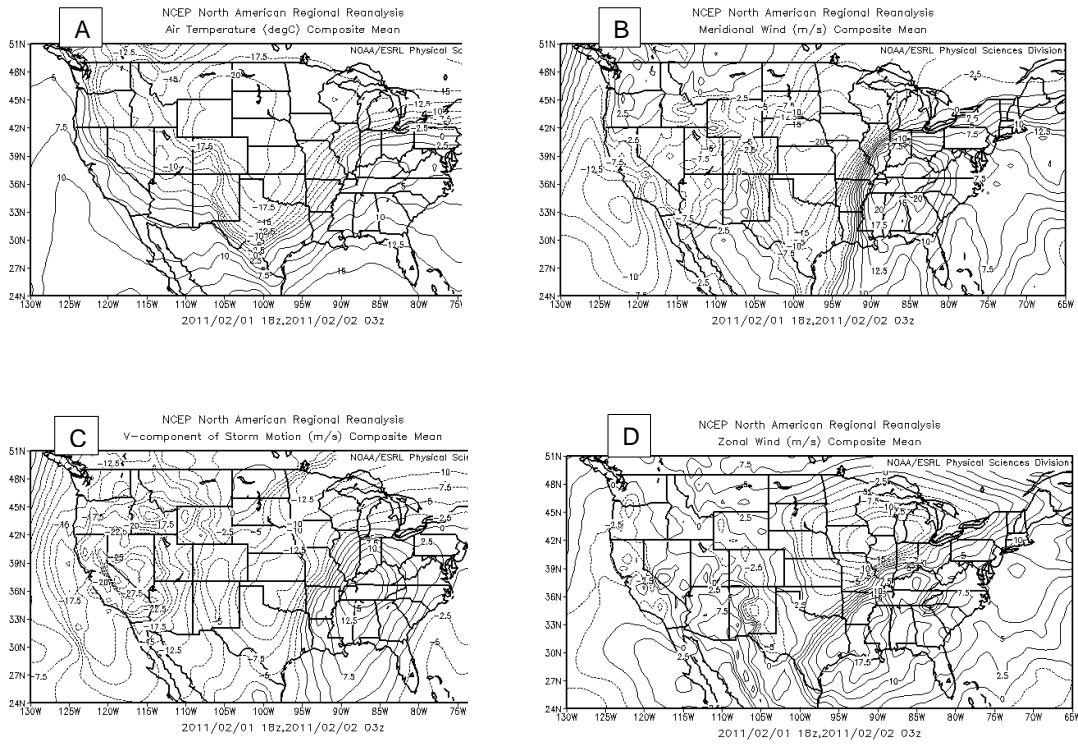
867

868

869

870

Figure 7. 1-2 February 2011 – Image [A] is event Pressure at Mean Sea Level ≤ 100850 . Image [B] is event 700hPa $RH \geq 80\%$. Image [C] is event 700hPa $\Omega \leq -1.2$. Image [D] is event Categorical Snow at Surface < 1 . Images [A], [B], [C] indicate a complex interaction of these variables to produce the regional distribution of snowfall shown in Image [D] and focus on the patterns of middle level moisture and ascent to north-northeast of the cyclone center that enhance snowfall rates and subsequently increase accumulations.



871

Figure 8. 1-2 February 2011 – Image [A] is event 850hPa Temperature. Image [B] is 850hPa Meridional Wind. Image [C] is event 700hPa V-Component of Storm Motion. Image [D] is event 850hPa Zonal Wind. Images [A], [B], [C], [D] indicate a complex interaction of these variables to produce the regional snowfall distribution shown in Figure 7 Image [D].

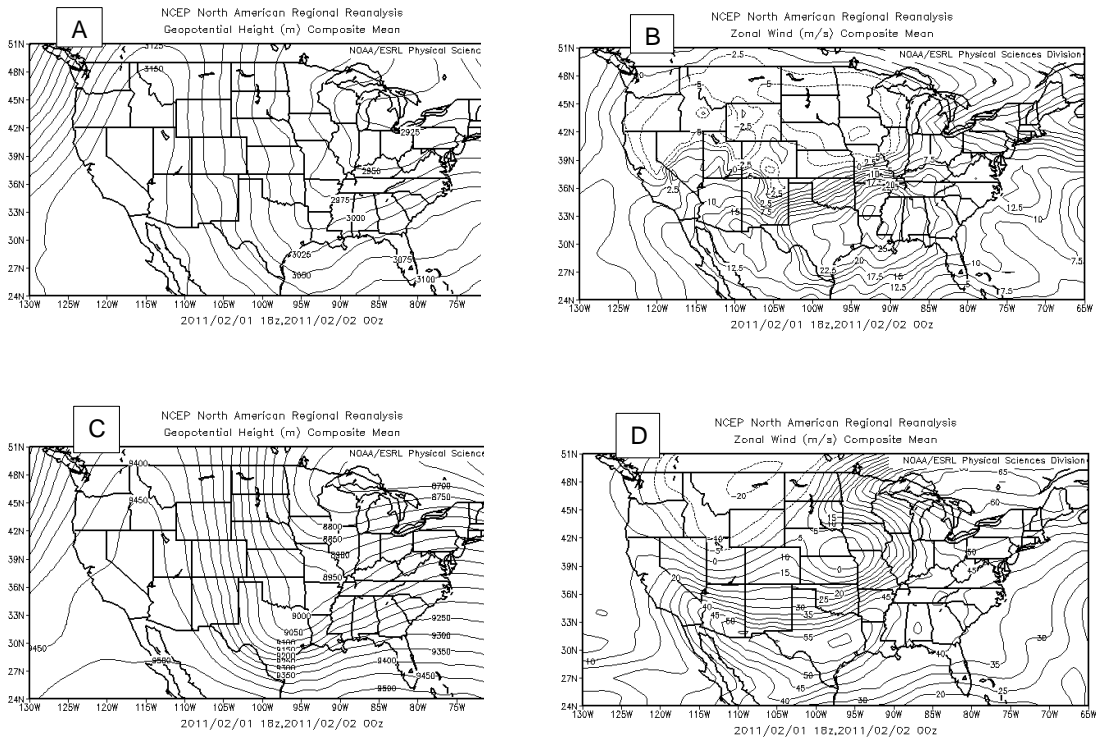
872

873

874

875

876

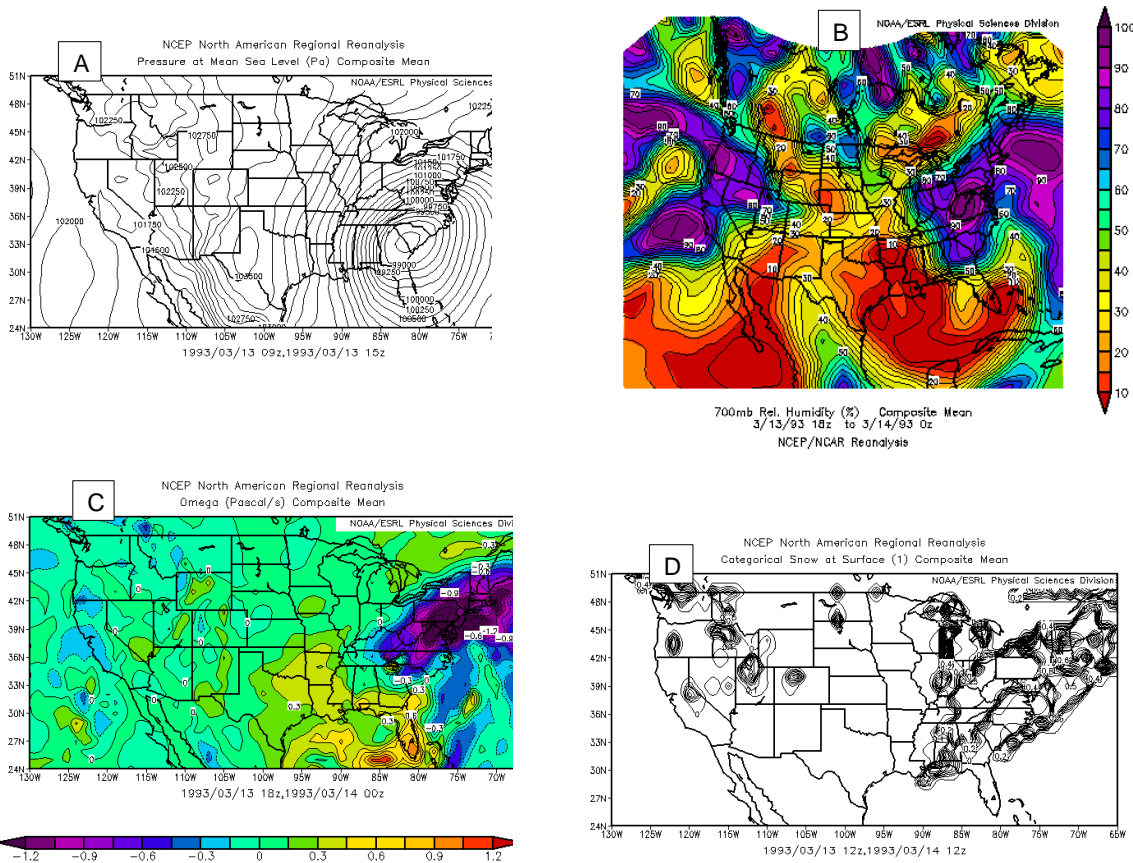


877 **Figure 9.** 1-2 February 2011 – Image [A] is event 700hPa Height. Image [B] is
 878 event 700hPa Zonal Wind. Image [C] is event 300hPa Height. Image [D] is
 879 event 300hPa Zonal Wind. Images [A], [B], [C], [D], also, indicate a complex
 interaction of these variables to produce the regional distribution of snowfall
 shown in Figure 7 Image D.

880

881

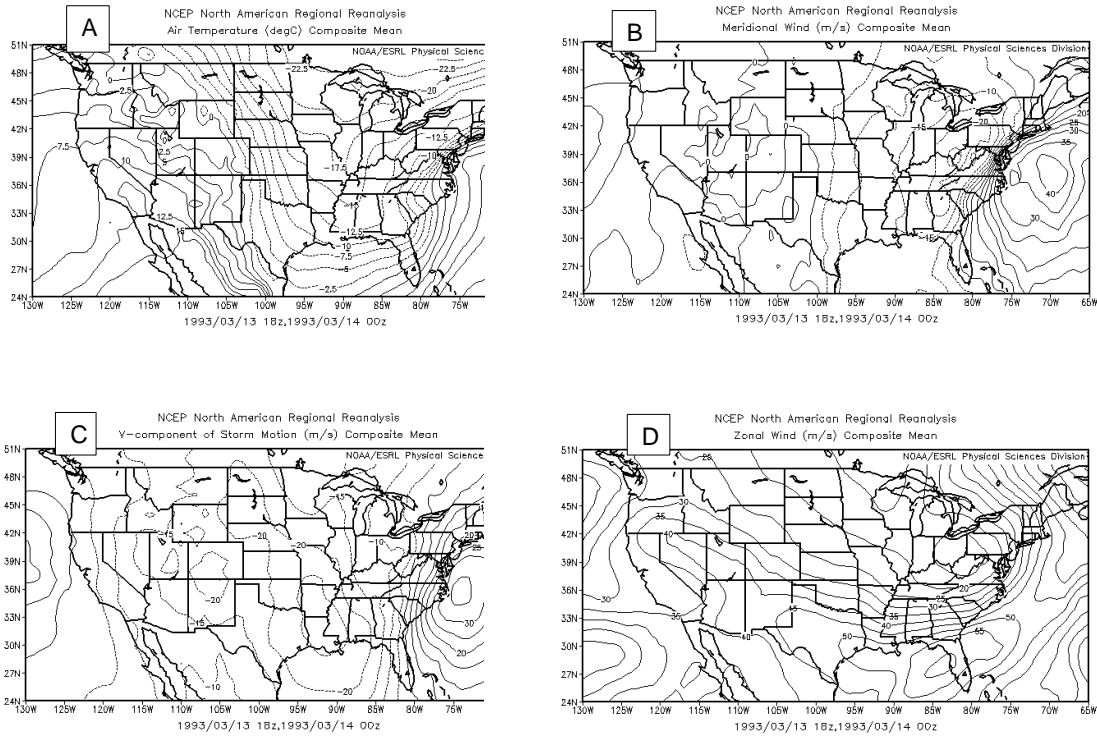
882



883 **Figure 10.** 13-14 March 1993 – Image [A] is event Pressure at Mean Sea
 884 Level ≤ 98750 . Image [B] is event 700hPa $RH \geq 80\%$. Image [C] is event 700hPa
 885 Omega ≤ -1.3 . Image [D] is event Categorical Snow at Surface < 1 . Images [A],
 886 [B], [C] indicate a complex interaction of these variables to produce the
 regional distribution of snowfall shown in Image [D] and focus on the patterns
 of middle level moisture and ascent north-northeast of the cyclone center that
 enhance snowfall rates, subsequently increase accumulations.

887

888



889 **Figure 11.** 13-14 March 1993 – Image [A] is event 850hPa Temperature. Image [B]
 890 is event 850hPa Meridional Wind. Image [C] is event 700hPa V-Component of
 891 Storm Motion. Image [D] is event 850hPa Zonal Wind. Images [A], [B], [C], [D]
 892 indicate a complex interaction of these variables to produce the regional
 893 distribution of snowfall shown in Figure 9 Image [D].
 894
 895

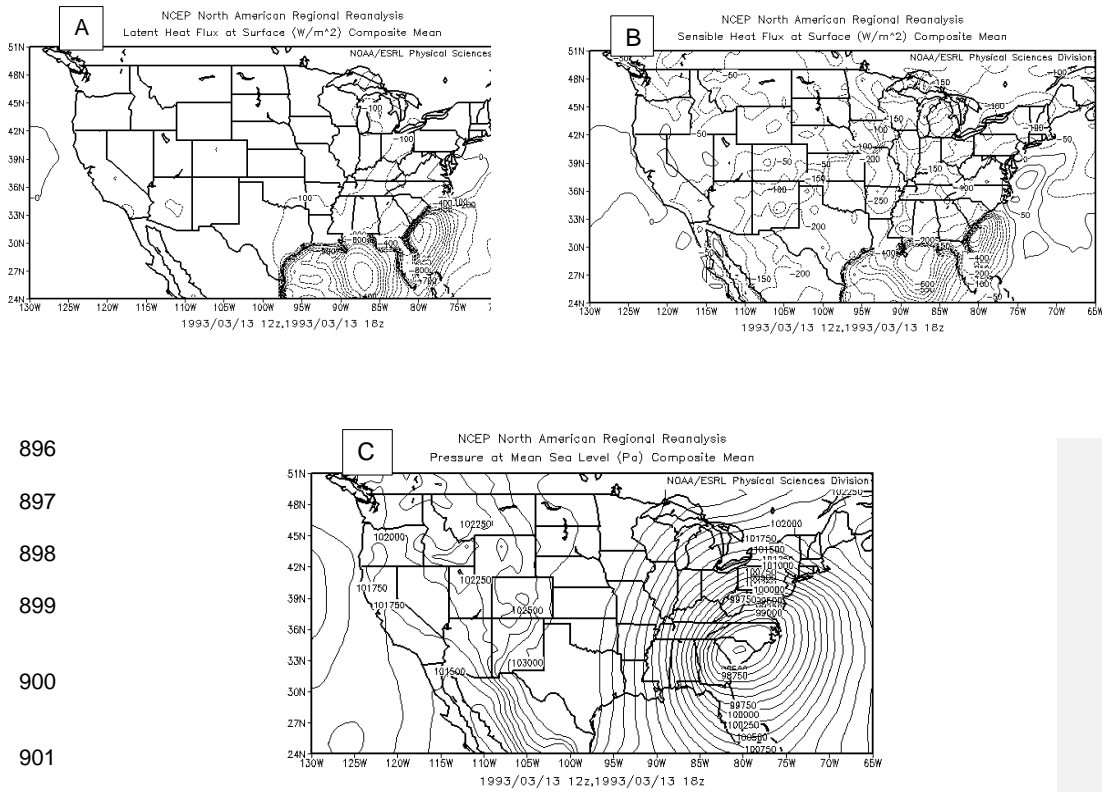
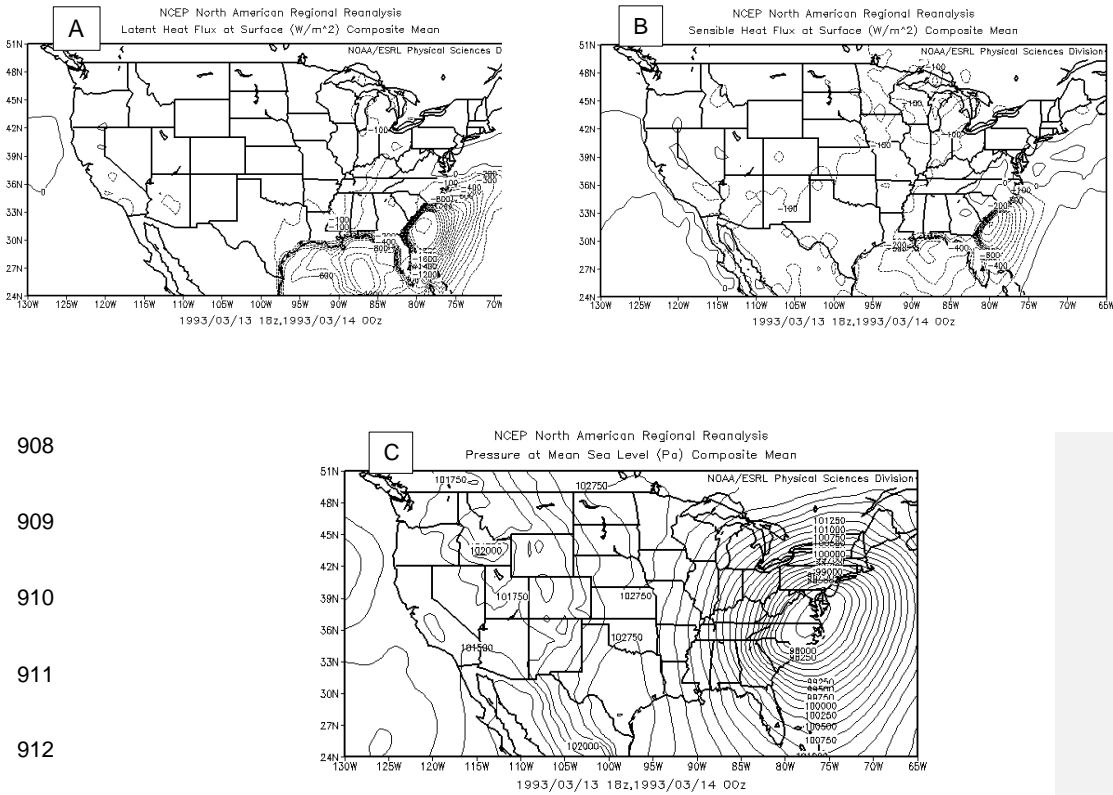


Figure 12. 13-14 March 1993 – Image [A] is event Latent Heat Flux at Surface 1200 – 1800 UTC 13 March 1993. Image [B] is event Sensible Heat Flux at Surface 1200 – 1800 UTC 13 March 1993. Image [C] is event Pressure at Mean Sea Level 1200 – 1800 UTC 13 March 1993.



908

909

910

911

912

913

914

915

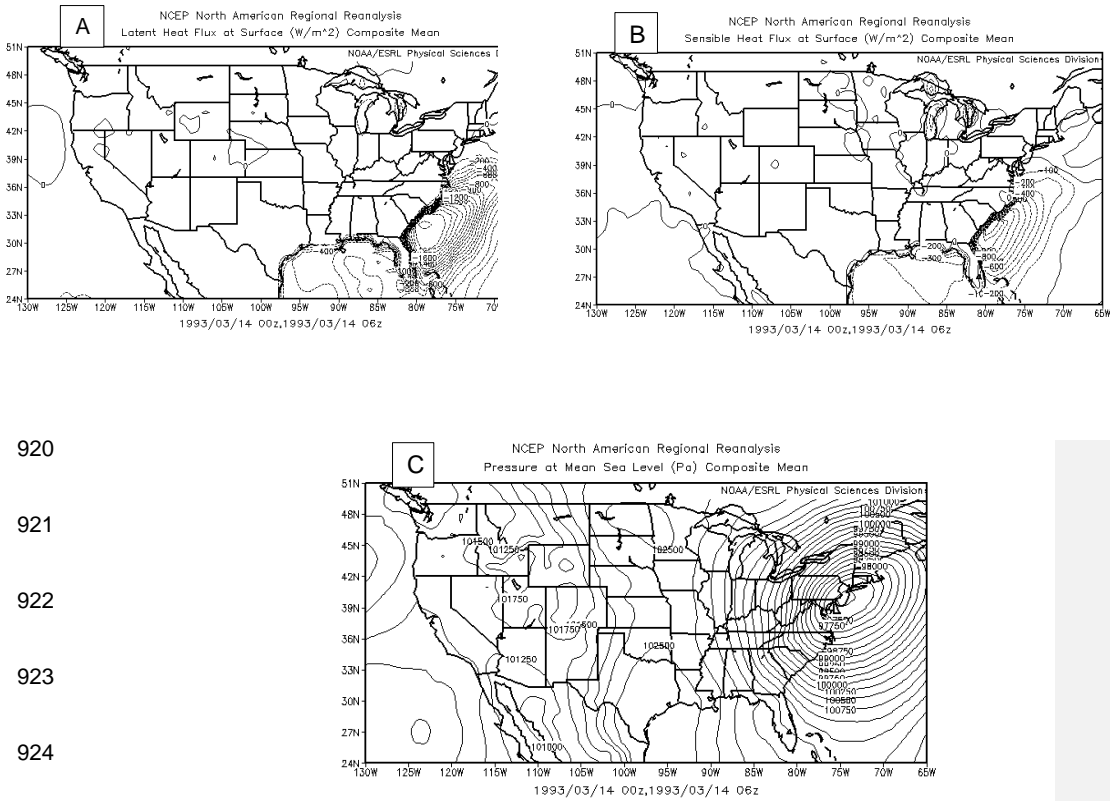
916

917

918

919

Figure 13. 13-14 March 1993 – Image [A] is event Latent Heat Flux at Surface 1800 UTC 13 March – 0000 UTC 14 March 1993. Image [B] is event Sensible Heat Flux at Surface 1800 UTC 13 March – 0000 UTC 14 March 1993. Image [C] is event Pressure at Mean Sea Level 1800 UTC 13 March – 0000 UTC 14 March 1993.



920

921

922

923

924

925

926

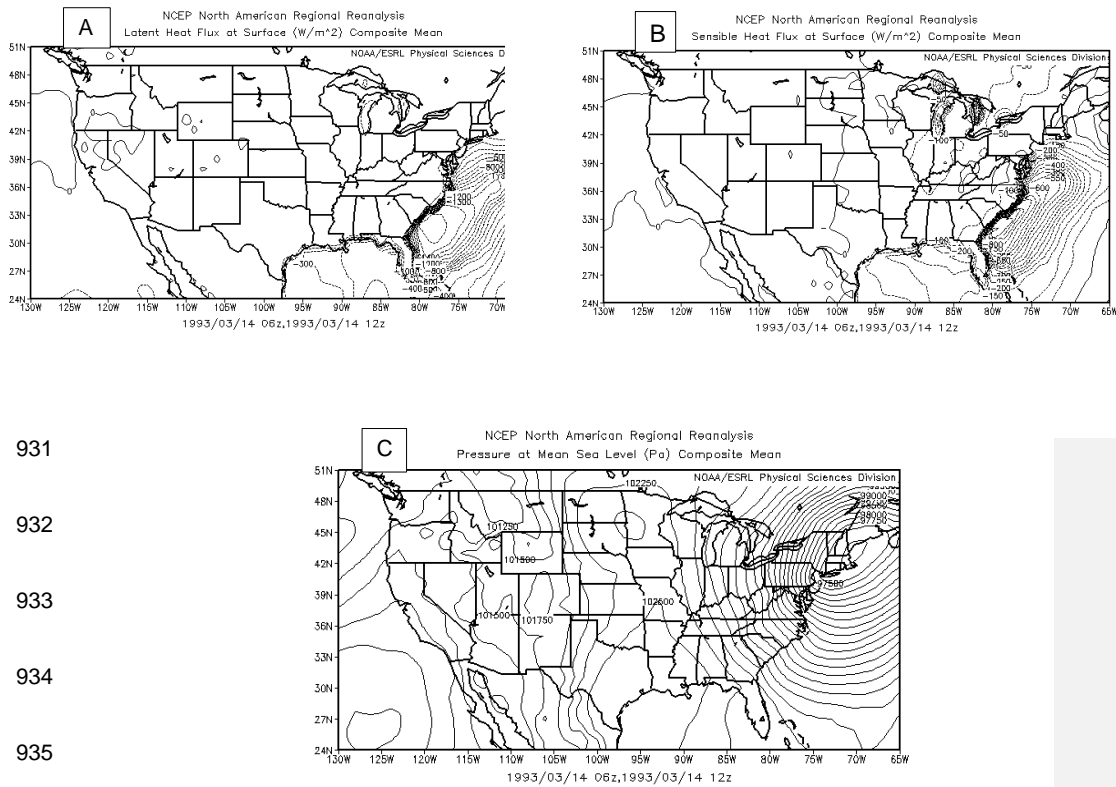
927

928

929

930

Figure 14. 13-14 March 1993 – Image [A] is event Latent Heat Flux at Surface 0000 – 0600 UTC 14 March 1993. Image [B] is event Sensible Heat Flux at Surface 0000 – 0600 UTC 14 March 1993. Image [C] is event Pressure at Mean Sea Level 0000 – 0600 UTC 14 March 1993.



931

932

933

934

935

936

937

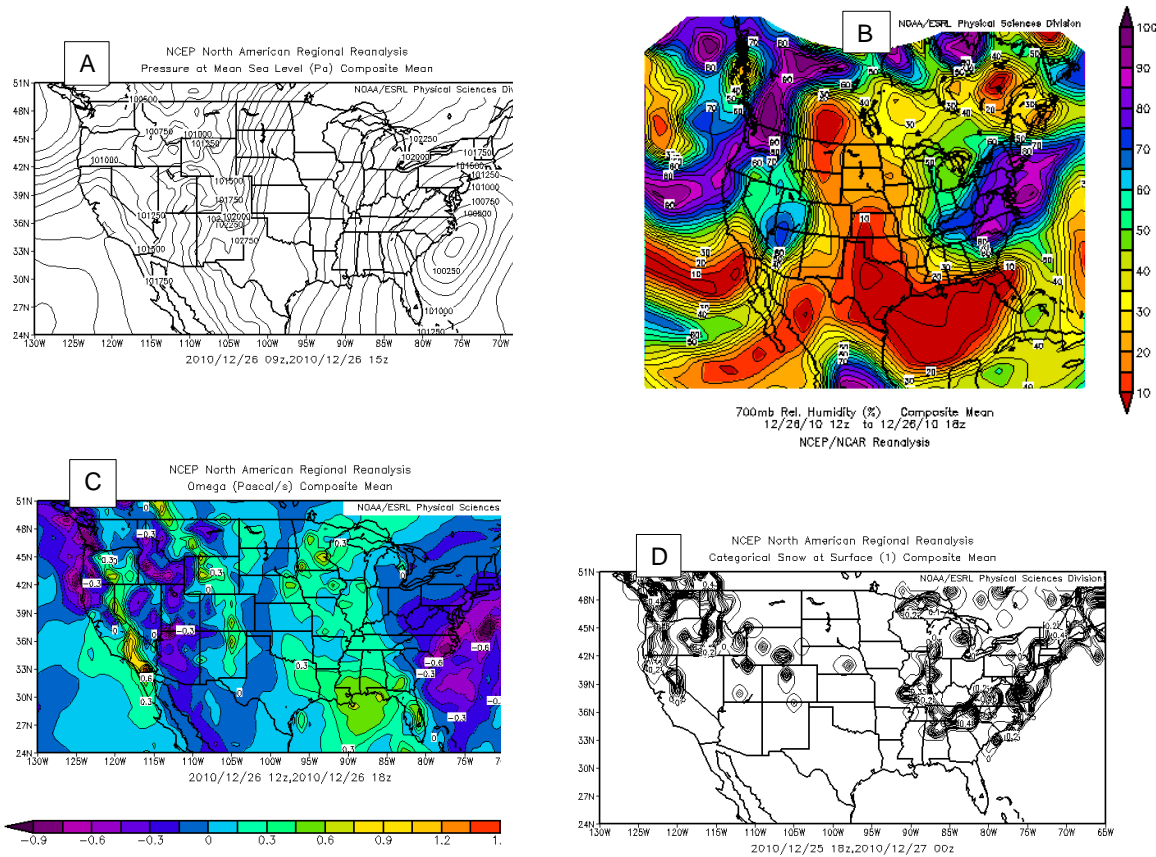
938

939

940

941

Figure 15. 13-14 March 1993 – Image [A] is event Latent Heat Flux at Surface 0600 – 1200 UTC 14 March 1993, Image [B] is event Sensible Heat Flux at Surface 0600 – 1200 UTC 14 March 1993. Image [C] is event Pressure at Mean Sea Level 0600 – 1200 UTC 14 March 1993.



942 **Figure 16.** 25-26 December 2010 – Image [A] is event Pressure at Mean Sea
 943 Level ≤ 100000 . Image [B] is event 700hPa $RH \geq 80\%$. Image [C] is event 700hPa
 944 Omega ≤ -0.90 . Image [D] is event Categorical Snow at Surface < 1 . Images [A], [B],
 945 [C] indicate a complex interaction of these variables to produce the regional
 distribution of snowfall shown in Image [D] and focus on the patterns of middle level
 moisture and ascent north-northeast of the cyclone center that enhance event
 snowfall rates, subsequently increase accumulations.

946

947

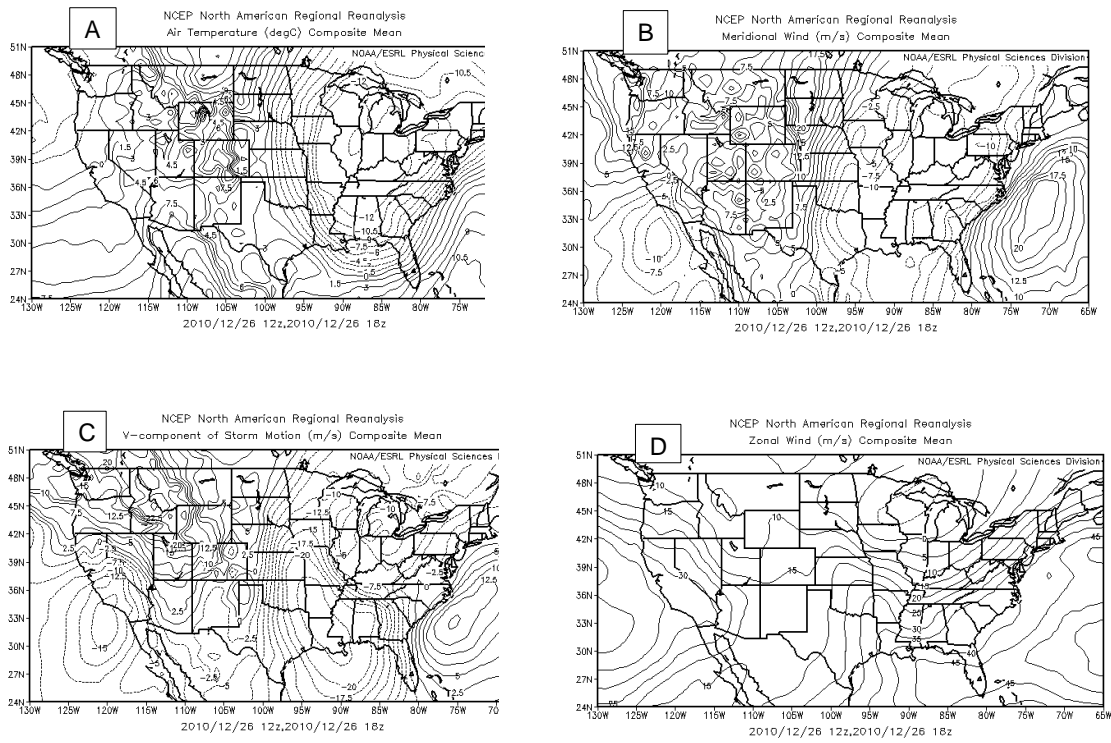


Figure 17. 25-26 December 2010 – Image [A] is event 850hPa Temperature. Image [B] is event 850hPa Meridional Wind. Image [C] is event 700hPa V-Component of Storm Motion. Image [D] is event 850hPa Zonal Wind. Images [A], [B], [C], [D] indicate a complex interaction of these variables to produce the regional distribution of snowfall shown Figure 11 Image [D].

948

949

950

951

952

953

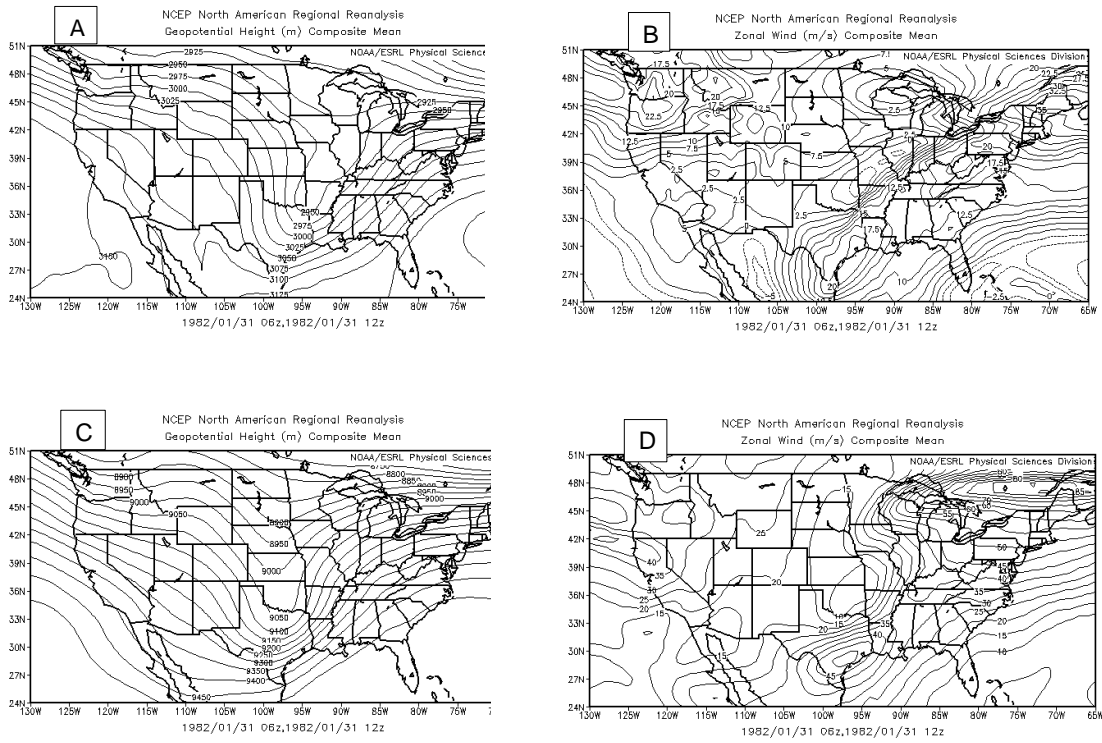


Figure 18. 30-31 January 1982 – Image [A] is event 700hPa Height. Image [B] is event 700hPa Zonal Wind. Image [C] is event 300hPa Height. Image [D] is event 300hPa Zonal Wind. Images [A], [B], [C], [D], also, indicate a complex interaction of these variables to produce the regional distribution of snowfall shown in Figure 1 Image D.

954

955

956

957

958

959

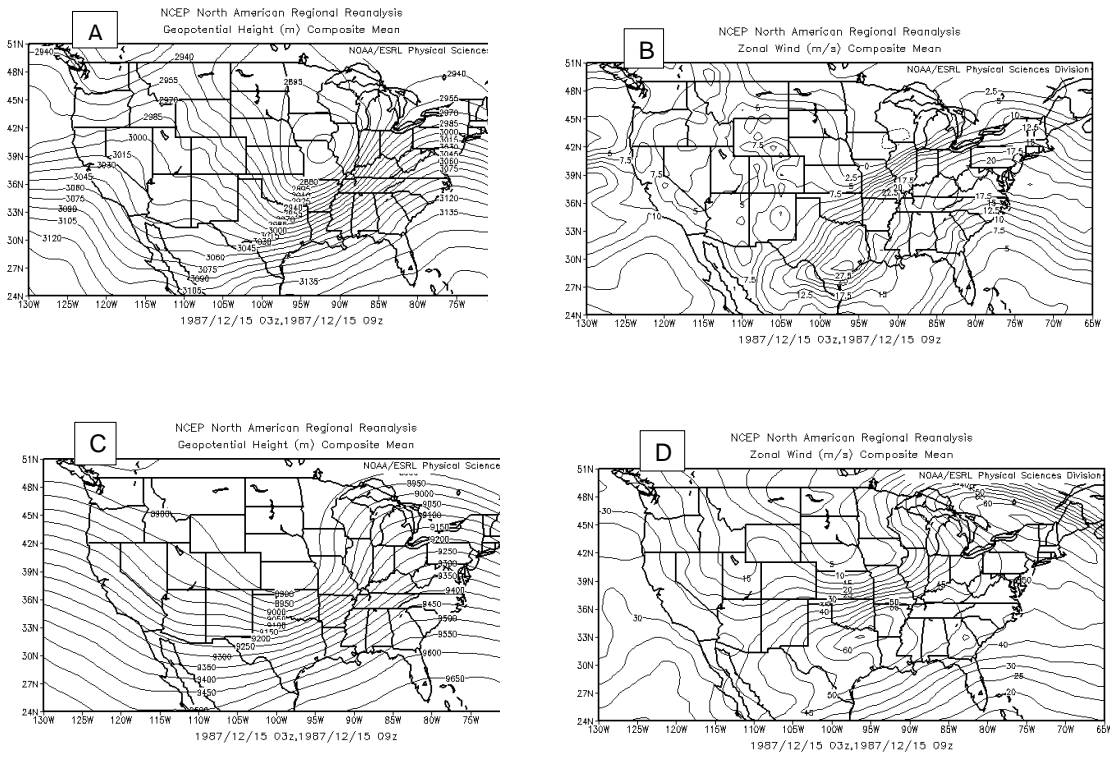


Figure 19. 14-15 December 1987 – Image [A] is event 700hPa Height. Image [B] is event 700hPa Zonal Wind. Image [C] is event 300hPa Height. Image [D] is event 300hPa Zonal Wind. Images [A], [B], [C], [D] indicate a complex interaction of these variables to produce the regional distribution of snowfall shown in Figure 3 Image D.

960

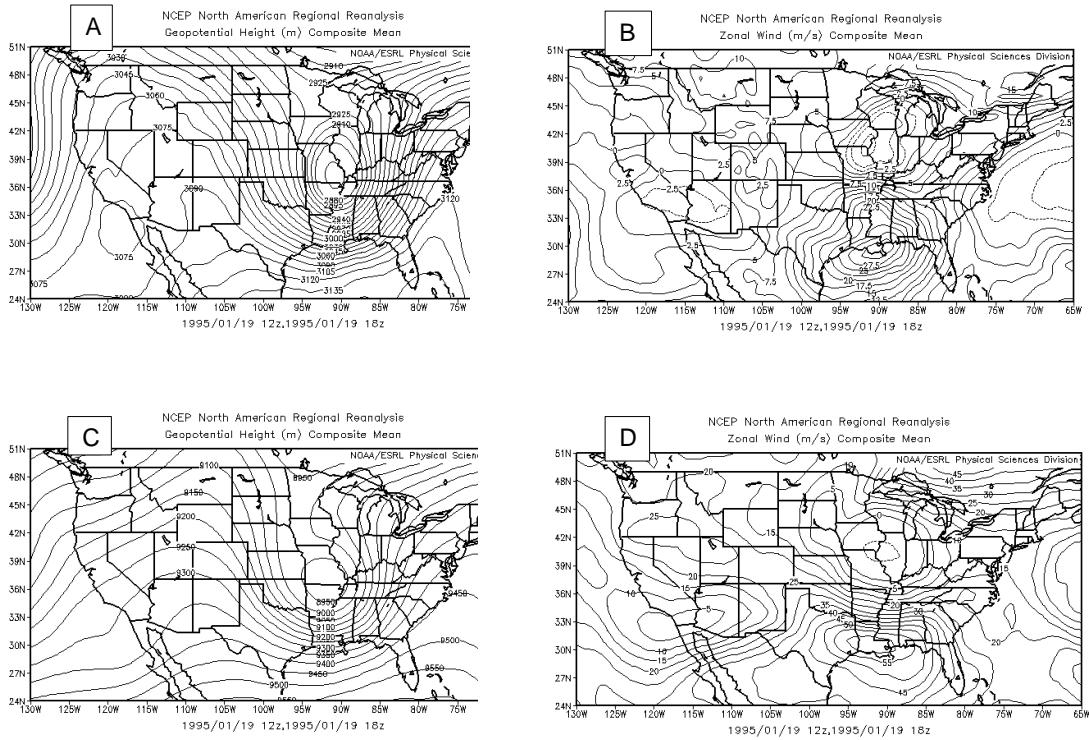
961

962

963

964

965



966 **Figure 20.** 19 January 1995 – Image [A] is event 700hPa Height. Image [B]
 967 is event 700hPa Zonal Wind. Image [C] is event 300hPa Height. Image [D] is
 968 event 300hPa zonal wind. Images [A], [B], [C], [D] indicate a complex
 969 interaction of these variables to produce the regional distribution of snowfall
 970 in Figure 5 Image D.
 971

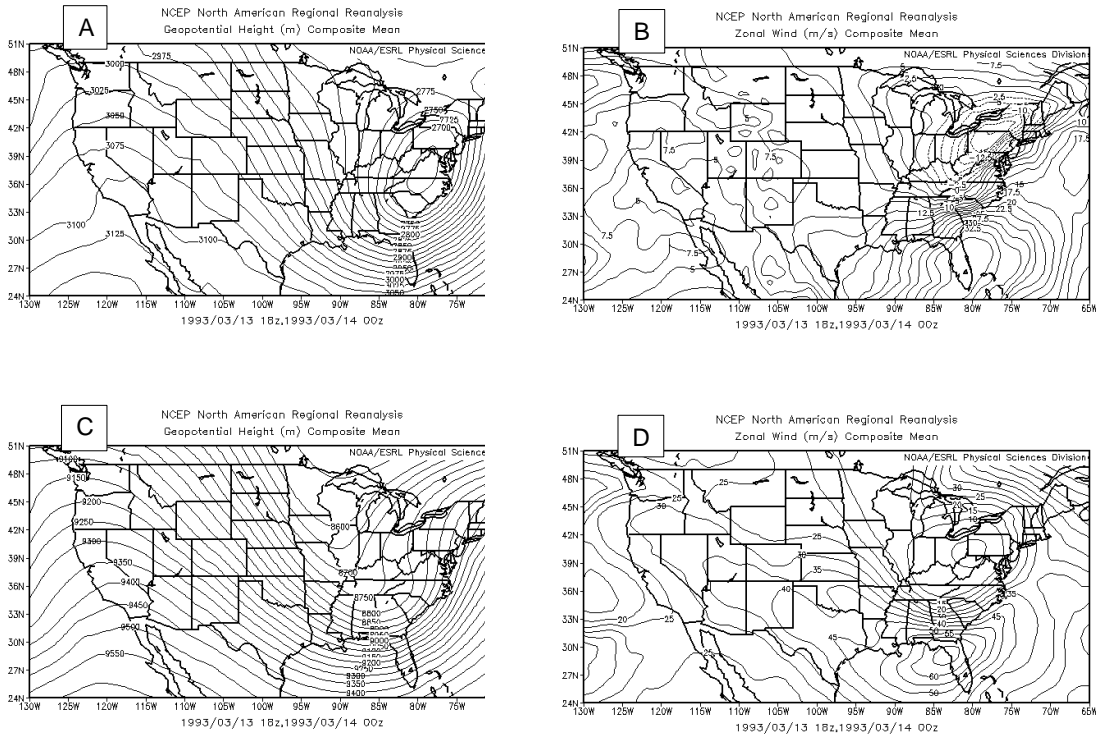


Figure 21. 13-14 March 1993 – Image [A] is event 700hPa Height. Image [B] is event 700hPa Zonal Wind. Image [C] is event 300hPa Height. Image [D] is event 300hPa Zonal Wind. Images [A], [B], [C], [D] indicate a complex of these variables to produce the regional distribution of snowfall shown in Figure 10 Image D.

972

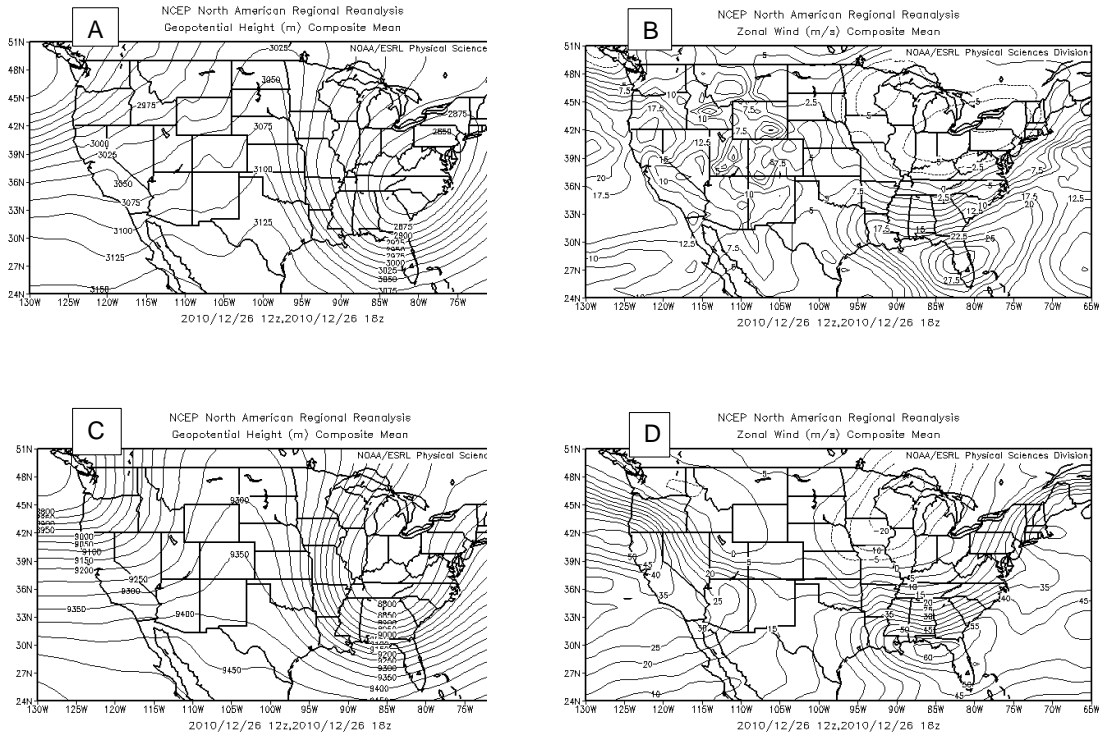
973

974

975

976

977



978

Figure 22. 25-26 December 2010 – Image [A], is event 700hPa Height. Image [B] is event 700hPa Zonal Wind. Image [C] is event 300hPa Height. Image [D] is event 300hPa Zonal Wind. Images [A], [B], [C], [D] indicate a complex interaction of these variables to produce the regional distribution of snowfall shown in Figure 16 Image D.

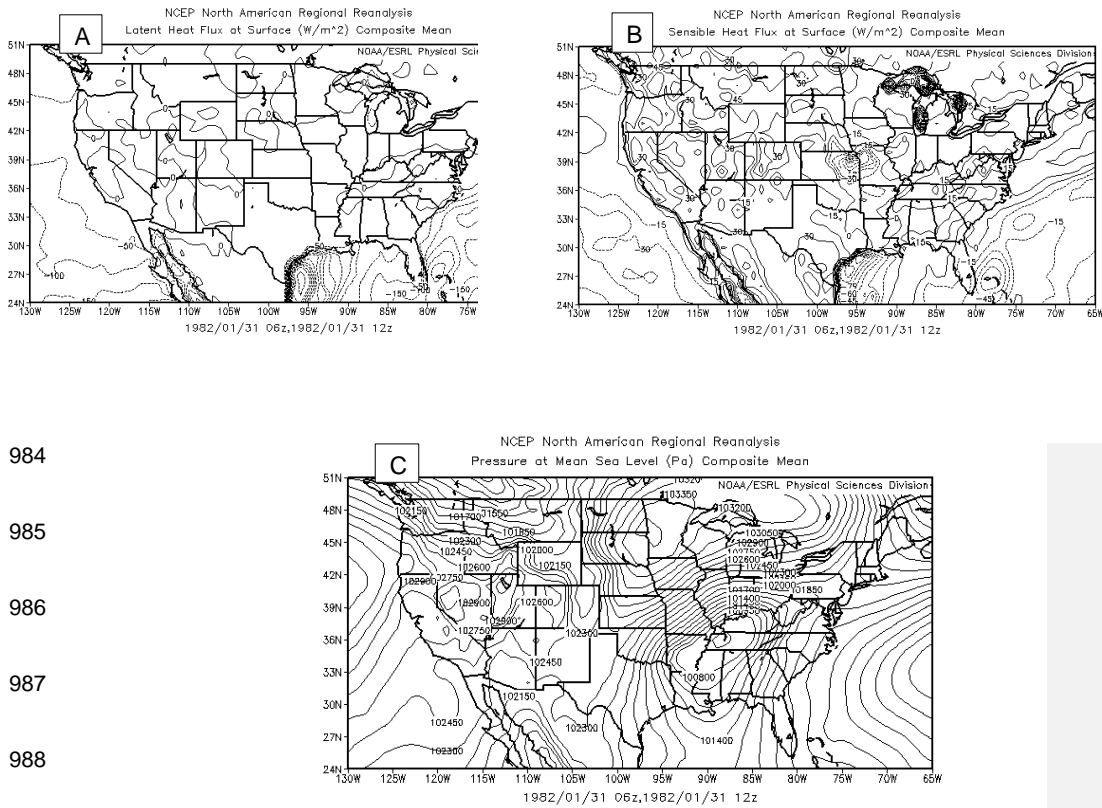
979

980

981

982

983



984

985

986

987

988

989

990

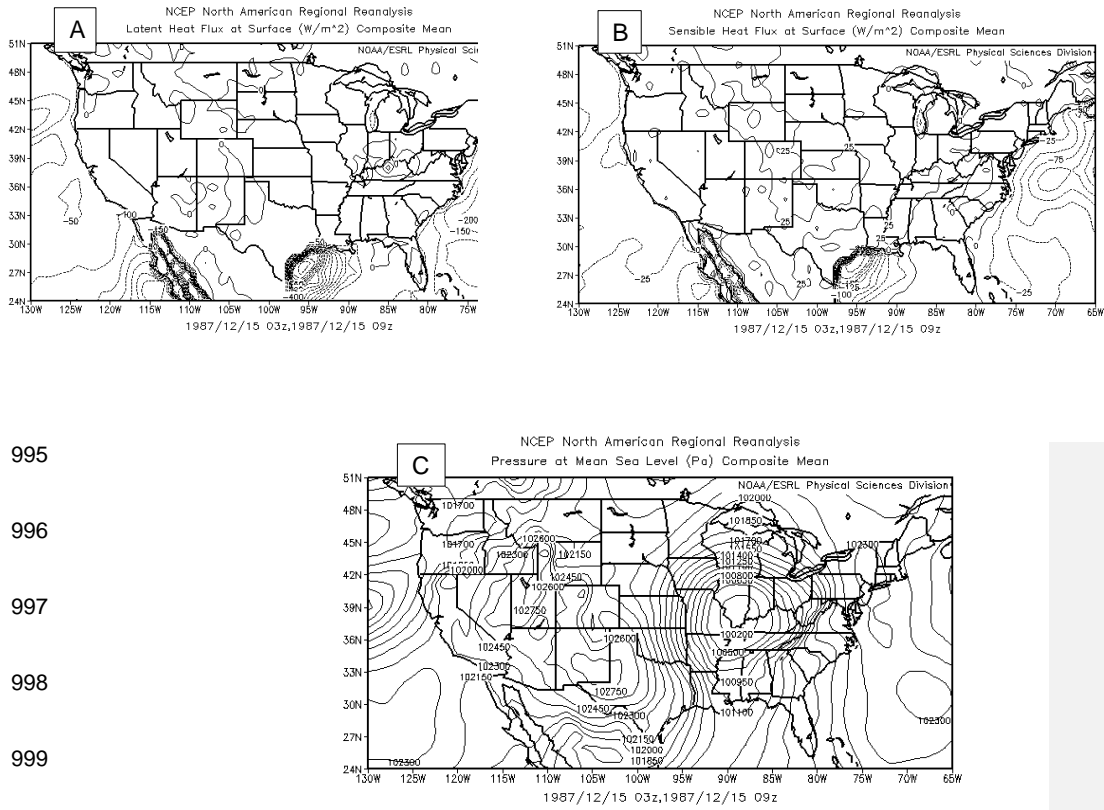
991

Figure 23. 30-31 January 1982 – Image [A] is selected event Latent Heat Flux at Surface. Image [B] is selected event Sensible Heat Flux at Surface. Image [C] is selected event Pressure at Mean Sea Level.

992

993

994



995

996

997

998

999

1000

1001

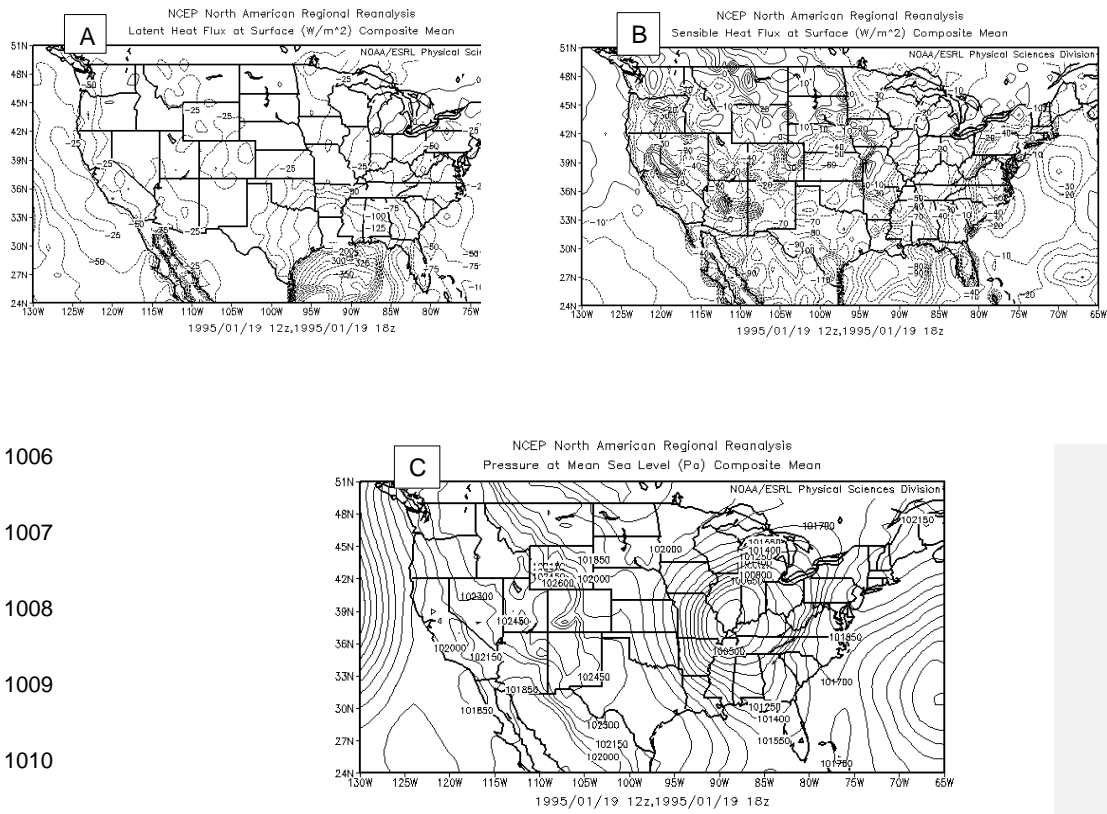
1002

1003

1004

1005

Figure 24. 14-15 December 1987 – Image [A] is selected event Latent Heat Flux at Surface. Image [B] is selected event Sensible Heat Flux at Surface. Image [C] is selected event Pressure at Mean Sea Level.



1006

1007

1008

1009

1010

1011

1012

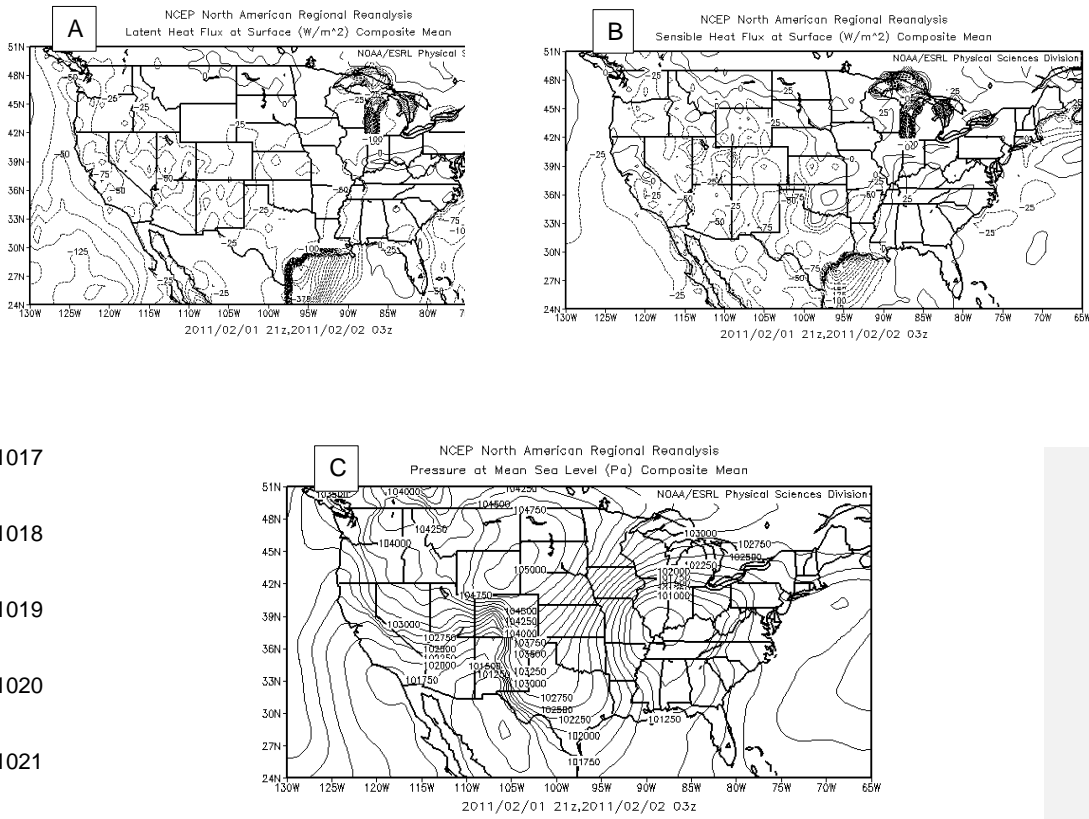
1013

Figure 25. 19 January 1995 – Image [A] is selected event Latent Heat Flux at Surface. Image [B] is selected event Sensible Heat Flux at Surface. Image [C] is selected event Pressure at Mean Sea Level.

1014

1015

1016



1017

1018

1019

1020

1021

1022

1023

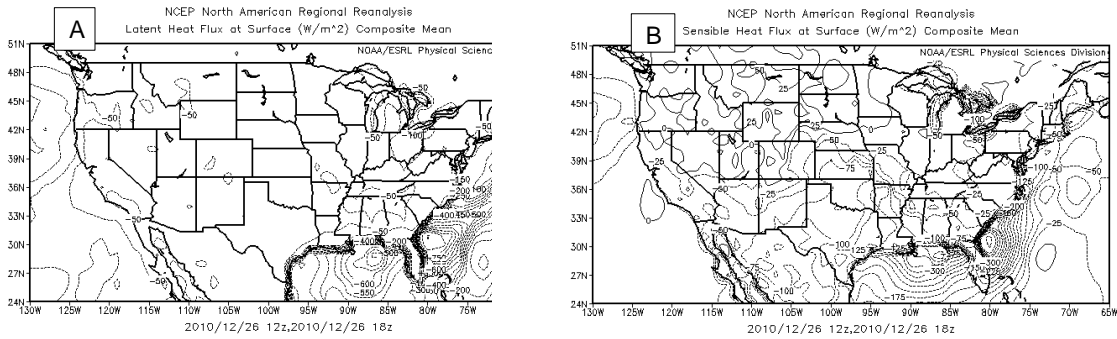
1024

1025

1026

1027

Figure 26. 1-2 February 2011 – Image [A] is selected event Latent Heat Flux at Surface. Image [B] is selected event Sensible Heat Flux at Surface. Image [C] is selected event Pressure at Mean Sea Level.



1028

1029

1030

1031

1032

1033

1034

1035

1036

1037

1038

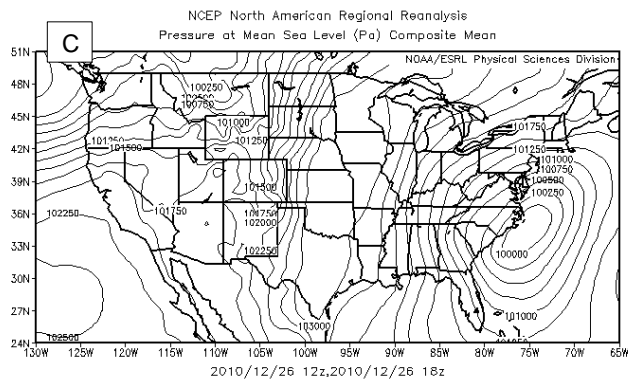
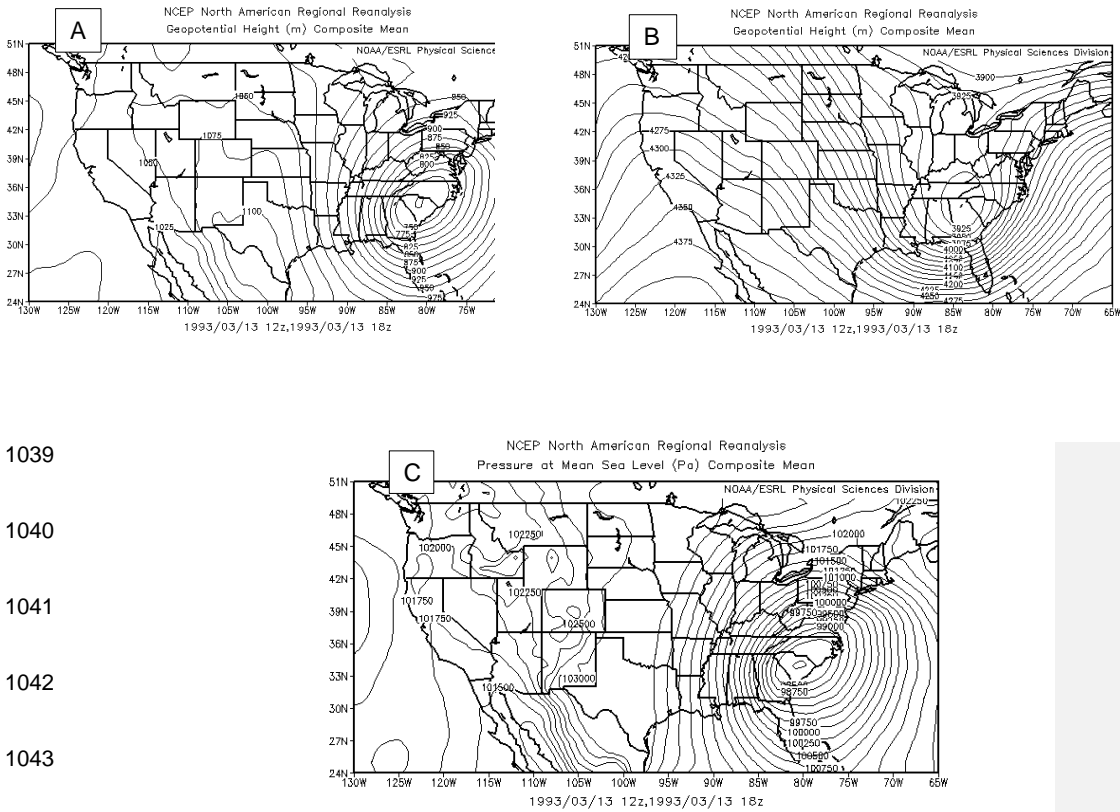


Figure 27. 25-26 December 2010 – Image [A] is selected event Latent Heat Flux at Surface. Image [B] is selected event Sensible Heat Flux at Surface. Image [C] is selected event Pressure at Mean Sea Level.



1039

1040

1041

1042

1043

1044

1045

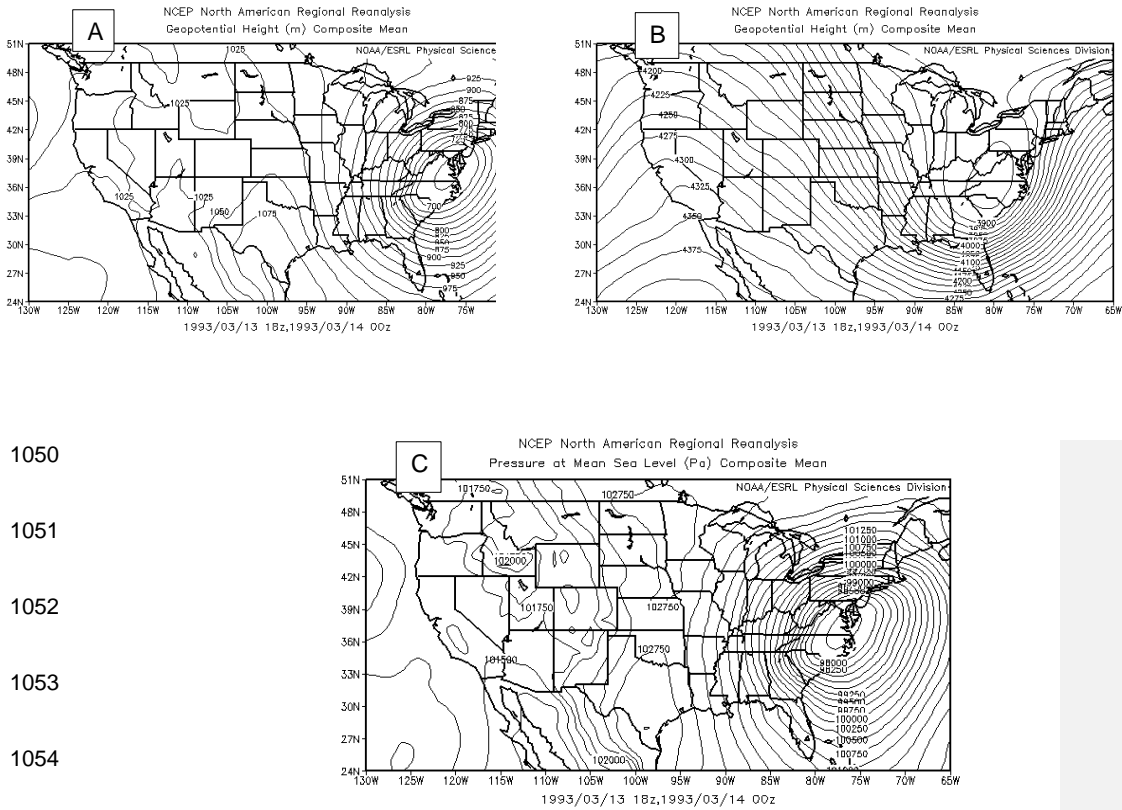
1046

1047

Figure 28. 13-14 March 1993 – Image A is 1200 – 1800 UTC 13 March 1993 900hPa Height. Image B is 1200 – 1800 UTC 13 March 1993 600hPa Height. Image C is 1200 – 1800 UTC 13 March 1993 Pressure at Mean Sea Level.

1048

1049



1050

1051

1052

1053

1054

1055

1056

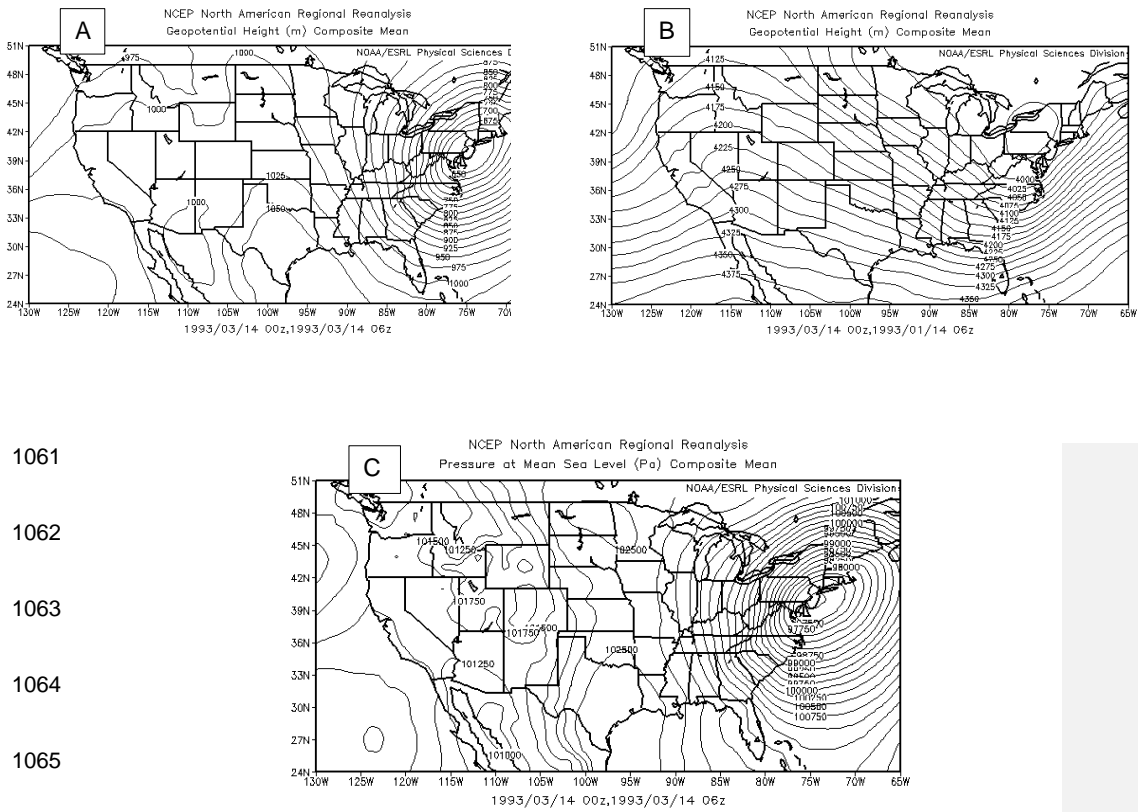
1057

1058

1059

1060

Figure 29. 13-14 March 1993 – Image A is 1800 UTC 13 March – 0000 UTC 14 March 1993 900hPa Height. Image B is 1800 UTC 13 March – 0000 UTC 14 March 1993 600hPa Height. Image C is 1800 UTC 13 March – 0000 UTC 14 March 1993 Pressure at Mean Sea Level.



1061

1062

1063

1064

1065

1066

1067

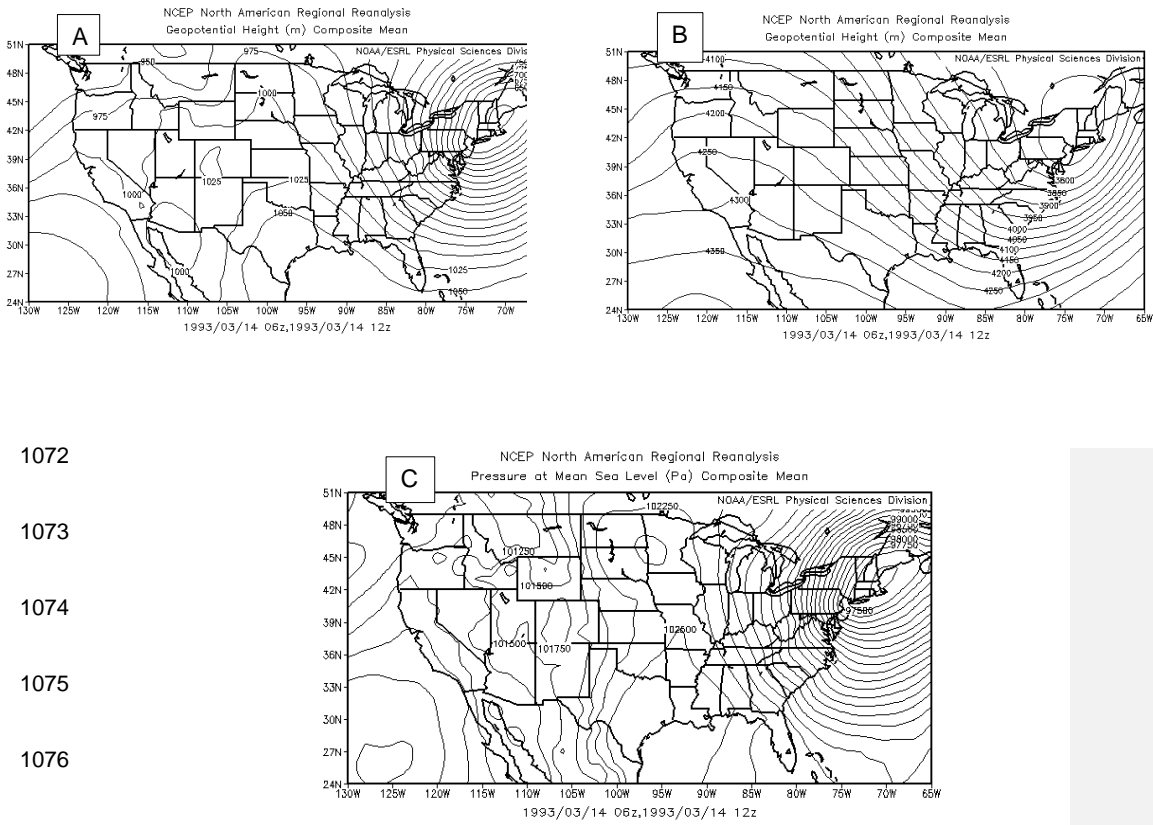
1068

Figure 30. 13-14 March 1993 – Image A is 0000 – 0600 UTC 14 March 1993 900hPa Height. Image B is 0000 – 0600 UTC 14 March 1993 600hPa Height. Image C is 0000 – 0600 UTC 14 March 1993 Pressure at Mean Sea Level.

1069

1070

1071



1072

1073

1074

1075

1076

1077

1078

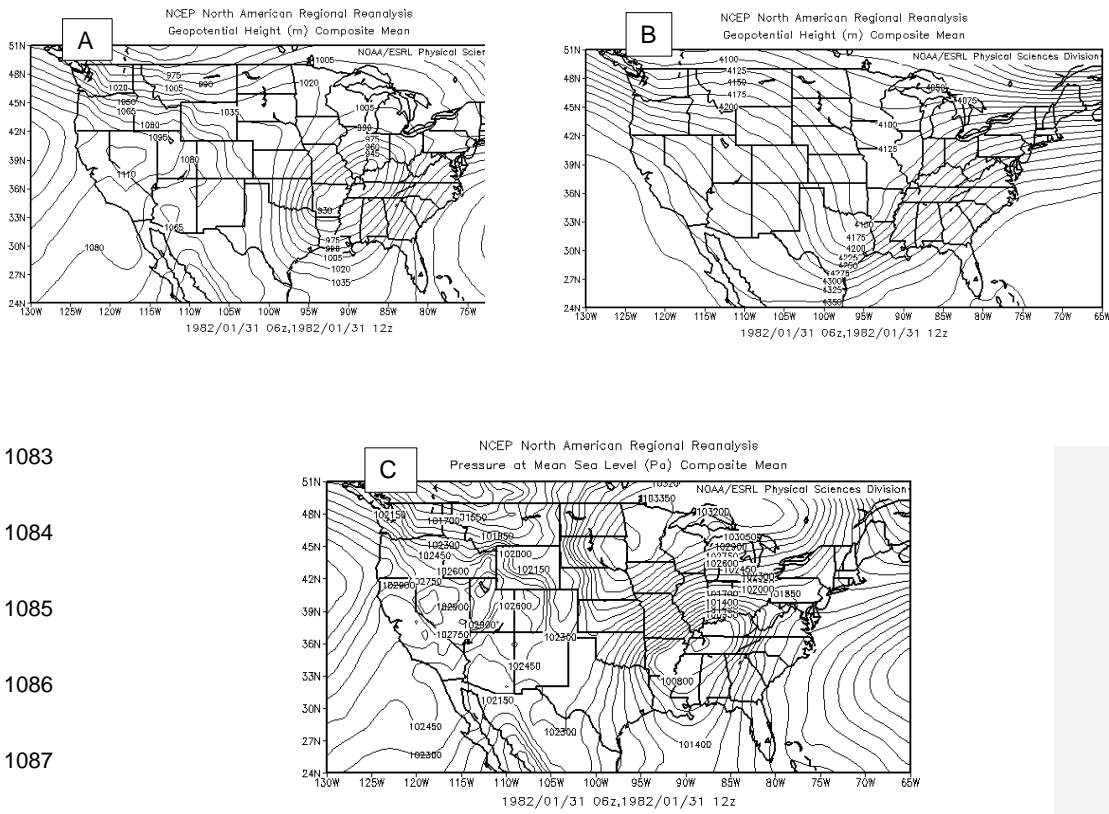
1079

1080

1081

1082

Figure 31. 13-14 March 1993 – Image A is 0600 – 1200 UTC 14 March 1993 900hPa Height. Image B is 0600 - 1200 UTC 14 March 1993 600hPa Height. Image C is 0600 - 1200 UTC Pressure at Mean Sea Level.



1083

1084

1085

1086

1087

1088

1089

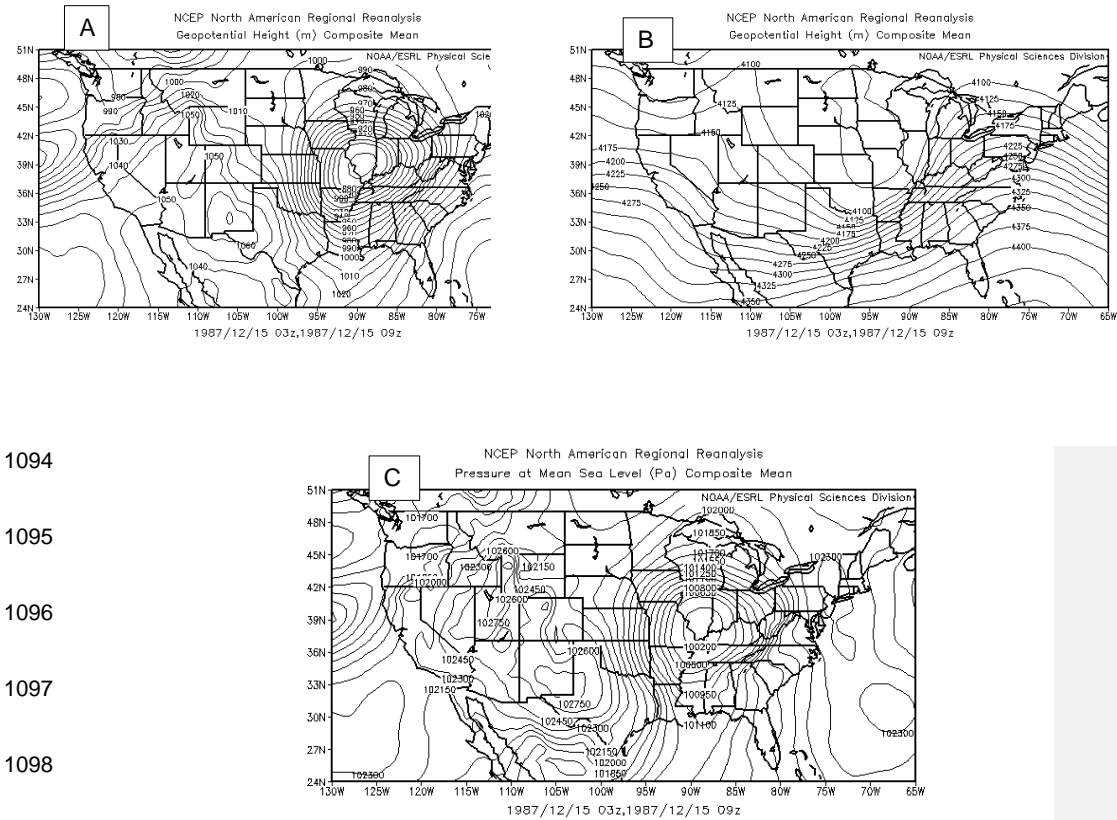
1090

1091

1092

1093

Figure 32. 30-31 January 1982 – Image A is 0600 – 1200 UTC 31 January 1982 900hPa Height. Image B is 0600 – 1200 UTC 31 January 1982 600hPa Height. Image C is 0600 – 1200 UTC 31 January 1982 Pressure at Mean Sea Level.



1094

1095

1096

1097

1098

1099

1100

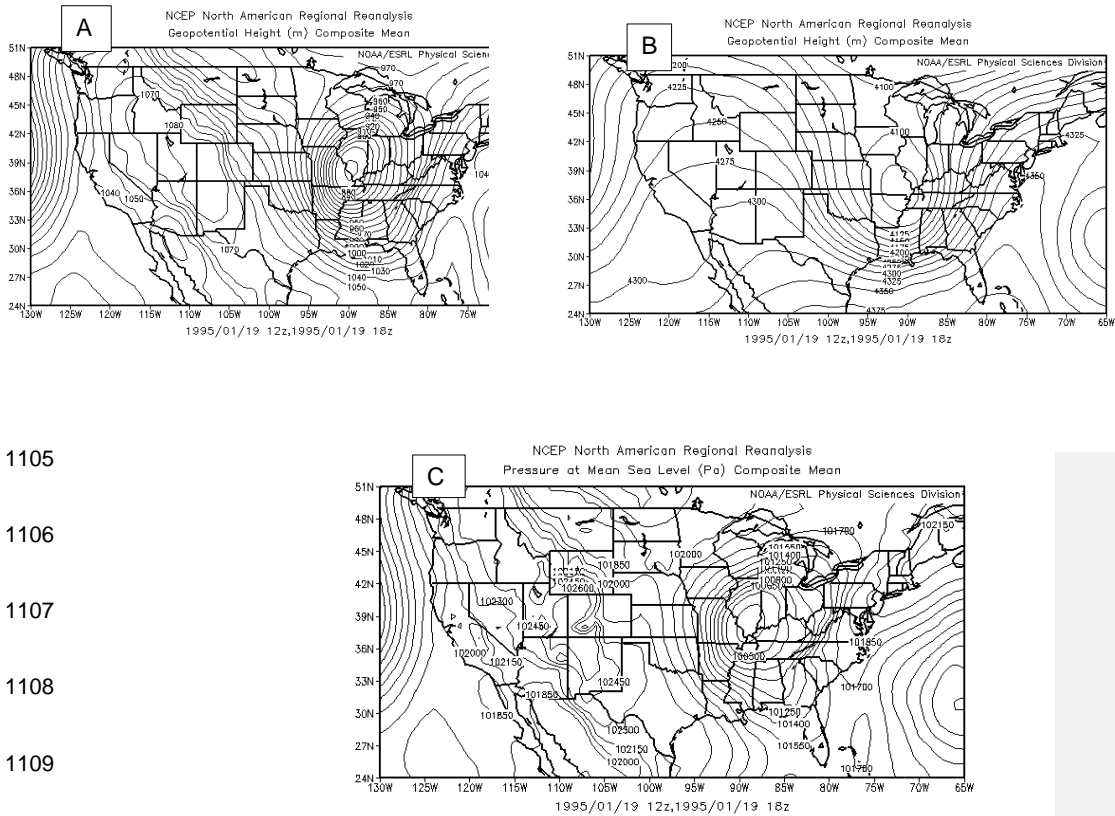
1101

1102

1103

1104

Figure 33. 14-15 December 1987 – Image A is 0300 – 0900 UTC 15 December 1987 900hPa Height. Image B is 0300 – 0900 UTC 15 December 1987 600hpa Height. Image C is 0300 – 0900 UTC 15 December 1987 Pressure at Mean Sea Level.



1105

1106

1107

1108

1109

1110

1111

1112

Figure 34. 19 January 1995 – Image A is 1200 – 1800 UTC 19 January 1995 900hPa Height. Image B is 1200 – 1800 UTC 19 January 1995 600hPa Height. Image C is 1200 – 1800 UTC 19 January 1995 Pressure at Mean Sea Level.

1113

1114

1115

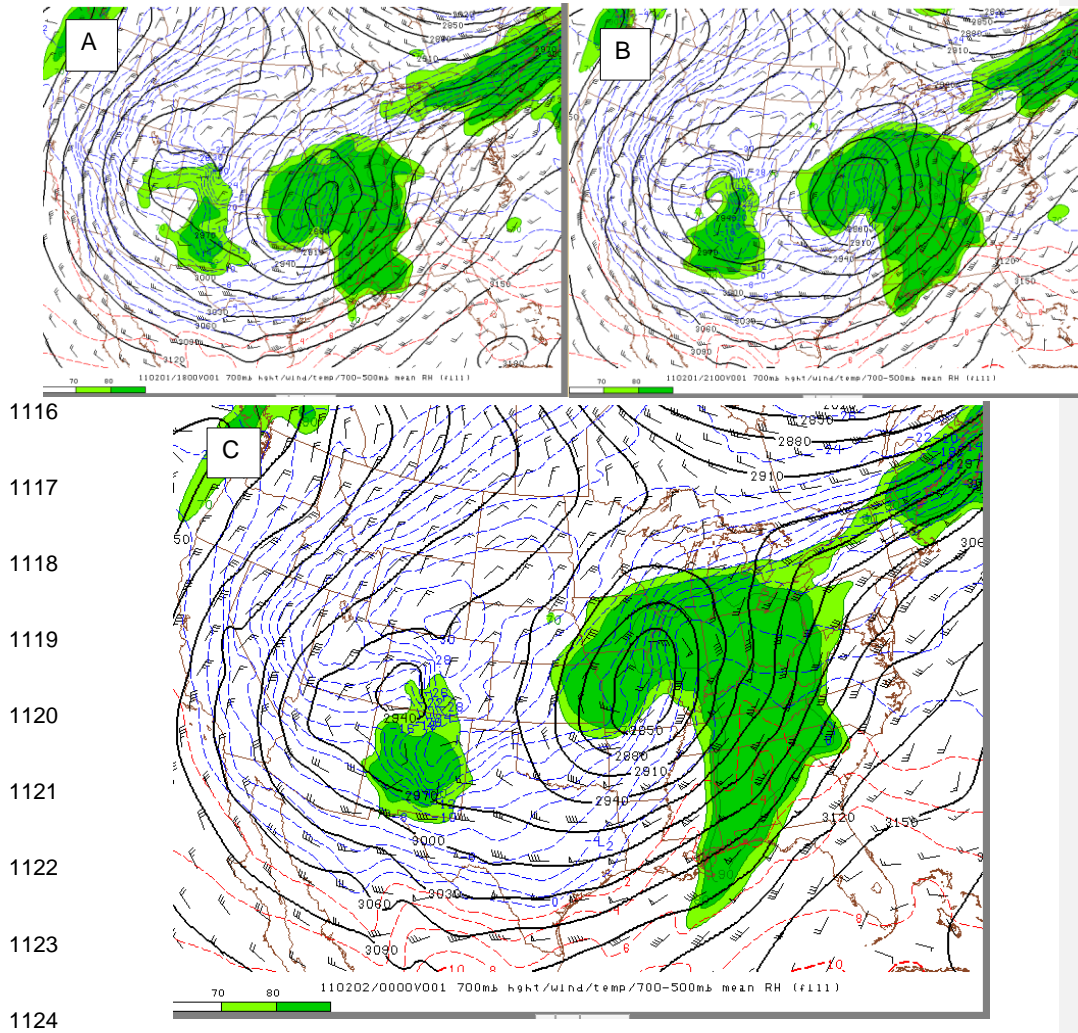


Figure 35. Image A is 1800 UTC 1 February 2011 700hPa Height, Wind, Temperature and 700-500hPa mean RH (fill). Image B is 2100 UTC 1 February 2011 700hPa Height, Wind, Temperature and 700-500hPa mean RH (fill). Image C is 0000 UTC 2 February 2011 700hPa Height, Wind, Temperature and 700 – 500hPa mean RH (fill).

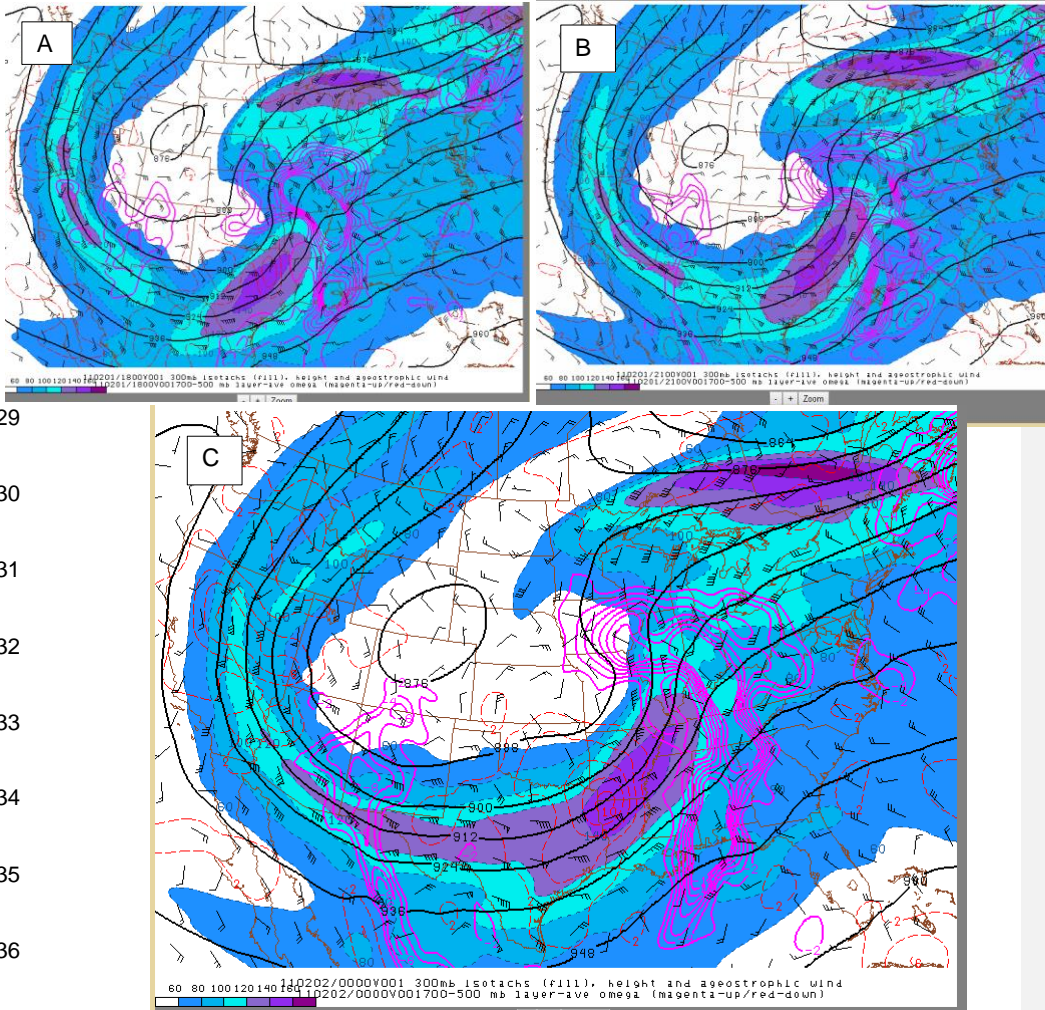


Figure 36. Image A is 1800 UTC 1 February 2011 300hPa Isotachs, Height and Ageostrophic Wind, 700-500hPa layer average Omega (magenta up). Image B is 2100 UTC 1 February 2011 300hPa Isotachs, Height and Ageostrophic Wind, 700-500hPa layer average Omega (magenta up). Image C is 0000 UTC 2 February 2011 300hPa Isotachs, Height and Ageostrophic Wind, 700-500hPa layer average Omega (magenta).

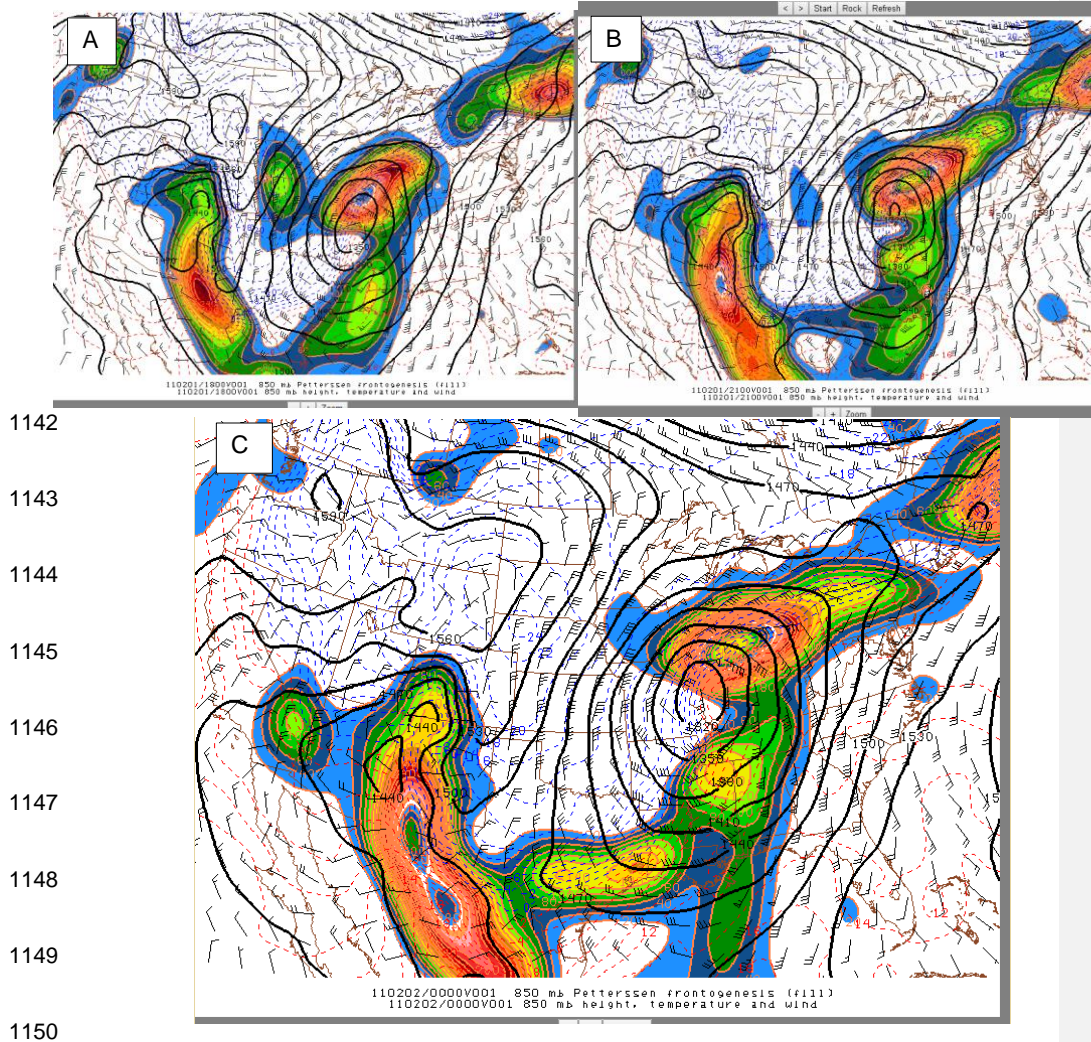


Figure 37. Image A is 1800 UTC 1 February 2011 850hPa Frontogenesis (fill), 850hPa Height, Temperature and Wind. Image B is 2100 UTC 1 February 2011 850hPa Frontogenesis (fill), 850hPa Height, Temperature and Wind. Image C is 0000 UTC 2 February 2011 850hPa Frontogenesis (fill), 850hPa Height, Temperature and Wind.

1153

1154

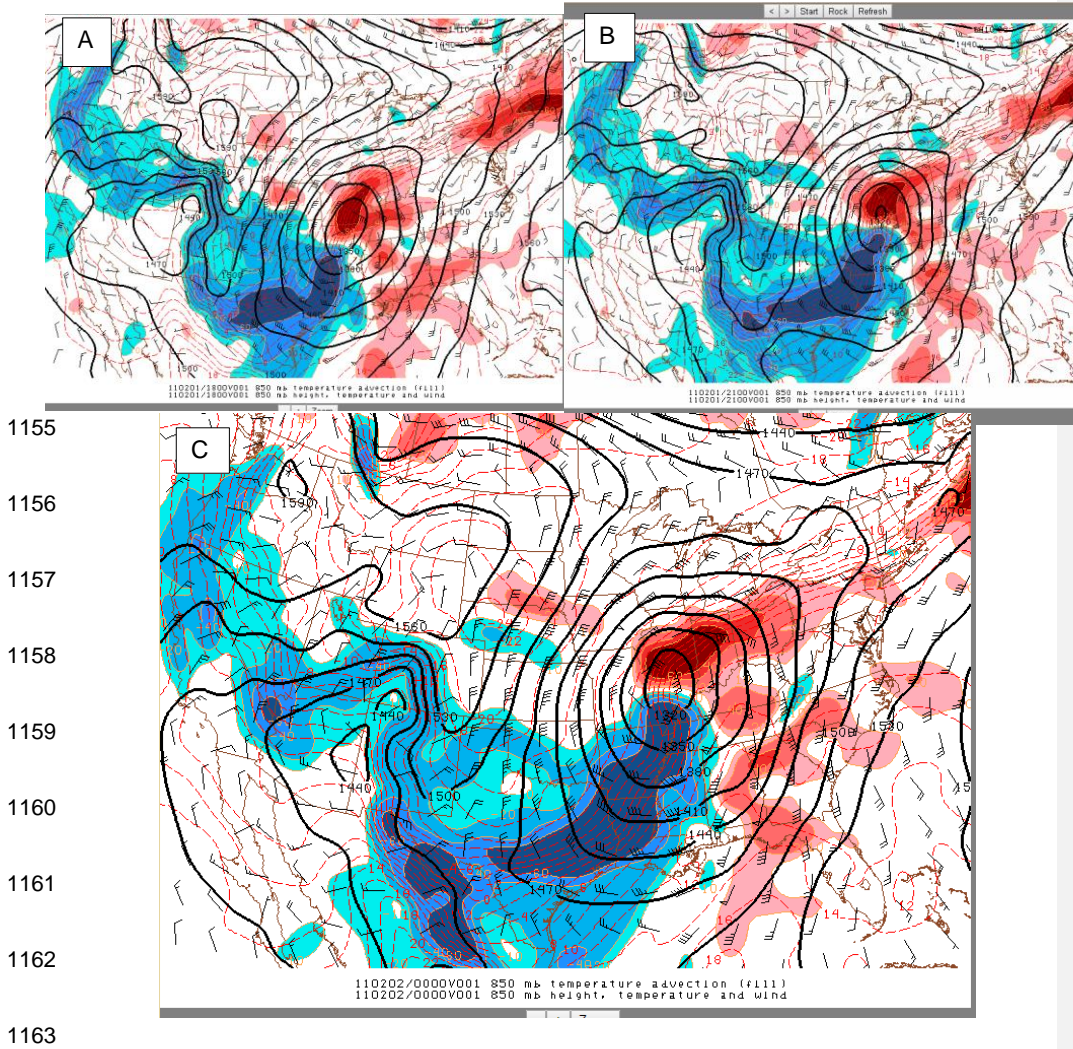


Figure 38. Image A is 1800 UTC 1 February 2011 850hPa Temperature Advection (fill), 850hPa Height, Temperature and Wind. Image B is 2100 UTC 1 February 2011 850hPa Temperature Advection (fill), 850hPa Height, Temperature and Wind. Image C is 0000 UTC 2 February 2011 850hPa Temperature Advection (fill), 850hPa Height, Temperature and Wind.

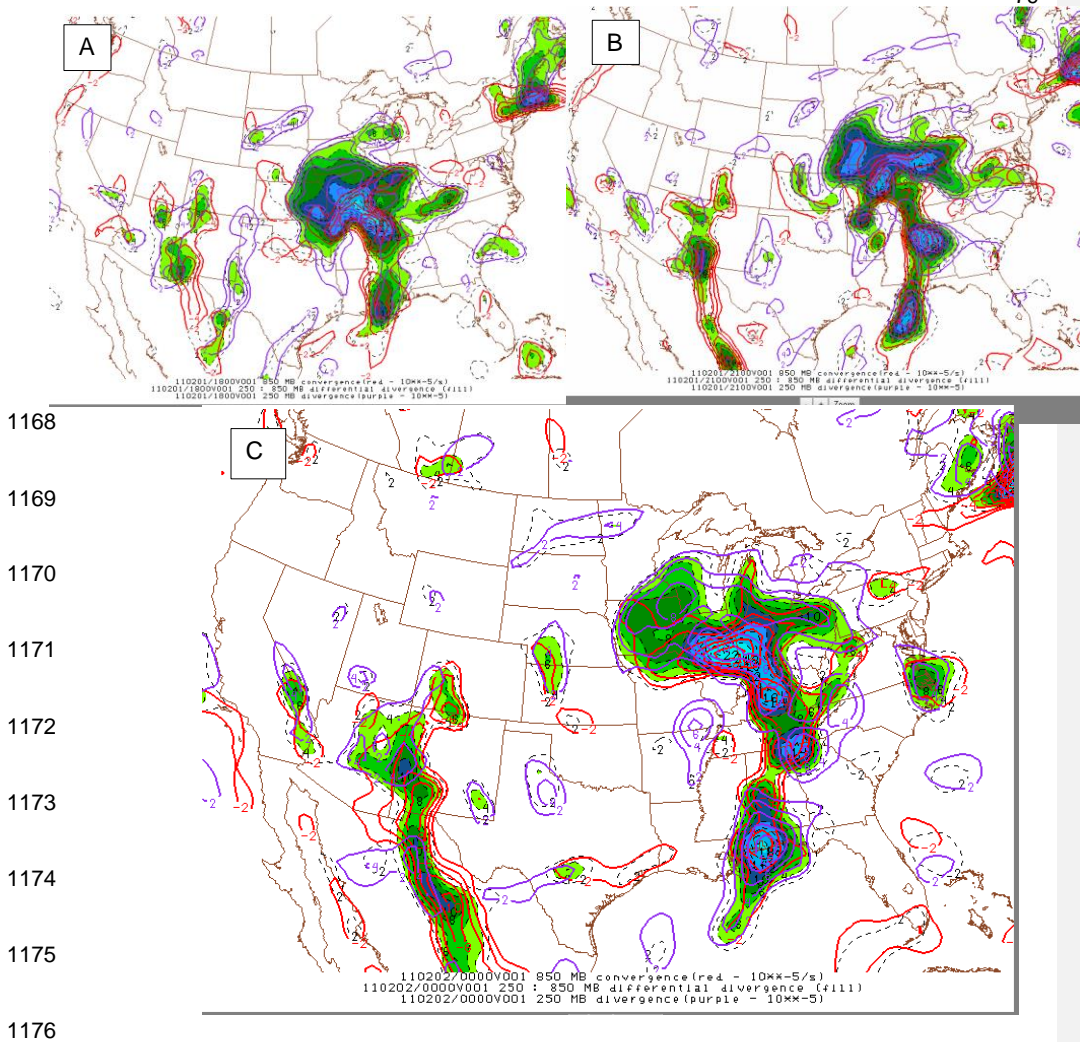


Figure 39. Image A is 1800 UTC 1 February 2011 850hPa Convergence (red), 250-850hPa Differential Divergence (fill) and 250hPa Divergence (purple). Image B is 2100 UTC 1 February 2011 850hPa Convergence (red), 250-850hPa Differential Divergence (fill) and 250hPa Divergence (purple). Image C is 0000 UTC 2 February 2011 850hPa Convergence (red), 250-850hPa Differential Divergence (fill) and 250hPa Divergence.

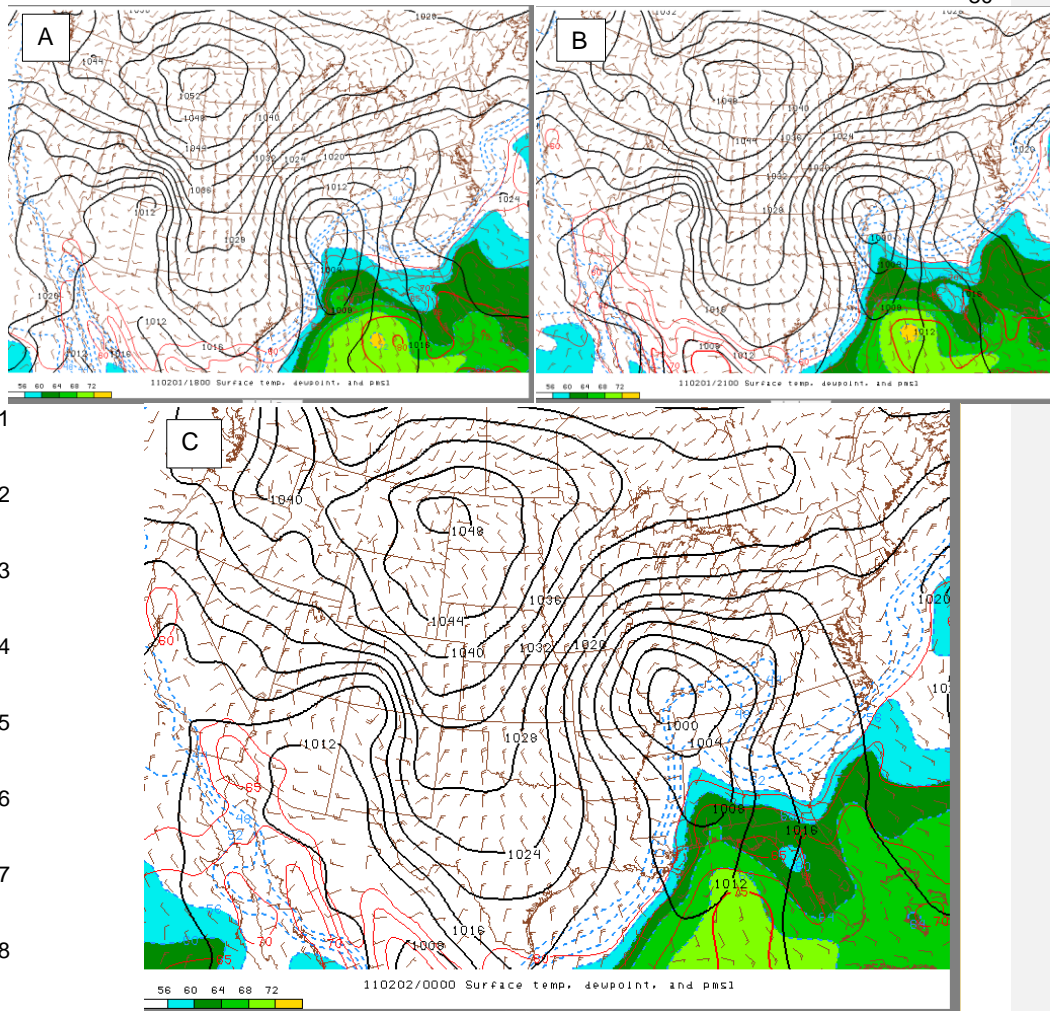


Figure 40. Image A is 1800 UTC 1 February 2011 Surface Temperature, Dewpoint and pmsl. Image B is 2100 UTC 1 February 2011 Surface Temperature, Dewpoint and pmsl. Image C is 0000 UTC 2 February 2011 Surface Temperature, Dewpoint and pmsl.

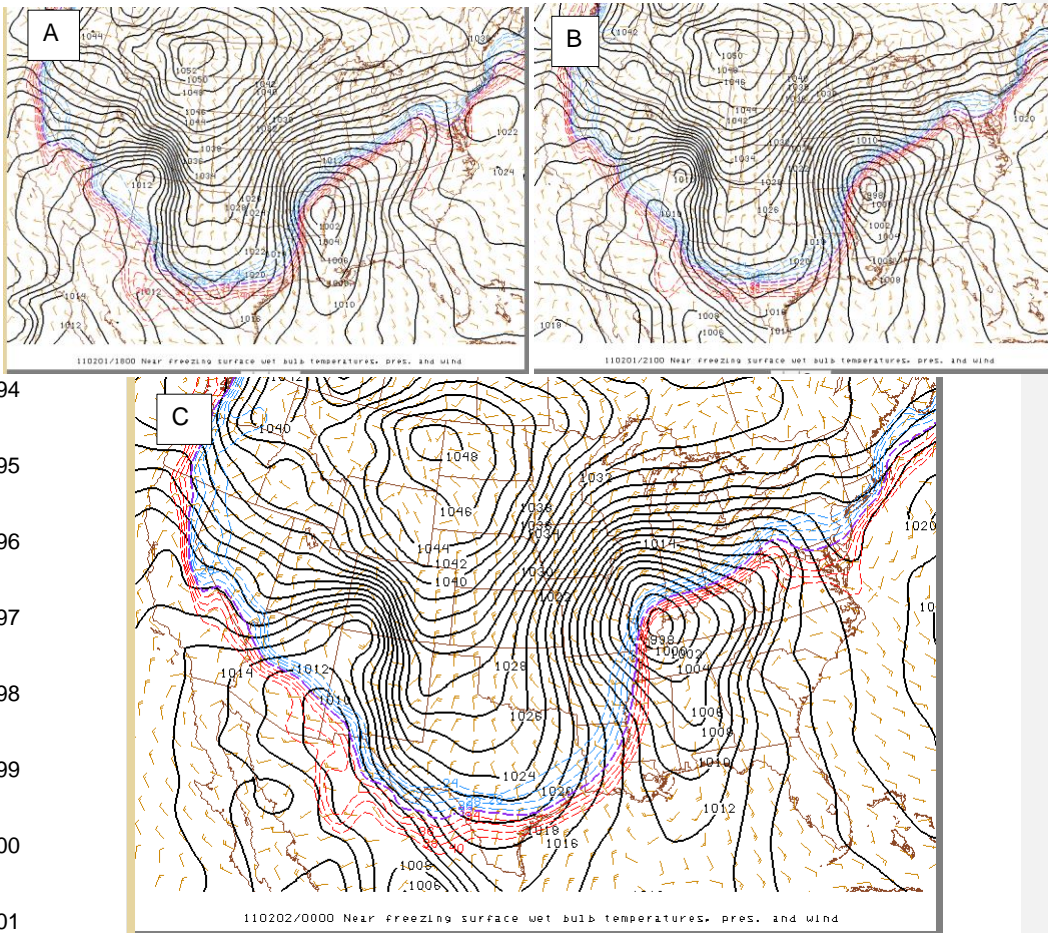


Figure 41. Image A is 1800 UTC 1 February 2011 Near Freezing Surface Wet Bulb Temperatures, Sea Level Pressure and Wind. Image B is 2100 UTC 1 February 2011 Near Freezing Surface Wet Bulb Temperatures, Sea Level Pressure and Wind. Image C is 0000 UTC 2 February 2011 Near Freezing Surface Wet Bulb Temperatures, Sea Level Pressure and Wind.

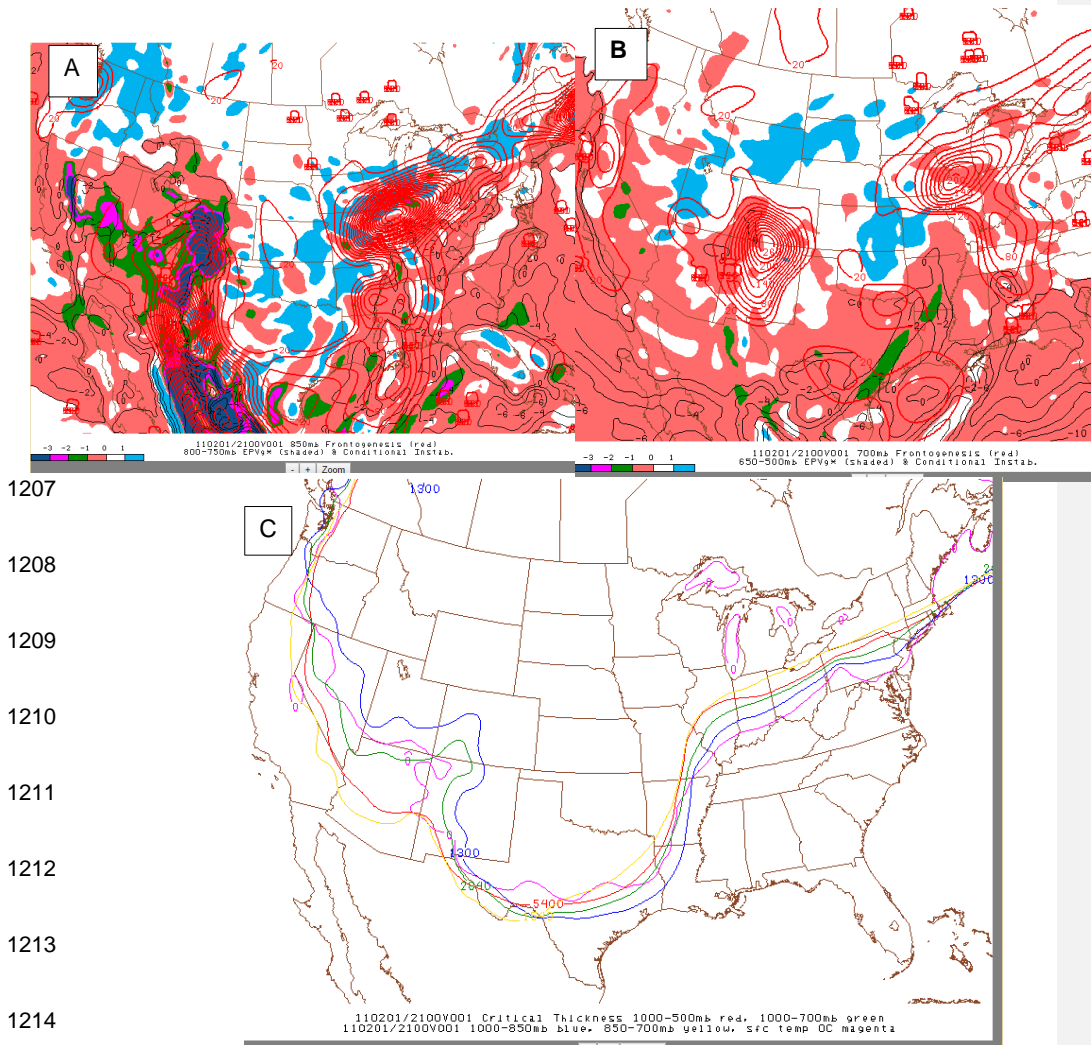


Figure 42. Image A is 2100 UTC 1 February 2011 850hPa Frontogenesis (red isolines), 800-750hPa EPVg (shaded) & Conditional Instability. Image B is 2100 UTC 1 February 2011 700hPa Frontogenesis (red isolines), 650-500hPa EPVg (shaded) & Conditional Instability. Image C is 2100 UTC 1 February 2011 Critical Thickness 1000-500hPa (red), 1000-700hPa (green), 1000-850hPa (blue), 850-700hPa (yellow), Surface Temperature 0C (magenta).

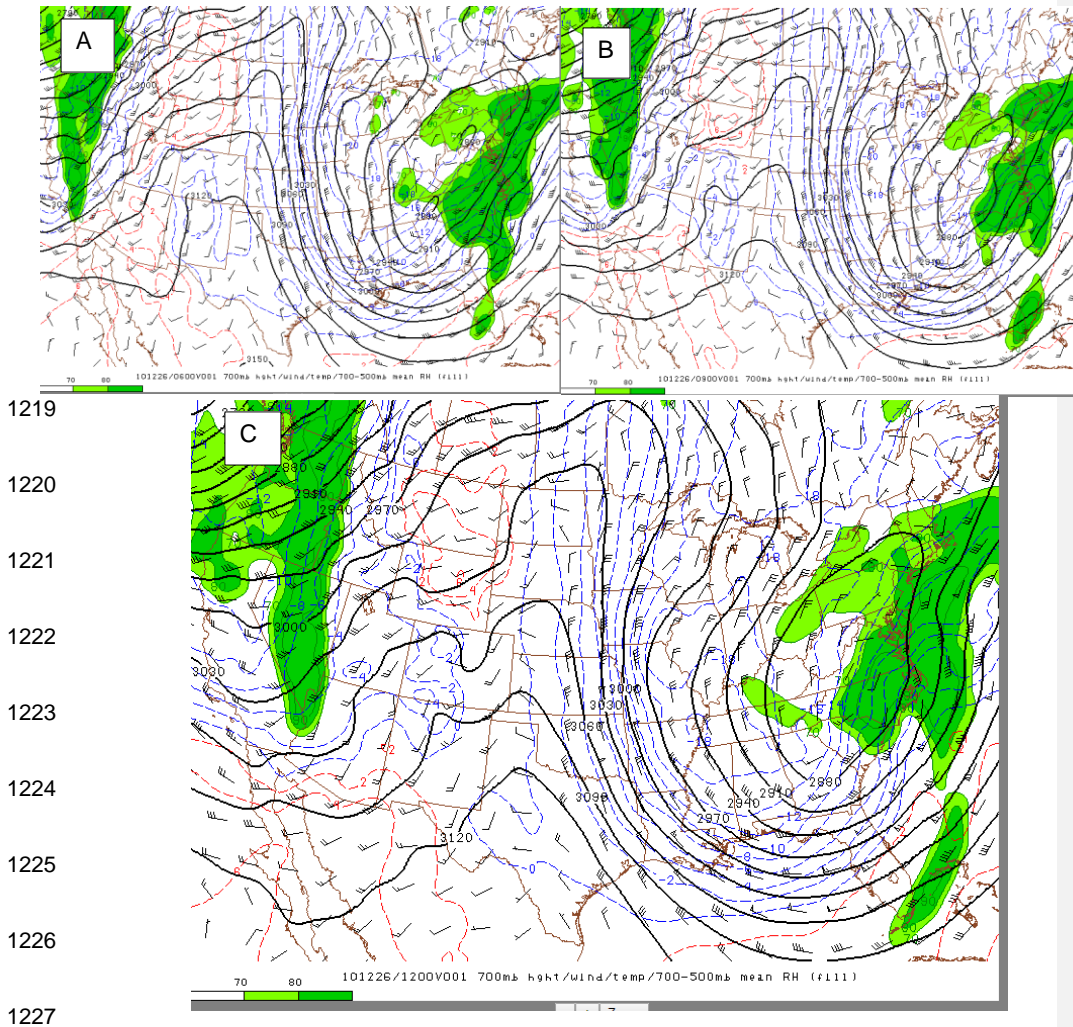


Figure 43. Image A is 0600 UTC 26 December 2010 700hPa height, wind, temperature and 700-500hPa mean RH (fill). Image B is 0900 UTC 26 December 2010 700hPa height, wind, temperature and 700-500hPa height, wind, temperature and 700-500hPa mean RH (fill). Image C is 1200 UTC 26 December 2010 700hPa height, wind, temperature and 700-500hPa mean RH (fill).

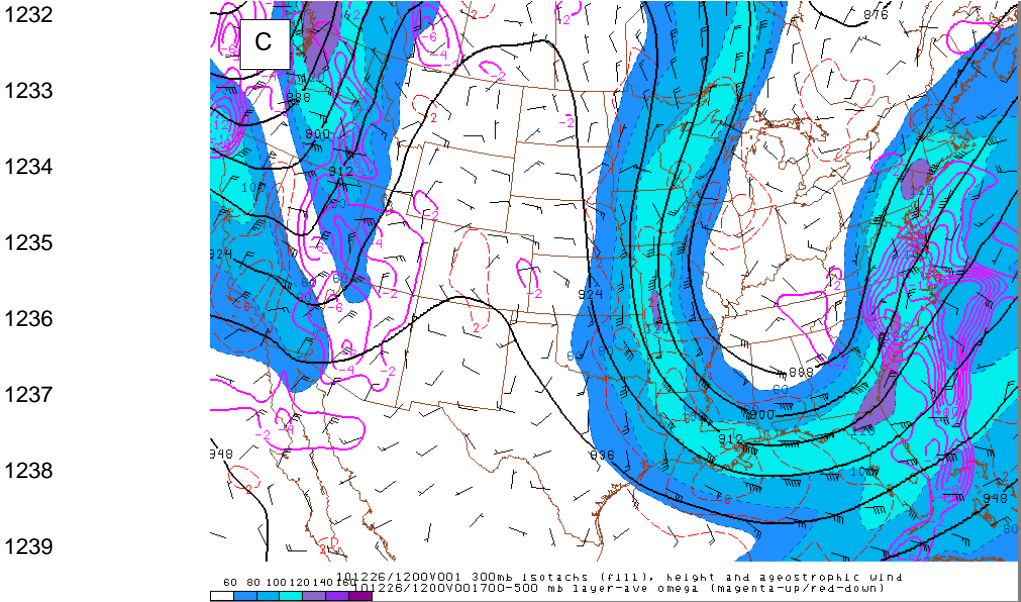
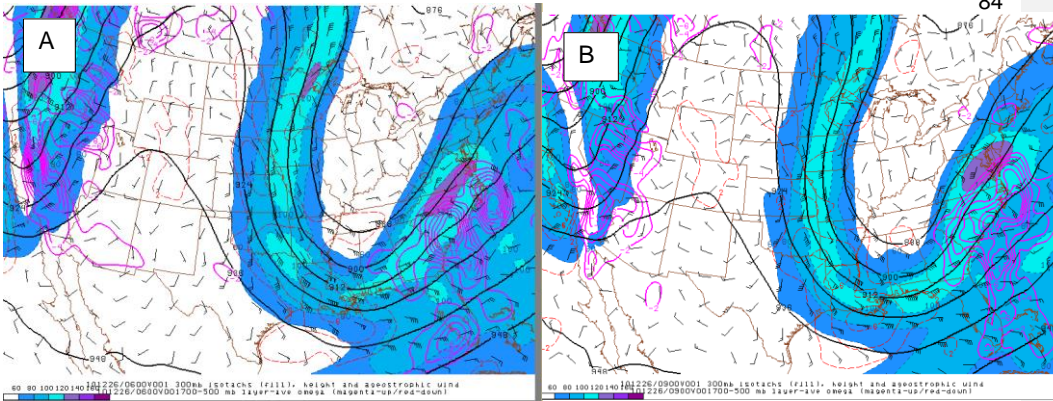


Figure 44. Image A is 0600 UTC 26 December 2010 300hPa isotachs (fill), height, ageostrophic wind and 700-500hPa layer average omega (magenta - up). Image B is 0900 UTC 26 December 2010 300hPa isotachs (fill), height, ageostrophic wind, and 700-500hPa layer average omega (magenta - up). Image C is 26 December 2010 300hPa isotachs (fill), height, ageostrophic wind and 700-500hPa layer average omega (magenta - up).

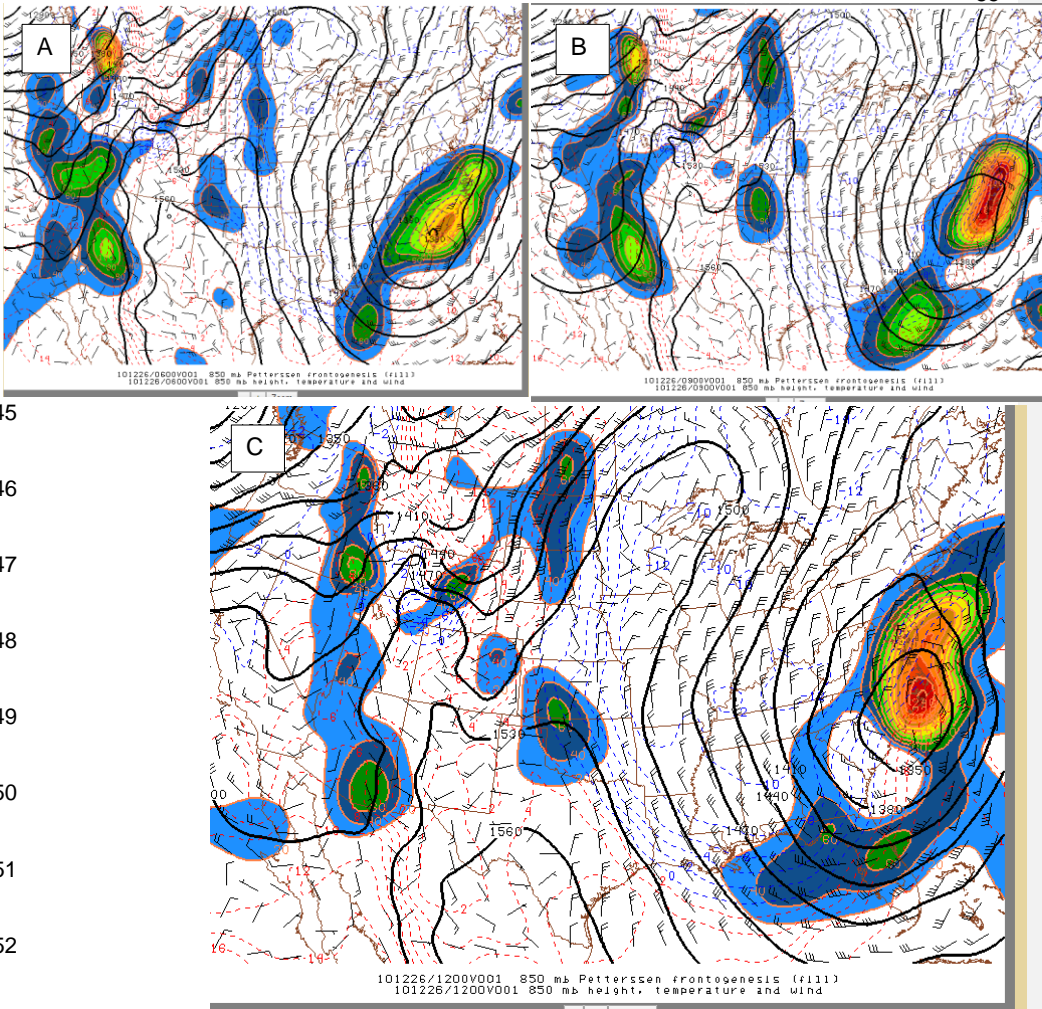


Figure 45. Image A is 0600 UTC 26 December 2010 850hPa frontogenesis (fill), 850hPa height, temperature and wind. Image B is 0900 UTC 26 December 2010 850hPa frontogenesis (fill), 850hPa height, temperature and wind. Image C is 1200 UTC 26 December 2010 850hPa frontogenesis (fill), 850hPa height, temperature and wind.

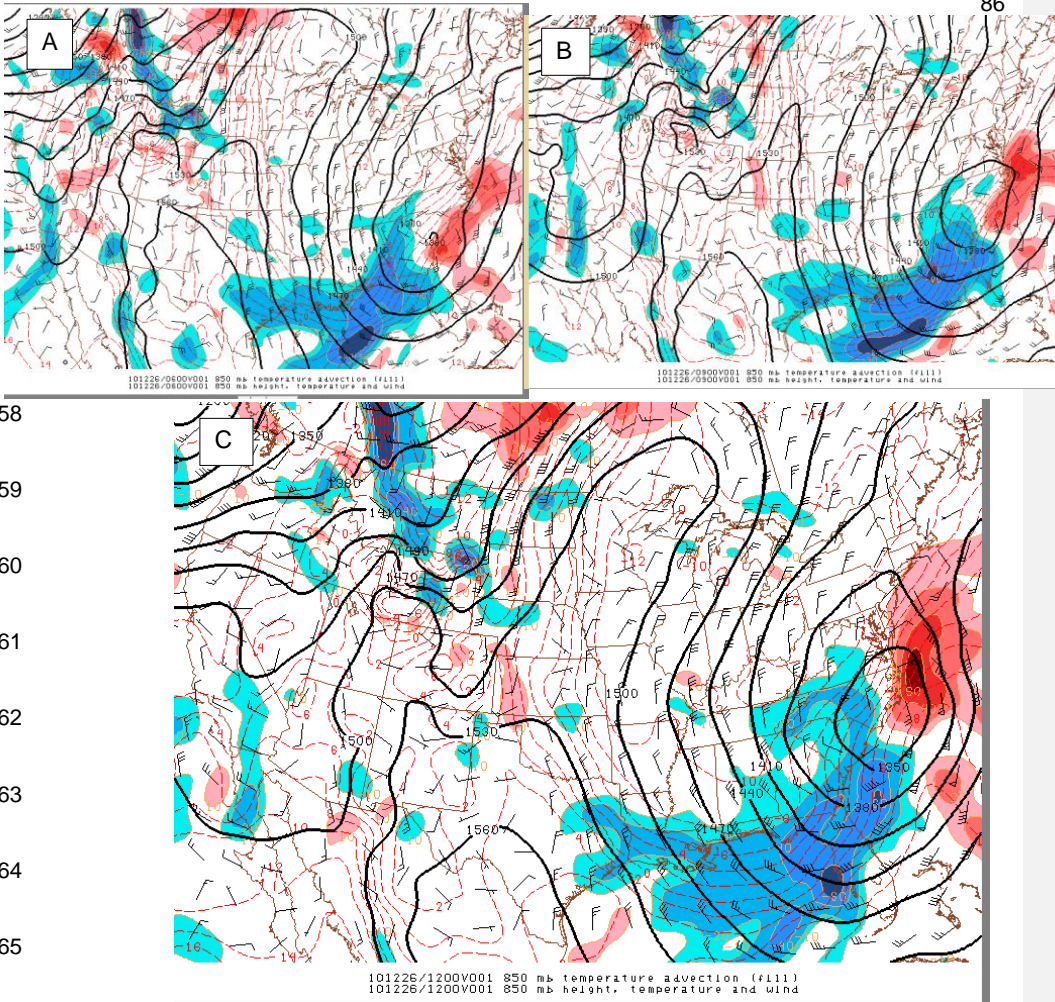
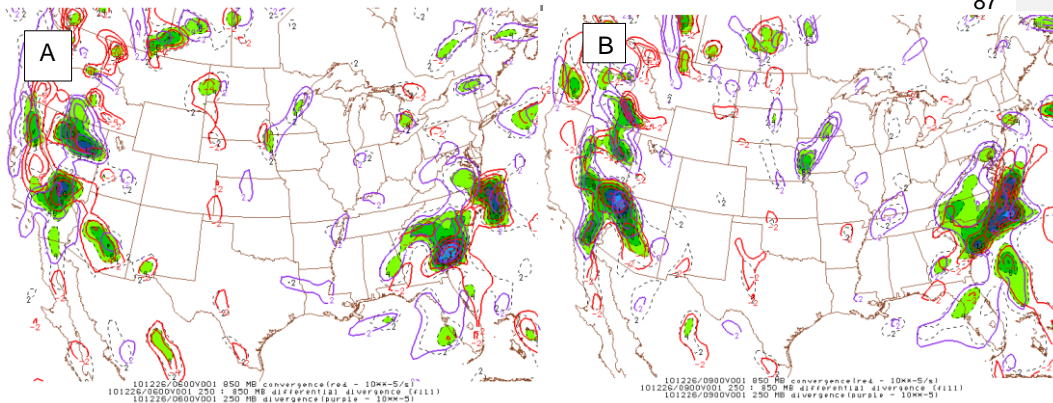


Figure 46. Image A is 0600 UTC 26 December 2010 850hPa temperature advection (fill), 850hPa height, temperature and wind. Image B is 0900 UTC 26 December 2010 temperature advection (fill), 850hPa height, temperature and wind. Image C is 1200 UTC 26 December 2010 850hPa temperature advection (fill), 850hPa height, temperature and wind.



1271

1272

1273

1274

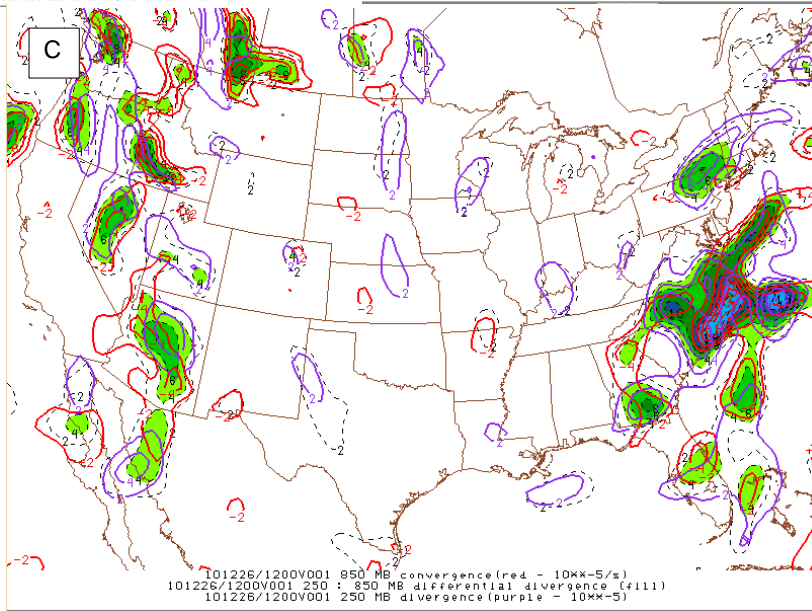
1275

1276

1277

1278

1279



1280

1281

1282

1283

Figure 47. Image A is 0600 UTC 26 December 2010 850hPa convergence (red isolines), 250-850hPa differential divergence (fill), 250hPa divergence (purple isolines). Image B is 0900 UTC 26 December 2010 850hPa convergence (red isolines), 250-850hPa differential divergence (fill), 250hPa divergence (purple isolines). Image C is 1200 UTC 26 December 2010 850hPa convergence (red isolines), 250-850hPa differential divergence (fill), 250hPa divergence (purple isolines).

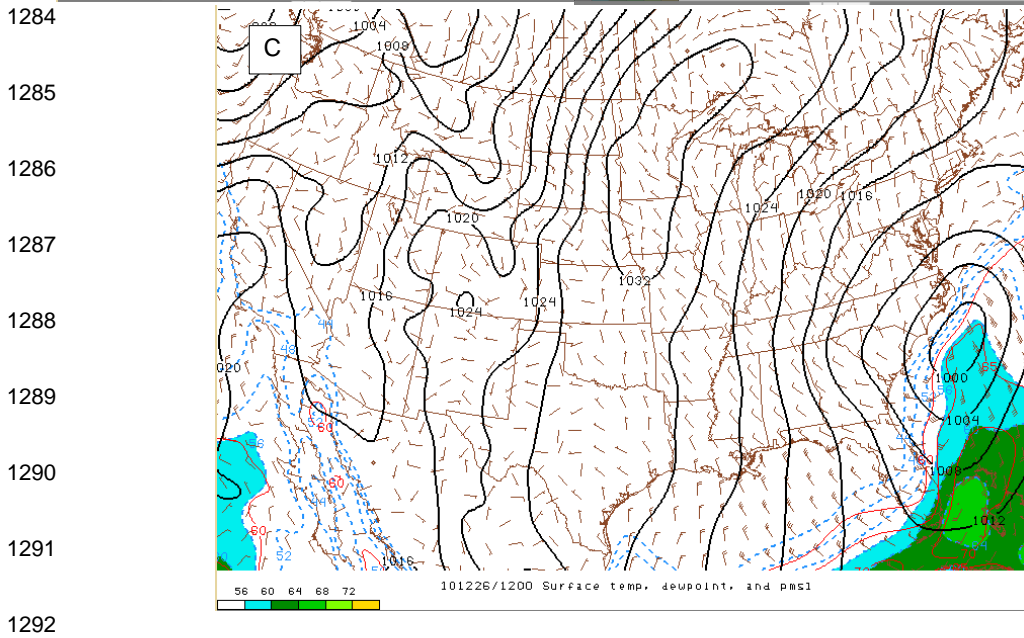
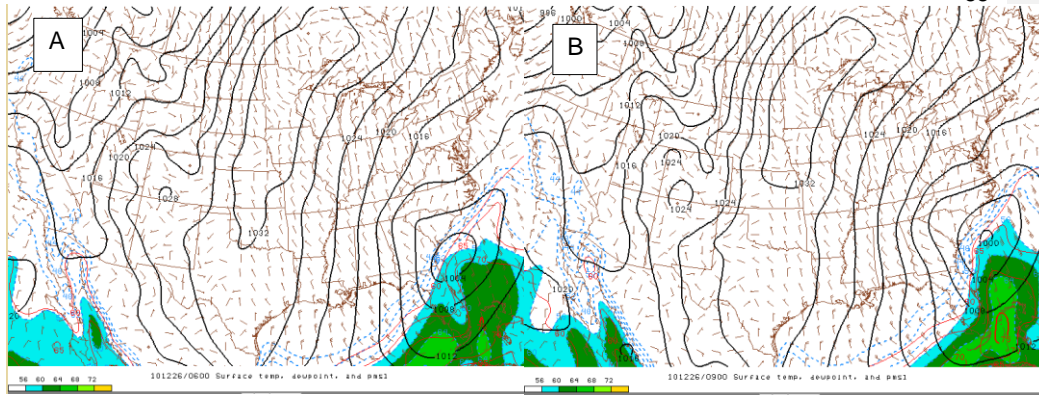
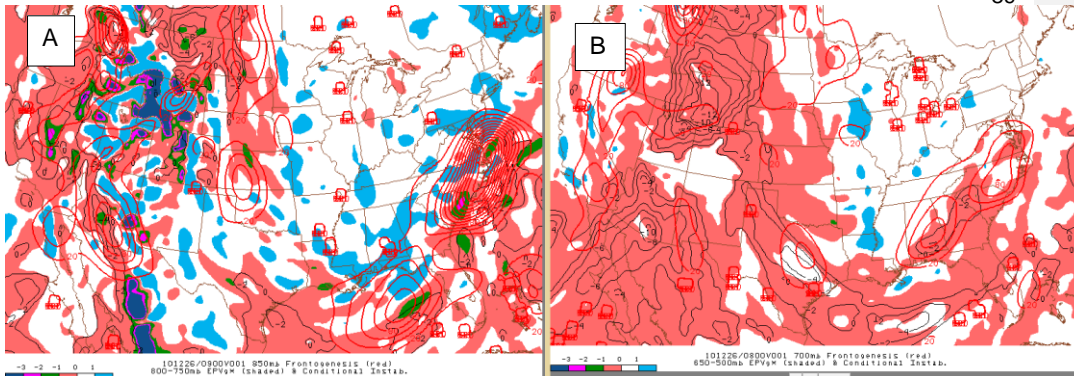


Figure 48. Image A is 0600 UTC 26 December 2010 Surface temperature, dewpoint and pmsl. Image B is 0900 UTC 26 December 2010 Surface temperature, dewpoint and pmsl. Image C is 26 December 2010 Surface temperature, dewpoint and pmsl.



1297

1298

1299

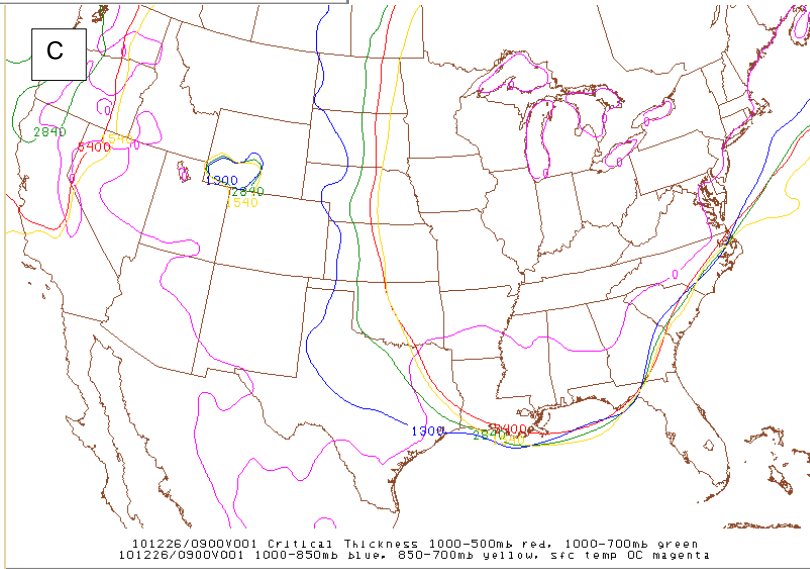
1300

1301

1302

1303

1304



1305

Figure 49. Image A is 0900 UTC 26 December 2010 850hPa Frontogenesis (red isolines), 800-750hPa EPVg (shaded) & conditional instability. Image B is 0800 UTC 700hPa Frontogenesis (red isolines), 650-500hPa EPVg (shaded) & conditional instability. Image C is 0900 UTC 26 December 2010 Critical Thickness 1000-500hPa (red), 1000-700hPa (green), 1000-850hPa (blue), 850-700hPa (yellow), surface temperature 0C (magenta).

1306

1307

1308

1309

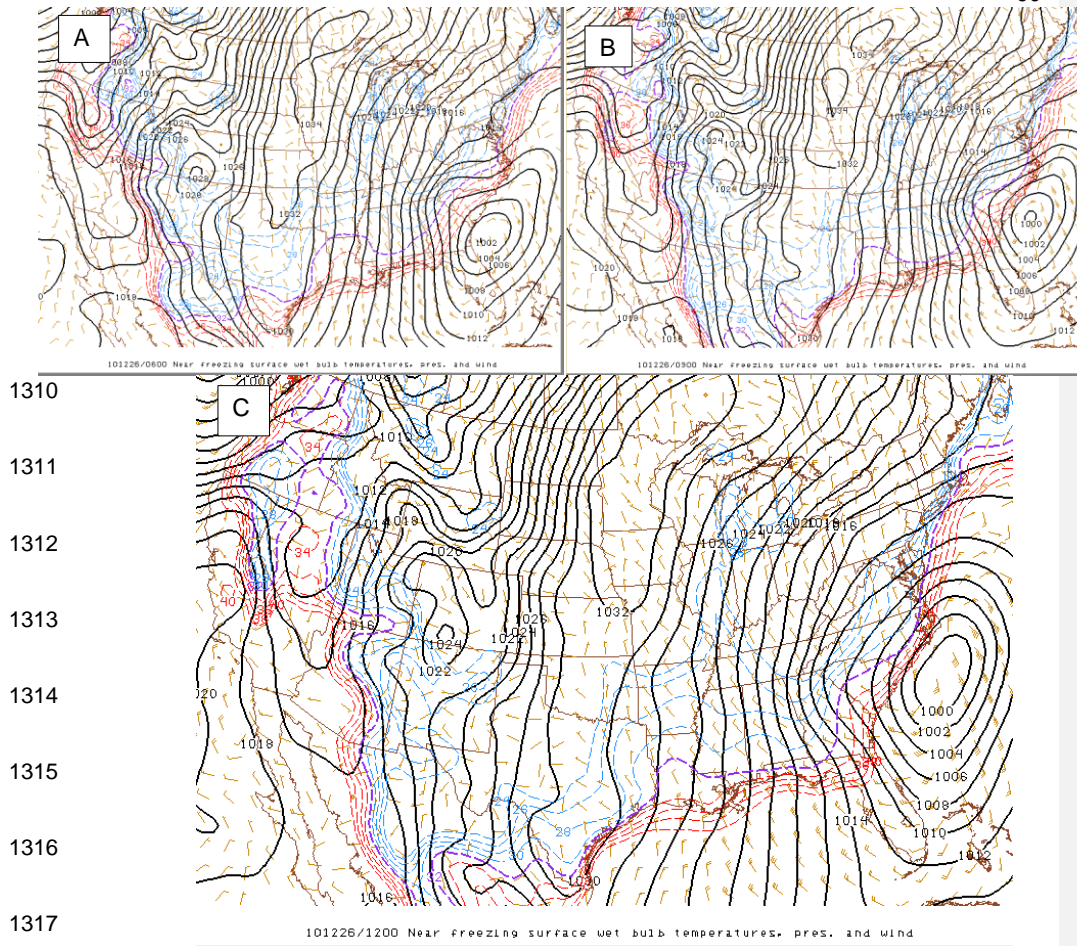


Figure 50. Image A is 0600 UTC 26 December 2010 Near freezing surface wet bulb temperatures, sea level pressure and wind. Image B is 0900 UTC 26 December 2010 Near freezing surface wet bulb temperatures, sea level pressure and wind. Image C is 1200 UTC 26 December 2010 Near freezing surface wet bulb temperatures, sea level pressure and wind.

1323

1324

1325

91

